

DELAWARE BAY AND RIVER CURRENT SURVEY 2021



**Silver Spring, Maryland
May 2024**



noaa National Oceanic and Atmospheric Administration

U.S. DEPARTMENT OF COMMERCE
National Ocean Service
Center for Operational Oceanographic Products and Services

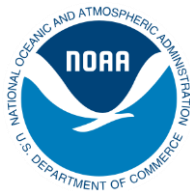
Center for Operational Oceanographic Products and Services
National Ocean Service
National Oceanic and Atmospheric Administration
U.S. Department of Commerce

The National Ocean Service (NOS) Center for Operational Oceanographic Products and Services (CO-OPS) provides the National infrastructure, science, and technical expertise to collect and distribute observations and predictions of water levels and currents to ensure safe, efficient and environmentally sound maritime commerce. The Center provides water level and tidal current products that support NOAA and NOS strategic priorities related to economic development, environmental stewardship, and climate resilience. For example, CO-OPS provides data and products required by the National Weather Service to meet its flood and tsunami warning responsibilities. The Center manages the National Water Level Observation Network (NWLON), a national network of Physical Oceanographic Real-Time Systems (PORTS[®]) in major U.S. harbors, and the National Current Observation Program consisting of current surveys in nearshore and coastal areas utilizing bottom-mounted platforms, subsurface buoys, horizontal sensors and quick-response real-time buoys. The Center: establishes standards for the collection and processing of water level and current data; collects and documents user requirements, which serve as the foundation for all resulting program activities; designs oceanographic observing systems; designs software to improve CO-OPS' data processing capabilities; maintains and operates oceanographic observing systems; performs operational data analysis and quality control; and produces and disseminates oceanographic products.

DELAWARE BAY AND RIVER CURRENT SURVEY 2021

Katie Kirk
Carl Kammerer
Ashley Barrett
Analise Keeney
Karen Kavanaugh
Rahwa Embaye
Christopher Paternostro
Lorraine Heilman

May 2024



U.S. DEPARTMENT OF COMMERCE

Gina Raimondo, Secretary

National Oceanic and Atmospheric Administration

**Dr. Richard Spinrad, NOAA Administrator and Under Secretary of
Commerce for Oceans and Atmosphere**

National Ocean Service

Nicole LeBoeuf, Assistant Administrator

Center for Operational Oceanographic Products and Services

Marian Westley, Director

NOTICE

Mention of a commercial company or product does not constitute an endorsement by NOAA. Use of information from this publication for publicity or advertising purposes concerning proprietary products or the tests of such products is not authorized.

TABLE OF CONTENTS

LIST OF FIGURES	2
LIST OF TABLES	7
LIST OF APPENDIX TABLES	7
EXECUTIVE SUMMARY	8
1.0 INTRODUCTION	9
2.0 PROJECT DESCRIPTION.....	14
2.1 Geographic Scope	19
2.2 Physical Oceanographic Overview	19
3.0 METHODS	21
3.1 Description of Instrumentation and Platforms.....	22
3.1.1 Bottom Mounts	26
3.1.2 Horizontal Mount.....	28
3.1.3 Surface Mounts	29
3.2 ADCP Setup and Data Collection	31
3.3 Description of Data Processing and Quality Control	32
3.4 CTD and Pressure Sensors	33
4.0 DATA ACQUIRED.....	34
5.0 STATION RESULTS	34
5.1 db1935 - Petty Island.....	35
5.2 DEB2101	40
5.3 DEB2105.....	45
5.4 DEB2117.....	51
5.5 DEB2119.....	56
5.6 DEB2128.....	62
5.7 DEB2132.....	68
6.0 SPATIAL VARIATION.....	74
6.1 Harmonic Constituents.....	74
6.2 Near-Surface Magnitude & Phases of the Tidal Current	88
6.3 Salinity	94
7.0 SUMMARY.....	104
ACKNOWLEDGEMENTS.....	104
REFERENCES CITED.....	106
APPENDIX A. STATION LISTING	108
APPENDIX B. STATION PLATFORM TYPES.....	110
ACRONYMS.....	111

LIST OF FIGURES

Figure 1. All stations deployed in the Delaware Bay and River (DEB) in 2019 (db1935) and 2021 (DEB21XX). Stations that had equipment or sensor failures limiting the days of good data to be less than 15 days are indicated by a blue circle. Stations where data was collected but was unusable due to an issue with the compass matrix are indicated by a red square. All other stations collected good data and are indicated by a gray circle. 11

Figure 2. All stations deployed in the Delaware Bay and River (DEB) in 2019 (db1935) and 2021 (DEB2101-DEB2136). The colors represent the number of days of good data collected at each station. Stations with less than 15 days of good data were not used to generate new predictions. 12

Figure 3. Current survey stations categorized by sensors deployed collecting time series data: gray circles represent acoustic Doppler current profiler (ADCP)-only stations; red squares represent stations with a conductivity, temperature, and depth (CTD) sensor co-located with the ADCP; and the yellow pentagon represents an external pressure sensor co-located with the ADCP. All stations were deployed in 2021 with the exception of db1935, which collected data in 2019. 13

Figure 4. The current survey stations color coded by the year data was last collected on site which was used to generate predictions at the historic stations. The black circles represent the active Physical Oceanographic Real-Time Systems (PORTS®) current meter stations (db0502 and db0301). The Currents Real Time Buoy (CURBY) deployment (db1935) was completed in 2019 as part of the current survey. Purple circles represent new stations occupied in 2021 where a historic station did not previously exist. 16

Figure 5. Lower Bay view of automatic identification system (AIS) tracks (from Vessel Traffic Data) for all vessels in the Delaware Bay, River, and vicinity. Current survey stations are represented by red circles. 17

Figure 6. Mid-River view of automatic identification system (AIS) tracks (from Vessel Traffic Data) for all vessels in the Delaware Bay, River, and vicinity. Current survey stations are represented by red circles. 18

Figure 7. Upper River view of automatic identification system (AIS) tracks (from Vessel Traffic Data) for all vessels in the Delaware Bay, River, and vicinity. Current survey stations are represented by red circles. 19

Figure 8. The great diurnal range of tidal height (meters) throughout the current survey area. ... 21

Figure 9. The NOAA R/V *Tornado* (7.6-meter [25-foot] Parker) equipped with a davit used for operations in the Delaware Bay and River. 22

Figure 10. Mount types for stations in the lower Bay: surface (red triangle), bottom (green circle), and side-looking (blue square). 24

Figure 11. Mount type for stations in the lower River: surface (red triangle), bottom (green circle), and side-looking (blue square). 25

Figure 12. Mount type for stations in the upper River: surface (red triangle), bottom (green circle), and side-looking (blue square). 26

Figure 13. Subsurface ellipsoid acoustic Doppler current profiler (ADCP) buoy (SEABY). The ellipsoid buoy holds the upward-facing ADCP and is attached to the acoustic release and anchor system with a taut wire line. 27

Figure 14. Mooring Systems, Inc. (MSI) H-TRBM-35 and H-TRBM-48 (formerly GP35 and GP48), which differ in diameter. The bottom mount holds an upward-facing acoustic Doppler current profiler (ADCP) and is lowered to the bottom to deploy and recovered with a grapnel that

is dragged to snag the ground line connecting the mount to an anchor. Specifications for the mount of both sizes are here: <https://www.mooringsystems.com/mounts.htm> (Image from MSI.)..... 27

Figure 15. Mooring Systems, Inc. (MSI) GP-TRBM (formerly mTRBM). The bottom mount holds an upward-facing acoustic Doppler current profiler (ADCP) and acoustic release system. The mount is lowered to the bottom for deployment and recovered by acoustically releasing to the surface a float that is tethered to the bottom mount. If the acoustic release fails, a grapnel is used to drag and snag the ground line connecting the mount to an anchor. Specifications for the mount are here <https://www.mooringsystems.com/mounts.htm>. (Image from MSI.) 28

Figure 16. Bridge cribbing side-looking mount (left). Side-looking acoustic Doppler current profiler (ADCP) deployed in the bridge cribbing mount (right)..... 29

Figure 17. Clamparatus on a green (left) and red (right) aid to navigation (ATON)..... 30

Figure 18. Mooring diagram (not to scale) of the Currents Real Time Buoy (CURBY). 31

Figure 19. Scatter plot of north-versus-east velocity (cm/s) for station db1935 at the near-surface prediction bin, bin 5 at 3 meters (m) below mean lower low water (MLLW). 36

Figure 20. Comparison of observed major axis velocity data (green points) to predicted tidal velocity (red line) along the major axis for station db1935. The lower figure shows the non-tidal residual (blue dots), which is the difference between the predicted and observed velocity from the upper panel..... 37

Figure 21. db1935 mean velocity (cm/s) profile along the major axis (red vectors) and minor axis (blue vectors) by depth. Only bins that passed quality control criteria are shown. This station was configured to collect 1-m bins. 38

Figure 22. db1935 maximum ebb current (MEC) timing (Greenwich Intervals [GI], red squares, upper x-axis) and speed (blue circles, lower x-axis) by depth..... 39

Figure 23. db1935 maximum flood current (MFC) timing (Greenwich Intervals [GI], red squares, upper x-axis) and speed (blue circles, lower x-axis) by depth..... 40

Figure 24. Scatter plot of north-versus-east velocity (cm/s) for station DEB2101 at the near-surface prediction bin, bin 13 at 1.5 meters below mean lower low water (MLLW)..... 41

Figure 25. Comparison of observed major axis velocity data (green points) to predicted tidal velocity (red line) along the major axis for station DEB2101. The sensor depth (magenta dots) is measured using the acoustic Doppler current profiler (ADCP) pressure sensor and shows the tidally-induced water level changes over time. The lower figure shows the non-tidal residual (blue dots), which is the difference between the predicted and observed velocity from the upper panel. 42

Figure 26. DEB2101 mean velocity (cm/s) profile along the major axis (red vectors) and minor axis (blue vectors) by depth. Only bins that passed quality control criteria are shown. This station was configured to collect 1-m bins. 43

Figure 27. DEB2101 maximum ebb current (MEC) timing (Greenwich Intervals [GI], red squares, upper x-axis) and speed (blue circles, lower x-axis) by depth..... 44

Figure 28. DEB2101 maximum flood current (MFC) timing (Greenwich Intervals [GI], red squares, upper x-axis) and speed (blue circles, lower x-axis) by depth..... 45

Figure 29. Scatter plot of north-versus-east velocity (cm/s) for station DEB2105 at the near-surface prediction bin, bin 12 at 1.4 m below mean lower low water (MLLW). 47

Figure 30. Comparison of observed major axis velocity data (green points) to predicted tidal velocity (red line) along the major axis for station DEB2105. The sensor depth (magenta dots) is measured using the acoustic Doppler current profiler (ADCP) pressure sensor and shows the tidally-induced water level changes over time. The lower figure shows the non-tidal residual (blue

dots), which is the difference between the predicted and observed velocity from the upper panel. 48

Figure 31. DEB2105 mean velocity (cm/s) profile along the major axis (red vectors) and minor axis (blue vectors) by depth. Only bins that passed quality control criteria are shown. This station was configured to collect 1-m bins. 49

Figure 32. DEB2105 maximum ebb current (MEC) timing (Greenwich Intervals [GI], red squares, upper x-axis) and speed (blue circles, lower x-axis) by depth..... 50

Figure 33. DEB2105 maximum flood current (MFC) timing (Greenwich Intervals [GI], red squares, upper x-axis) and speed (blue circles, lower x-axis) by depth..... 51

Figure 34. Scatter plot of north-versus-east velocity (cm/s) for station DEB2117 at the near-surface prediction bin, bin 13 at 2.3 m below mean lower low water (MLLW). 52

Figure 35. Comparison of observed major axis velocity data (green points) to predicted tidal velocity (red line) along the major axis for station DEB2117. The sensor depth (magenta dots) is measured using the acoustic Doppler current profiler (ADCP) pressure sensor and shows the tidally-induced water level changes over time. The lower figure shows the non-tidal residual (blue dots), which is the difference between the predicted and observed velocity from the upper panel. 53

Figure 36. DEB2117 mean velocity (cm/s) profile along the major axis (red vectors) and minor axis (blue vectors) by depth. Only bins that passed quality control criteria are shown. This station was configured to collect 1-m bins. 54

Figure 37. DEB2117 maximum ebb current (MEC) timing (Greenwich Intervals [GI], red squares, upper x-axis) and speed (blue circles, lower x-axis) by depth..... 55

Figure 38. DEB2117 maximum flood current (MFC) timing (Greenwich Intervals [GI], red squares, upper x-axis) and speed (blue circles, lower x-axis) by depth..... 56

Figure 39. Scatter plot of north-versus-east velocity (cm/s) for station DEB2119 at the near-surface prediction bin, bin 6 at 1.9 m below mean lower low water (MLLW). 58

Figure 40. Comparison of observed major axis velocity data (green points) to predicted tidal velocity (red line) along the major axis for station DEB2119. The lower figure shows the non-tidal residual (blue dots), which is the difference between the predicted and observed velocity from the upper panel..... 59

Figure 41. DEB2119 mean velocity (cm/s) profile along the major axis (red vectors) and minor axis (blue vectors) by depth. Only bins that passed quality control criteria are shown. This station was configured to collect 1-m bins. 60

Figure 42. DEB2119 maximum ebb current (MEC) timing (Greenwich Intervals [GI], red squares, upper x-axis) and speed (blue circles, lower x-axis) by depth..... 61

Figure 43. DEB2119 maximum flood current (MFC) timing (Greenwich Intervals [GI], red squares, upper x-axis) and speed (blue circles, lower x-axis) by depth..... 62

Figure 44. Scatter plot of north-versus-east velocity (cm/s) for station DEB2128 at the near-surface prediction bin, bin 12 at 2.5 meters (m) below mean lower low water (MLLW). 64

Figure 45. Comparison of observed major axis velocity data (green points) to predicted tidal velocity (red line) along the major axis for station DEB2128. The sensor depth (magenta dots) is measured using the acoustic Doppler current profiler (ADCP) pressure sensor and shows the tidally induced water level changes over time. The lower figure shows the non-tidal residual (blue dots), which is the difference between the predicted and observed velocity from the upper panel. 65

Figure 46. DEB2128 mean velocity (cm/s) profile along the major axis (red vectors) and minor axis (blue vectors) by depth. Only bins that passed quality control criteria are shown. This station was configured to collect 1-m bins. 66

Figure 47. DEB2128 maximum ebb current (MEC) timing (Greenwich Intervals [GI], red squares, upper x-axis) and speed (blue circles, lower x-axis) by depth..... 67

Figure 48. DEB2128 maximum flood current (MFC) timing (Greenwich Intervals [GI], red squares, upper x-axis) and speed (blue circles, lower x-axis) by depth..... 68

Figure 49. Scatter plot of north-versus-east velocity (cm/s) for station DEB2132 at the near-surface prediction bin, bin 9 at 1.8 meters (m) below mean lower low water (MLLW). 69

Figure 50. Comparison of observed major axis velocity data (green points) to predicted tidal velocity (red line) along the major axis for station DEB2132. The sensor depth (magenta dots) is measured using the acoustic Doppler current profiler (ADCP) pressure sensor and shows the tidally induced water level changes over time. The lower figure shows the non-tidal residual (blue dots), which is the difference between the predicted and observed velocity from the upper panel. 70

Figure 51. DEB2132 mean velocity (cm/s) profile along the major axis (red vectors) and minor axis (blue vectors) by depth. Only bins that passed quality control criteria are shown. This station was configured to collect 1-m bins. 71

Figure 52. DEB2132 maximum ebb current (MEC) timing (Greenwich Intervals [GI], red squares, upper x-axis) and speed (blue circles, lower x-axis) by depth..... 72

Figure 53. DEB2132 maximum flood current (MFC) timing (Greenwich Intervals [GI], red squares, upper x-axis) and speed (blue circles, lower x-axis) by depth..... 73

Figure 54. Defant ratios for the lower Bay for the near-surface prediction bin at survey stations. Semidiurnal tides (Defant ratio < 0.25) are observed at all stations. 74

Figure 55. Defant ratios for the lower River for the near-surface prediction bin at survey stations. Semidiurnal tides (Defant ratio < 0.25) are observed at all stations. 75

Figure 56. Defant ratios for the upper River for the near-surface prediction bin at survey stations. Semidiurnal tides (Defant ratio < 0.25) are observed at all stations. 76

Figure 57. M2 tidal ellipses for prediction stations in Delaware Bay, showing the topographic steering of the ellipses..... 77

Figure 58. M2 tidal ellipses for prediction stations in the lower Delaware River, showing the topographic steering of the ellipses..... 78

Figure 59. M2 tidal ellipses for prediction stations in upper Delaware River, showing the topographic steering of the ellipses..... 79

Figure 60. K1 tidal ellipses for prediction stations in Delaware Bay, showing the topographic steering of the ellipses. Note that these are on a different scale than M2 in order to better visualize the ellipses. These data are at about 1/4 the scale of the M2 data. 80

Figure 61. K1 tidal ellipses for prediction stations in the lower Delaware River, showing the topographic steering of the ellipses. Note that these are on a different scale than M2 in order to better visualize the ellipses. These data are at about 1/4 the scale of the M2 data. 81

Figure 62. K1 tidal ellipses for prediction stations in the upper Delaware River, showing the topographic steering of the ellipses. Note that these are on a different scale than M2 in order to better visualize the ellipses. These data are at about 1/4 the scale of the M2 data. 82

Figure 63. O1 tidal ellipses for prediction stations in Delaware Bay, showing the topographic steering of the ellipses. Note that these are on a different scale than M2 in order to better visualize the ellipses. These data are at about 1/4 the scale of the M2 data. 83

Figure 64. O1 tidal ellipses for prediction stations in the lower Delaware River, showing the topographic steering of the ellipses. Note that these are on a different scale than M2 in order to better visualize the ellipses. These data are at about 1/4 the scale of the M2 data.	84
Figure 65. O1 tidal ellipses for prediction stations in the upper Delaware River, showing the topographic steering of the ellipses. Note that these are on a different scale than M2 in order to better visualize the ellipses. These data are at about 1/4 the scale of the M2 data.	85
Figure 66. S2 tidal ellipses for prediction stations in Delaware Bay, showing the topographic steering of the ellipses. Note that these are on a different scale than M2 in order to better visualize the ellipses. These data are at about 1/2 the scale of the M2 data.	86
Figure 67. S2 tidal ellipses for prediction stations in the lower Delaware River, showing the topographic steering of the ellipses. Note that these are on a different scale than M2 in order to better visualize the ellipses. These data are at about 1/2 the scale of the M2 data.	87
Figure 68. S2 tidal ellipses for prediction stations in the upper Delaware River, showing the topographic steering of the ellipses. Note that these are on a different scale than M2 in order to better visualize the ellipses. These data are at about 1/2 the scale of the M2 data.	88
Figure 69. Mean values for the tidal currents during maximum flood and ebb for near-surface bins at all stations in the lower Delaware Bay.....	89
Figure 70. Mean values for the tidal currents during maximum flood and ebb for near-surface bins at all stations in the lower Delaware River.	90
Figure 71. Mean values for the tidal currents during maximum flood and ebb for near-surface bins at all stations in the upper Delaware River.	91
Figure 72. GI timing of maximum flood (top) and ebb (bottom) at stations in the lower Delaware Bay. Note that the colors represent hours from 0 to 12.42 with the end interval limits having the same colors to represent the cyclical tides.....	92
Figure 73. GI timing of maximum flood (top) and ebb (bottom) at stations in the lower Delaware River. Note that the colors represent hours from 0 to 12.42 with the end interval limits having the same colors to represent the cyclical tides.....	93
Figure 74. GI timing of maximum flood (top) and ebb (bottom) at stations in the upper Delaware River. Note that the colors represent hours from 0 to 12.42 with the end interval limits having the same colors to represent the cyclical tides.....	94
Figure 75. Delaware Bay Operation Forecast (DBOFS) nowcast surface salinity practical salinity units (PSU) output on January 24, 2021, showing the salinity gradient from the mouth of the Bay (>30 PSU) that decreases moving upriver (~0 PSU).	96
Figure 76. Raw conductivity, temperature, and depth (CTD) sensor (YSI Castaway) vertical downcast at DEB2101 upon deployment (on July 15, 2021) of the acoustic Doppler current profiler (ADCP) and CTD platform. The subsurface ellipsoid ADCP buoy (SEABY) released early and drifted to shore, so a recovery CTD cast was not completed.....	97
Figure 77. Raw water temperature (top), conductivity (middle), and depth (bottom) data collected with an SBE37 conductivity, temperature, and depth (CTD) sensor at DEB2101. The data was trimmed to exclude the time period at the end of the deployment when the subsurface ellipsoid ADCP buoy (SEABY) released early and drifted to shore.....	98
Figure 78. Raw conductivity, temperature, and depth (CTD) sensor (YSI Castaway) vertical downcast at DEB2105 upon deployment (on September 14, 2021) and recovery (on November 3, 2021) of the acoustic Doppler current profiler (ADCP) and CTD platform.....	99
Figure 79. Raw water temperature (top), practical salinity (middle), and depth (bottom) data collected with an SBE37 conductivity, temperature, and depth (CTD) sensor at DEB2105.	100

Figure 80. Raw conductivity, temperature, and depth (CTD) sensor (YSI Castaway) vertical downcast at DEB2117 upon deployment (on July 21, 2021) and recovery (on November 5, 2021) of the acoustic Doppler current profiler (ADCP) and CTD platform. 101

Figure 81. Raw conductivity, temperature, and depth (CTD) sensor (SBE37) time series of water temperature (top), salinity (middle), and depth (bottom) collected at DEB2117. 102

Figure 82. Raw conductivity, temperature, and depth (CTD) sensor (YSI Castaway) vertical downcast at DEB2119 upon deployment (on July 21, 2021) and recovery (on November 5, 2021) of the acoustic Doppler current profiler (ADCP) and CTD platform. 103

Figure 83. Raw conductivity, temperature, and depth (CTD) sensor (In Situ Aqua TROLL) time series of water temperature (top), conductivity (middle), and pressure (bottom) collected at DEB2119..... 104

LIST OF TABLES

Table 1. Great diurnal tidal ranges (in meters) and Defant ratios for the current survey area..... 20

LIST OF APPENDIX TABLES

Table A1. Station location and deployment information. Measurements in meters (m)109

Table B1. Platform and sensor information. Stations not used for predictions are italicized. ADCP = acoustic Doppler current profiler. MLLW = mean lower low water. Measurements in meters (m).....111

EXECUTIVE SUMMARY

The National Oceanic and Atmospheric Administration (NOAA) National Ocean Service (NOS) Center for Operational Oceanographic Products and Services (CO-OPS) works to promote safe navigation throughout the U.S. waterways. As part of this effort, the CO-OPS National Current Observation Program (NCOP) acquires, archives, and disseminates information on tidal currents in the coastal U.S., which is used to update the NOAA tidal current predictions. Through oceanographic analysis and prioritization of stakeholder needs, CO-OPS identified the Delaware Bay and River (DEB) region as a location in need of updated tidal current predictions and for further study. Tidal current data are collected at new locations to help increase spatial coverage in tidal current observations and predictions, as well as through reoccupations of historical stations to update the observations and predictions with increased quality and accuracy. The data products generated are utilized by NOAA and the user community to help ensure safe navigation, make informed coastal zone management decisions, and support the protection of life and property. Furthermore, data collected can be used to inform the development of new hydrodynamic models or provide validation to existing ones.

This report summarizes the data collection and analysis completed by NCOP in the 2021 Delaware Bay and River Current Survey as well as the joint effort between NCOP and the Ocean System Test and Evaluation Program (OSTEP) at CO-OPS to complete the first operational deployment of the real-time CURrents BuoY (CURBY) in 2019 at Petty Island (db1935). In 2021, the first operational deployment of the SEABY (subsurface ellipsoid ADCP buoy) was also completed, and the platform was used at 5 stations.

A total of 35 stations were successfully deployed in 2021 for at least 1 lunar month (29 days). Currents were measured at each station with an acoustic Doppler current profiler (ADCP) moored with a configuration determined by factors such as station depth, seafloor composition, expected maritime activities, anticipated currents, and available inventory. Each ADCP was configured to collect data in evenly spaced ensembles of averaged velocity observations. These data include vertical or horizontal current profiles (speed and direction), water temperature, pressure, and additional quality control variables. These ensembles were typically 6 minutes (min). Of the 35 stations, 3 collected data for over 100 days. However, due to a variety of sensor or equipment failures, 4 stations (DEB2120, DEB2125, DEB2127, and DEB2136) collected either an insufficient duration of data (< 15 days) or data of quality too poor to generate reliable tidal current predictions. Currents were analyzed for tidal constituents using harmonic analysis of the velocity time series data collected by the ADCP. Tidal current predictions for 32 stations (including db1935) were made available online via the CO-OPS Tides and Currents website (NOAA Current Predictions).

Concurrent with each deployment and recovery of an ADCP, a vertical conductivity-temperature-depth (CTD) profile was taken to ascertain the physical properties of the seawater at the approximate location of each station. Additionally, CTDs were deployed at a single depth co-located with 6 of the ADCP stations, 1 SeaBird SBE 35 with the 2019 CURBY station, and 5 at ADCP stations in 2021. These provided a time series of water temperature, salinity, and pressure data that will be useful to the research and modeling community. These instruments were part of ongoing coordination with OSTEP to test the Aqua TROLL 200 CTD manufactured by In-Situ, which is a cheaper, smaller, and lighter alternative to the SeaBird CTD that NCOP has traditionally used.

1.0 INTRODUCTION

The National Ocean Service (NOS) Center for Operational Oceanographic Products and Services (CO-OPS) manages the National Current Observation Program (NCOP). The program's primary goal is to improve the quality and accuracy of tidal current predictions. Improving this information is a critical part of the NOS's efforts toward promoting safe navigation in our Nation's waterways. Mariners require accurate and dependable information on the movement of the waters in which they navigate. As increasingly larger ships use our ports and as seagoing commerce continues to increase, there is an increased risk to safe navigation in the Nation's ports (NOAA 2018). CO-OPS acquires, archives, and disseminates information on tides and tidal currents in U.S. ports and estuaries, a vital NOS function since the 1840s. The main source of this information for the public is the CO-OPS Tides and Currents website (NOAA Current Predictions). The National Oceanic and Atmospheric Administration (NOAA) previously published Tidal Current Tables annually as required by the Navigation and Safety Regulations section of the U.S. Code of Federal Regulations (Charts and Publications 2022). NOAA discontinued the production of these tables in 2020 due to changes in paper carriage requirements as set forth by the U.S. Coast Guard (2016), and the predictions are now digitally available and accessible through NOAA. Both the collection and analysis of current observations, as well as the dissemination of the data, fall under the authority of the Navigation and Navigable Waters title of the U.S. Code (Dissemination of data 2021).

The flow dynamics of an estuary or tidal river can be modified by changes in natural factors, such as land motion and other morphologic changes, or through man-made alterations, such as the deepening of channels by dredging, harbor construction, bridge construction, the deposition of dredge materials, and the diversion of river flow. Changes in water flow and tidal dynamics can affect the accuracy of tidal current predictions; therefore, new data must be collected periodically to ensure that predictions remain reliable and are adjusted when necessary.

CO-OPS has developed expertise in deploying current profilers throughout the Nation's coastal waters via the NCOP program. These data are used for a number of products. In addition to updating existing tidal current predictions and establishing new tidal current prediction locations (Fanelli et al. 2014), data collected through this program are used by NOAA and the user community in the production and refinement of other products, such as the validation of hydrodynamic forecast systems (Lanerolle et al. 2011) and integration into commercial navigation software. These products are used to ensure safe navigation, make informed coastal zone management decisions, and protect life and property.

The data described in this report were collected by NCOP at a total of 36 stations, including 1 station occupied from July-October 2019 (Figure 1) and 35 stations occupied from May-October 2021. Of the 35 stations deployed in 2021, 31 were occupied for at least 1 lunar month (29 days), sufficient to complete a harmonic analysis and generate reliable tidal current predictions. The remaining 4 stations (DEB2120, DEB2125, DEB2127, and DEB2136) collected insufficient data. DEB2125 had unusable data due to a corrupted compass matrix and significantly high pitch values that exceed the manufacturer's recommendation for quality velocity data. DEB2136 was co-located with DEB2125 with the intention of testing a modified mount on a smaller diameter aid to navigation (ATON) buoy in an effort to expand the available platforms for future NCOP and Physical Oceanographic Real-Time System (PORTS[®]) stations, and it only collected 8 days of good data. DEB2120 was dragged and buried, limiting the good data to only the first 10 days of the deployment. DEB2127 had equipment mounting failures likely due to impacts from marine debris floating subsurface and only collected less than 2 days of good data. DEB2111 had equipment mounting failures for the same reason and collected 16 days of good data, which allows

for a custom analysis but does not meet the typical requirement of 33 days of data collection for the standard analysis. An acoustic Doppler current profiler (ADCP) was lost at DEB2132 due to a recreational vessel allision with the ATON; however, this station was still occupied in the second half of the survey, collecting sufficient data to generate predictions. Figure 2 shows the number of good days of data at each station. These data include vertical (35 stations) or horizontal (only at DEB2123) current profiles (speed and direction), water temperature, pressure, and additional quality control variables. Currents were analyzed for tidal constituents using harmonic analysis of the velocity time series data collected by the ADCP.

Conductivity, temperature, and depth (CTD) sensors were deployed co-located with 6 of the ADCP stations in an effort to support the research and modeling community (Figure 3). One of the 6 stations was the Currents Real Time Buoy (CURBY) deployment (db1935) in 2019, and the other 5 deployments occurred in 2021. The CTDs recorded a time series of water temperature, salinity, and depth measurements at a single vertical location aligned with the ADCP. Stations were chosen based on internal modeling needs to help resolve the salinity gradient near the mouth of the Bay and on external needs of partners at the U.S. Geological Survey (USGS) analyzing the drinking water clarity farther upriver. In coordination with the Ocean System Test and Evaluation Program (OSTEP), In-Situ Aqua TROLL CTDs—which are a cheaper, smaller, and lighter alternative sensor to the SeaBird instruments that NCOP traditionally has used—were tested and used in some deployments.

Additionally, an external pressure sensor was deployed at 1 station near the mouth of the Bay on a fixed anchor (Figure 3). These data will be used in comparison with the ADCP pressure sensor that was mounted on the subsurface ellipsoid ADCP buoy (SEABY). The analysis of the difference in pressure between the 2 sensors allows better understanding of the buoy motion and evaluation of equipment performance for the platforms tested in conjunction with OSTEP.

All of the data and analysis presented herein are available on the Tides and Currents website (<https://tidesandcurrents.noaa.gov/>) or by contacting CO-OPS (Tide.Predictions@noaa.gov).

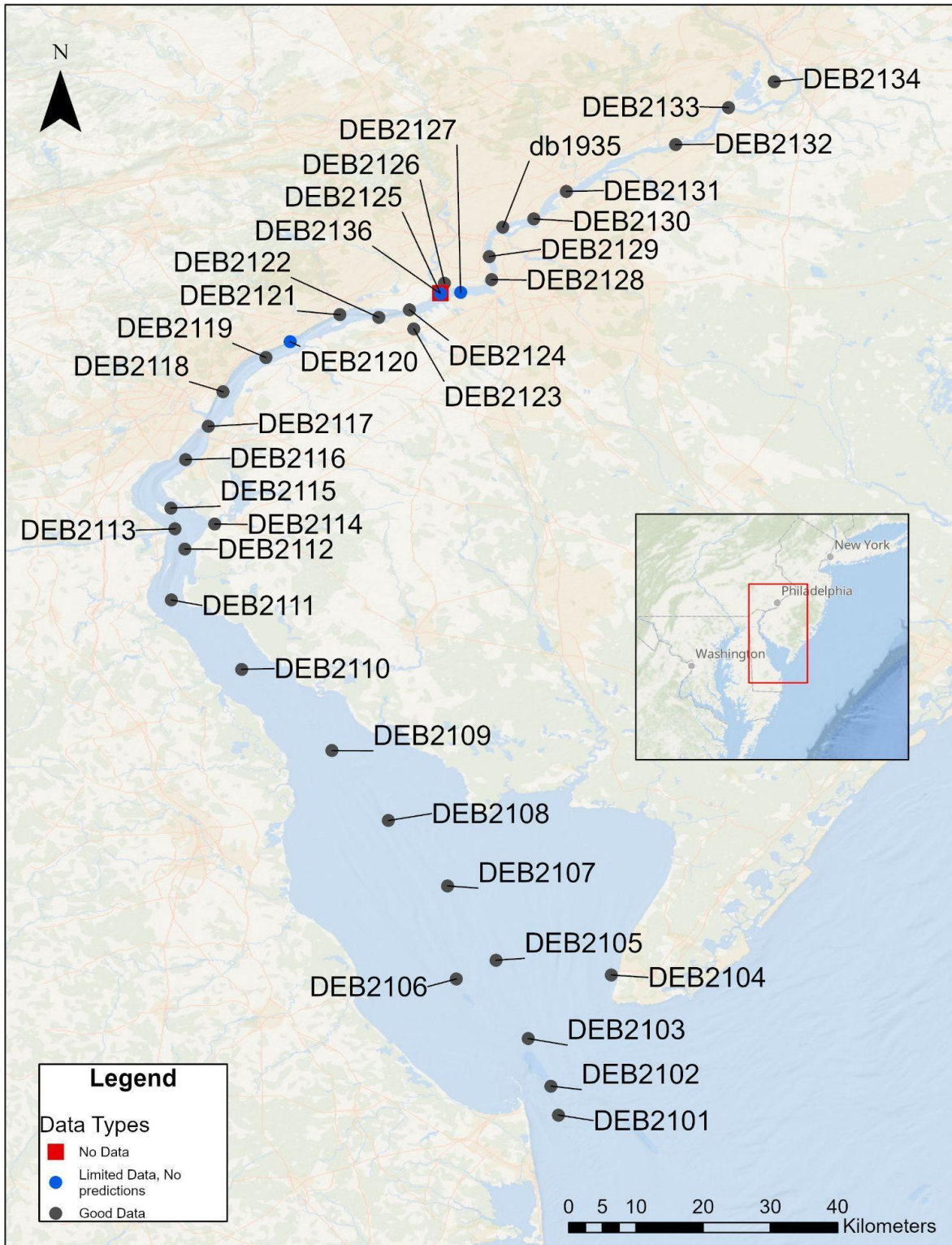


Figure 1. All stations deployed in the Delaware Bay and River (DEB) in 2019 (db1935) and 2021 (DEB21XX). Stations that had equipment or sensor failures limiting the days of good data to be less than 15 days are indicated by a blue circle. Stations where data was collected but was unusable due to an issue with the compass matrix are indicated by a red square. All other stations collected good data and are indicated by a gray circle.

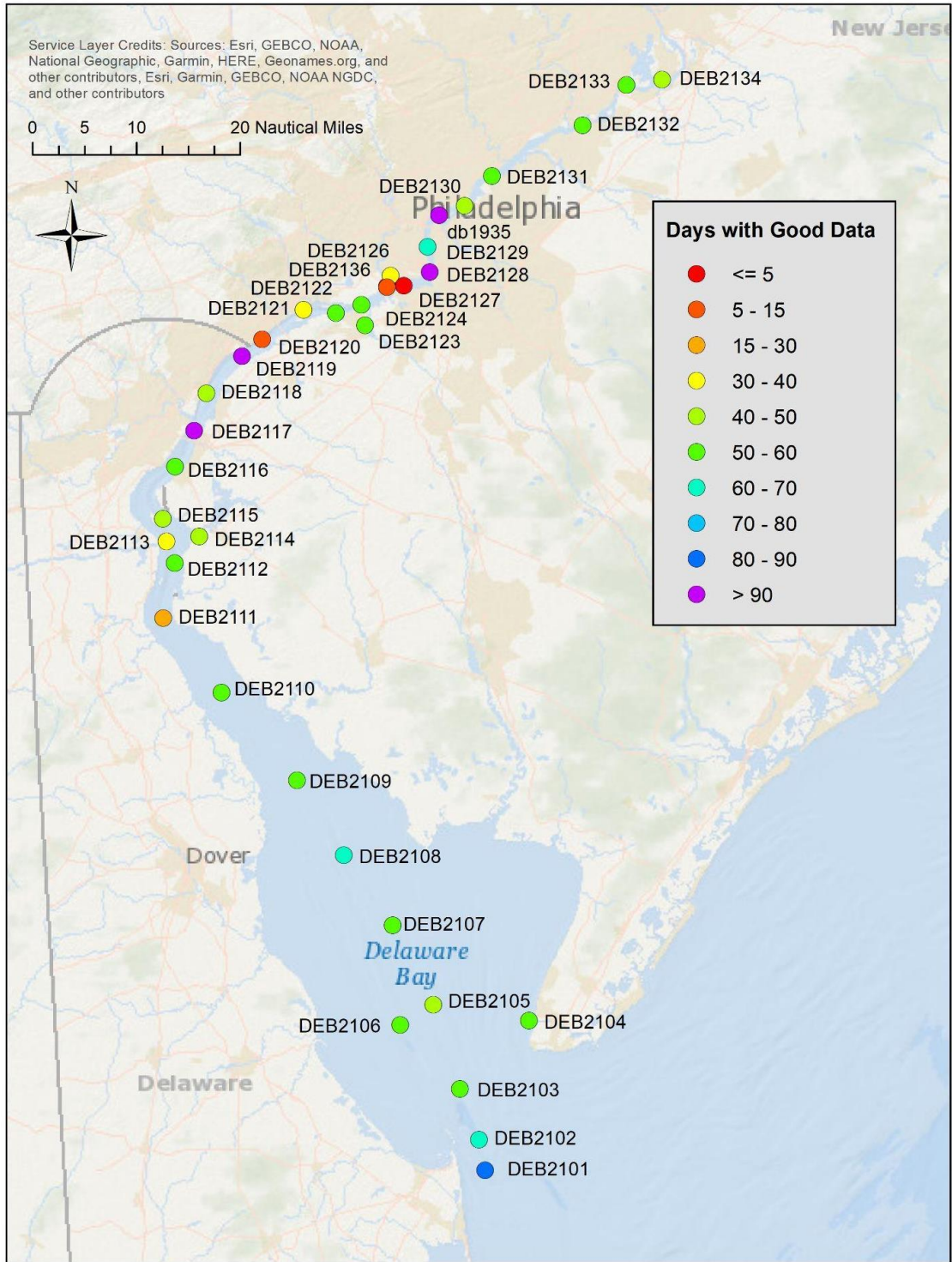


Figure 2. All stations deployed in the Delaware Bay and River (DEB) in 2019 (db1935) and 2021 (DEB2101-DEB2136). The colors represent the number of days of good data collected at each station. Stations with less than 15 days of good data were not used to generate new predictions.

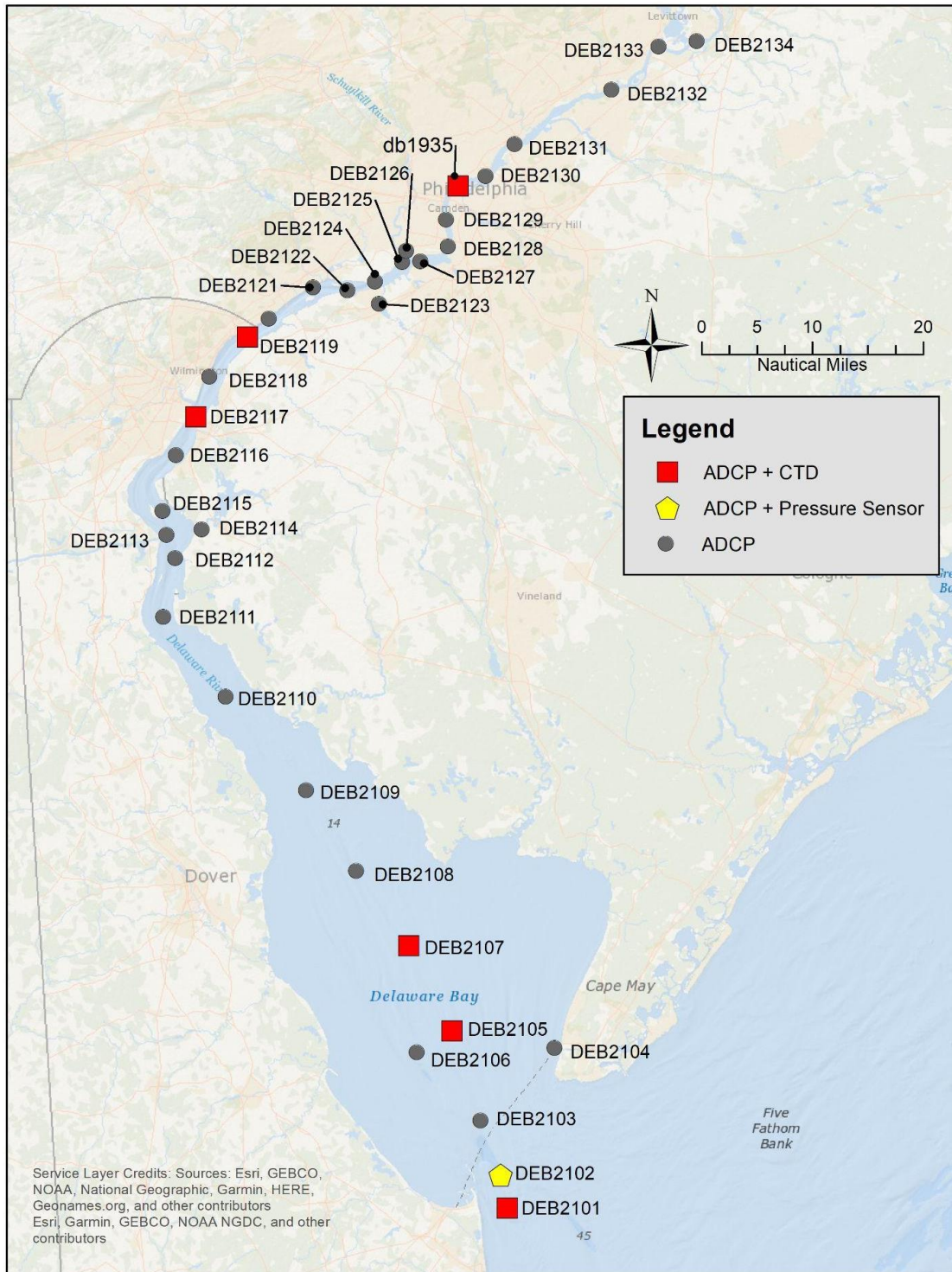


Figure 3. Current survey stations categorized by sensors deployed collecting time series data: gray circles represent acoustic Doppler current profiler (ADCP)-only stations; red squares represent stations with a conductivity, temperature, and depth (CTD) sensor co-located with the ADCP; and the yellow pentagon represents an external

pressure sensor co-located with the ADCP. All stations were deployed in 2021 with the exception of db1935, which collected data in 2019.

2.0 PROJECT DESCRIPTION

The Delaware Bay and River (DEB) region was identified by an internal assessment (Fanelli et al. 2014) as a top-10 high priority region in need of updating predictions with an NCOP project utilizing modern oceanographic equipment. This assessment took into account information such as the number of vessel accidents (15 as of 2006), average tidal current (0.59 m/s), fish tonnage (43.1 million pounds as of 2010), commercial tonnage (89,509,200 short tons as of 2010), and approximate year of last survey (1985). Major seaports along the Delaware River include Philadelphia, PA (ranked #25 by tonnage in the U.S.; USACE 2018), Paulsboro, NJ (#39), Marcus Hook, PA (#44), Wilmington and New Castle, DE (#64 and 65, respectively), and Camden, NJ (#74). These ports serve a population of approximately 8.6 million people living in the Delaware Estuary and Basin as of 2020 (Technical Report for the Delaware Estuary and Basin 2022). The Delaware River ports were rated 22nd in the top container port rankings in North America (The Top 25 Container...2017).

The most recent NOS current survey in the Delaware River and Bay began in 1984, lasted 15 months, and included 43 stations, 1 of which was the Delaware Bay Entrance reference station (ACT4071) that was occupied for 221 days. The NOS Delaware Bay reference station at Brandywine Shoal Light, 0.5 nautical miles (nm) west of (ACT4131), was originally occupied in 1916 for 29 days, and the predictions were later revised in 1943. The majority of the subordinate stations in the region were based on data collected over short time periods (5-10 days) in the 1920s and 1940s (Figure 4). Since 1985, CO-OPS has deployed several current meters in the Bay to test mooring and mounting designs, the results of which include updating the harmonic reference station at the entrance of the Bay (DEB0002). There have been a total of 6 PORTS[®] currents stations that were deployed as early as 2002. Of these 6 PORTS[®] stations, 2 are still active: Delaware Bay Channel LB10 (db0502) near the mouth and Philadelphia (db0301).

NOAA's Delaware Bay Operational Forecast System (DBOFS) was put into operation in 2012, and the model domain spans the current survey area and includes 10 vertical levels. The currents data as well as the CTD observations collected both in the 2019 field reconnaissance and the deployment and recovery of the current meters in 2021 help support DBOFS model validation and the development of new models. The Delaware River Basin is the first location in which USGS piloted its Next Generation Water Observing System (NGWOS) program, which uses advanced modeling to predict water quantity and quality. The data collected in the reconnaissance and survey was also shared with USGS to support their NGWOS model development and validation efforts.

Captains from the Delaware River and Bay Pilots' Association requested updated tidal current predictions at the historic Petty Island station just north of Philadelphia. In response to this request, the first operational deployment of CURBY was completed from July-October 2019 at this site (db1935). Based on a harmonic analysis of the buoy data, the tidal current predictions at this historic station were updated in the January 2020 Tidal Current Table quarterly update. The recent observations were also compared to the historic predictions and the DBOFS nowcast output at a nearby location and depth. The results were presented at the American Meteorological Society Conference in a Precision Navigation session in January 2020. More detailed explanation of the CURBY buoy performance along with the data results are described in Fiorentino et al. (2022).

The U.S. Army Corps of Engineers (USACE) completed the Delaware River Main Channel Deepening project in February 2020 (USACE 2021). This project involved deepening the federal navigation channel from 12.2 meter (m; 40 feet [ft]) to 13.7 m (45 ft) over 160 km (100 m), extending from the mouth of the Bay up through Philadelphia and Camden. Updating the tidal

current predictions based on data collected in 2021 is timely given that the bathymetric changes will likely impact the historic tidal current directions and speeds.

Initial site locations were proposed based upon the internal needs and capabilities of NOAA. Additional station recommendations were provided through meetings and correspondence with stakeholders, including professional mariners and federal, state, and local partners, as well as academics and researchers. The final survey study was conducted by incorporating oceanographic needs, engineering restrictions, and criteria set forth by the International Hydrographic Organization (IHO 2008). As an example of the type of criteria used for site selection, Figures 5-7 show maps of ship traffic density from automatic identification system (AIS) ship tracks (data retrieved from Vessel Traffic). Traffic density is a key determination of current meter placement.

In 2019, a reconnaissance was conducted to gather information about the physical characteristics of proposed sites. This reconnaissance provided the necessary information for exact locations, platform engineering, and instrument frequencies for the proposed stations. All proposed sites were visited to gather data about their physical characteristics such as depth, bottom type, and vertical profiles of water temperature and salinity. This information was then used to plan the platform and sensor configurations for each current observation station. During reconnaissance operations, each site was visited using a vessel equipped with a fathometer to determine the depth of the site, a CTD sensor to determine salinity and water temperature, and a Ponar-style bottom sampler to determine the nature of the seabed at the site (e.g., mud, silt, sand). Based upon the reconnaissance, 34 deployment locations were identified, which were occupied using methods described in section 3. This technical report focuses on the results of these ADCP current meter deployments.

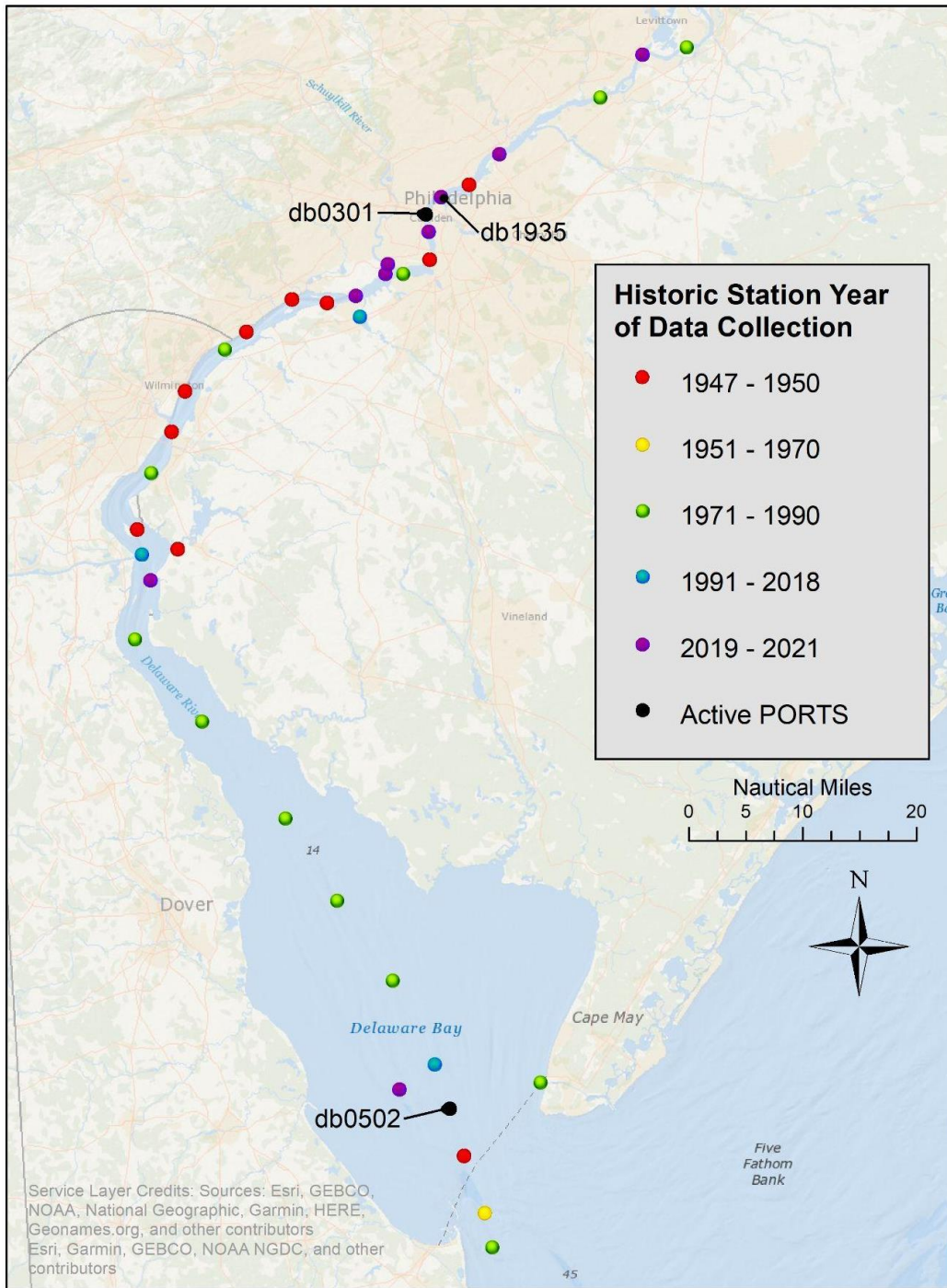


Figure 4. The current survey stations color coded by the year data was last collected on site which was used to generate predictions at the historic stations. The black circles represent the active Physical Oceanographic Real-Time Systems (PORTS[®]) current meter stations (db0502 and db0301). The Currents Real Time Buoy (CURBY) deployment (db1935) was completed in 2019 as part of the current survey. Purple circles represent new stations occupied in 2021 where a historic station did not previously exist.

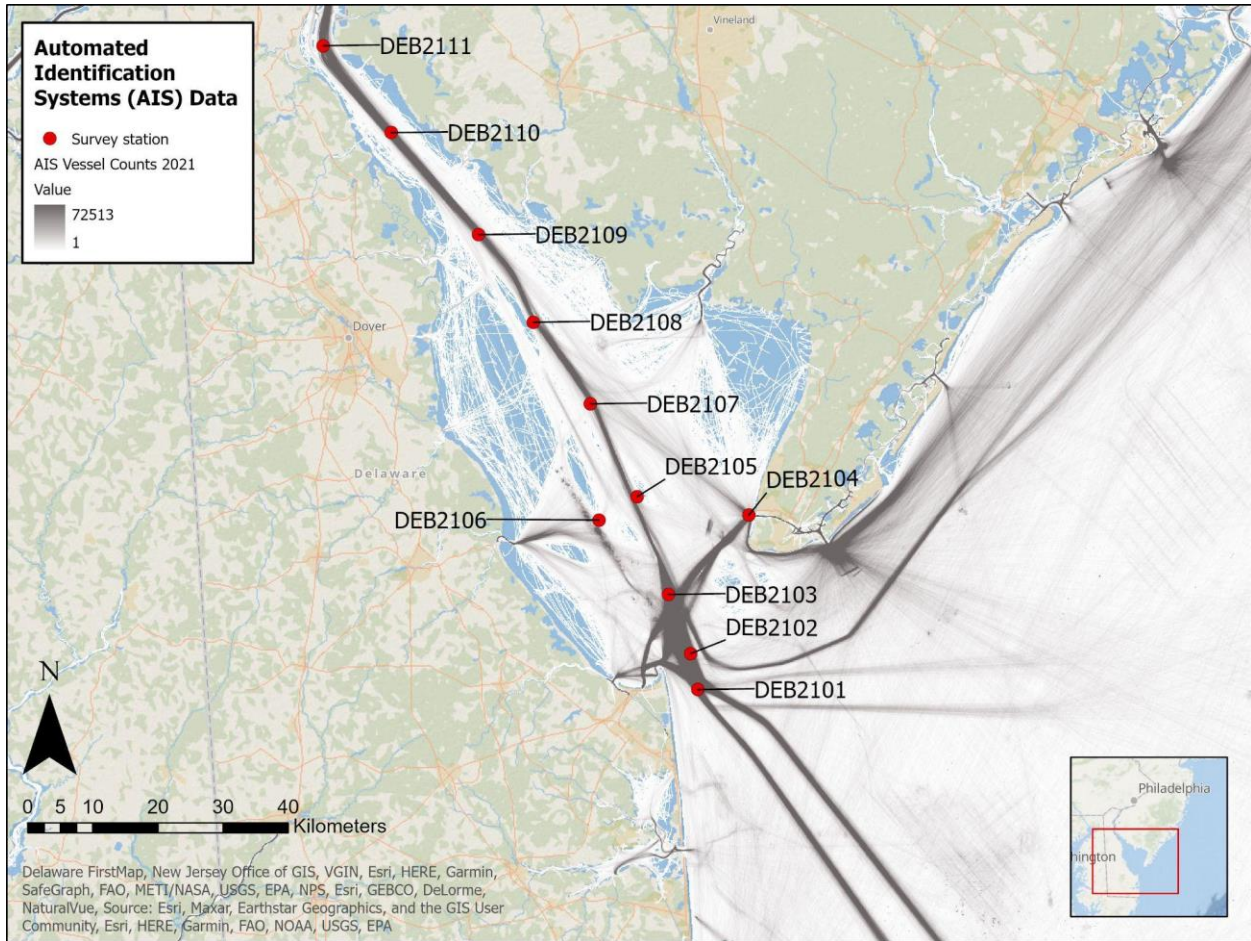


Figure 5. Lower Bay view of automatic identification system (AIS) tracks (from Vessel Traffic Data) for all vessels in the Delaware Bay, River, and vicinity. Current survey stations are represented by red circles.

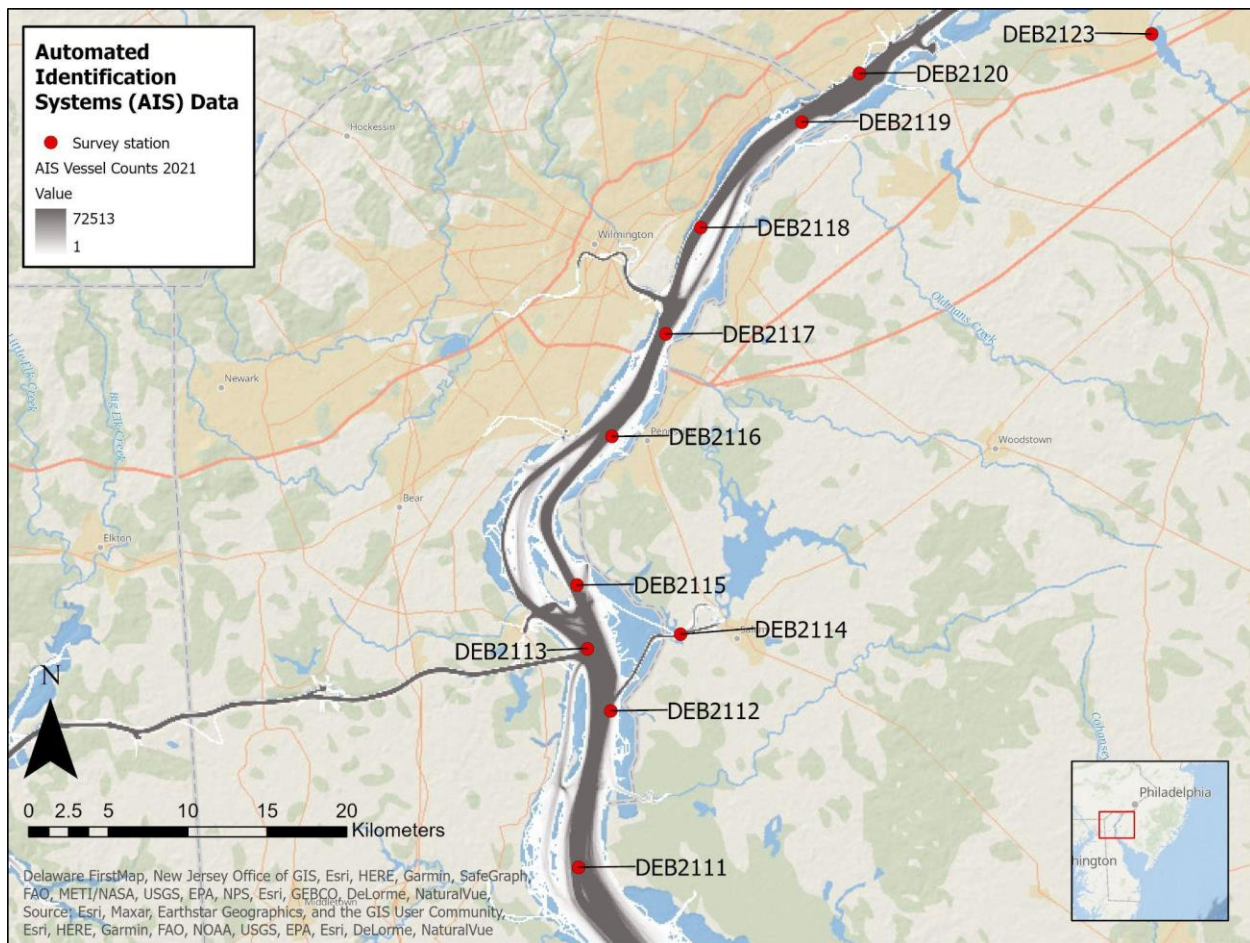


Figure 6. Mid-River view of automatic identification system (AIS) tracks (from Vessel Traffic Data) for all vessels in the Delaware Bay, River, and vicinity. Current survey stations are represented by red circles.

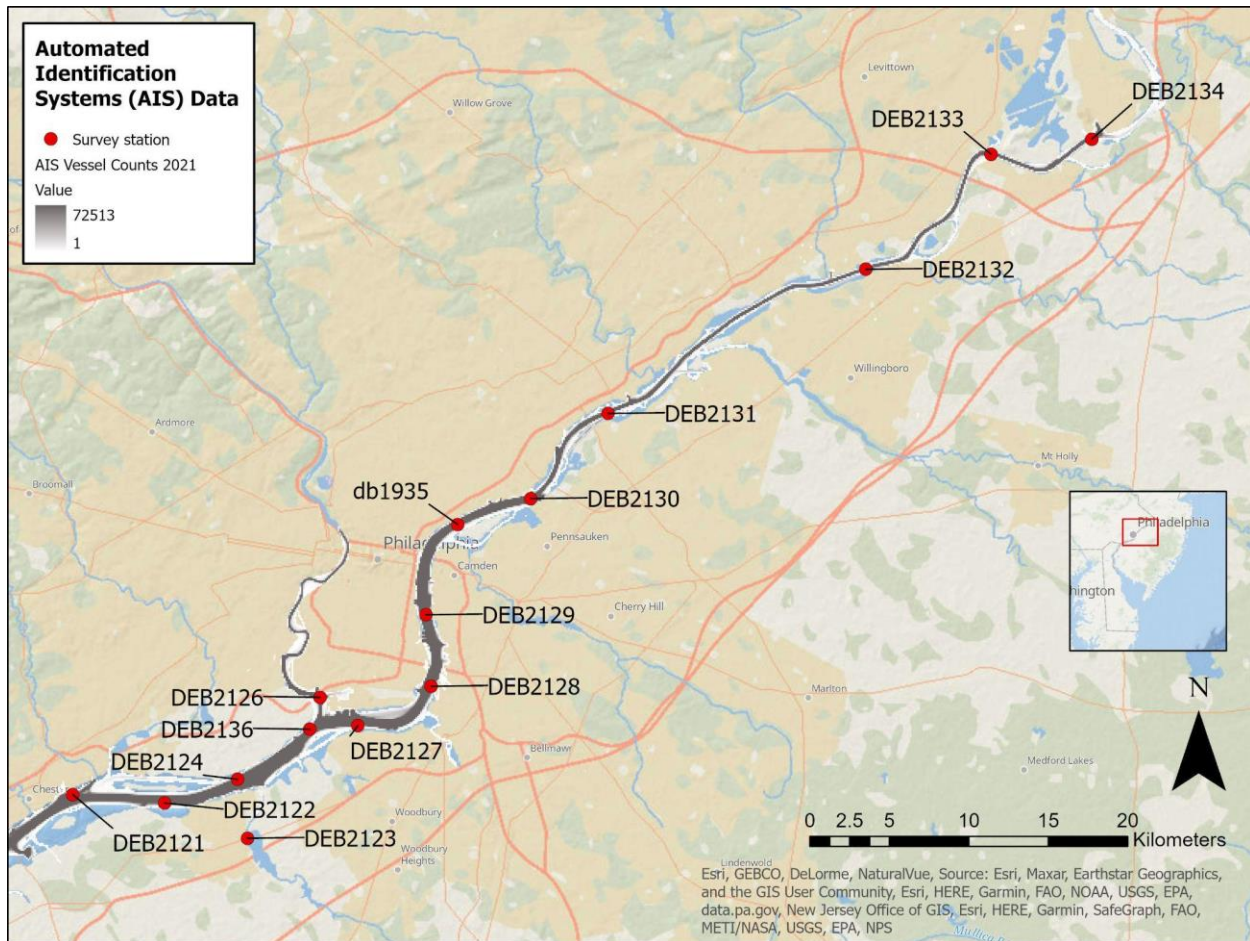


Figure 7. Upper River view of automatic identification system (AIS) tracks (from Vessel Traffic Data) for all vessels in the Delaware Bay, River, and vicinity. Current survey stations are represented by red circles.

2.1 Geographic Scope

Located within the Mid-Atlantic Bight along the U.S. eastern coast, the greater oceanographic region in this study is formally known as the Delaware Bay Estuary. The geographic scope of this project extended over 200 km from the mouth of the Delaware Bay where water flows into the Atlantic Ocean between Cape Henlopen in Delaware and Cape May in New Jersey up to nearly the tidal limit of the Delaware River in Trenton, NJ (Klavans et al. 1986).

2.2 Physical Oceanographic Overview

Delaware Bay is a drowned river valley with a progressive tidal wave and is classified as a partially- to well-mixed estuary depending on location within the Bay (more stratified and partially mixed) or River (well mixed; Klavans et al. 1986; Valle-Levinson 2010). This is evident in the salinity data discussed in Section 6.3. The primary source of freshwater into the Bay flows from the Delaware River at Trenton (51%) and the Schuylkill River (15%) near Philadelphia (Klavans et al. 1986).

Due primarily to the shape of the estuary, the tidal amplitude increases upstream as seen in Figure 8 showing the great diurnal tidal range (in meters), which is the difference in height between mean higher high water (MHHW) and mean lower low water (MLLW). High water propagates from the mouth of the Bay upstream to Trenton over approximately 7 hours while it takes approximately 8 hours for low water to return to the mouth (Klavans et al. 1986).

Tides and tidal currents are semidiurnal, as determined by their Defant ratio (Table 2.1), which is defined as: $(K1 + O1) / (M2 + S2)$ and discussed in sections 5 and 6. This ratio is used to define the nature of the tide as it changes from strict semidiurnal to strict diurnal: for a Defant ratio less than 0.25, the tides are semidiurnal; for a Defant ratio between 0.25 and 1.5, the tides are mixed, primarily semidiurnal; for a ratio between 1.5 and 3.0, the tides are mixed but mostly diurnal; and for a ratio greater than 3, the tides are diurnal (Defant 1958).

This report focuses on the tidal forcing of the currents; non-tidal currents are primarily driven by winds and density-driven mixing between fresh and saltwater masses (Klavans et al. 1986). The gravitational flow is modified by Coriolis and frictional drag from both the seafloor roughness and shoreline irregularities (Klavans et al. 1986).

Table 1. Great diurnal tidal ranges (in meters) and Defant ratios for the current survey area.

Station ID	Station Name	Great Diurnal Range (m)	Defant Ratio
8537121	Ship John Shoal, NJ	1.8920	0.2039
8551910	Reedy Point, DE	1.7790	0.1814
8555889	Brandywine Shoal Light, DE	1.6760	0.2284
8557380	Lewes, DE	1.4180	0.2643
8536110	Cape May, NJ	1.6590	0.2271
8540433	Marcus Hook, PA	1.8800	0.2109
8545240	Philadelphia, PA	2.0390	0.2017
8538886	Tacony-Palmyra Bridge, NJ	2.1790	0.1800
8539094	Burlington, Delaware River, NJ	2.3930	0.1718
8548989	Newbold, PA	2.5580	0.1646

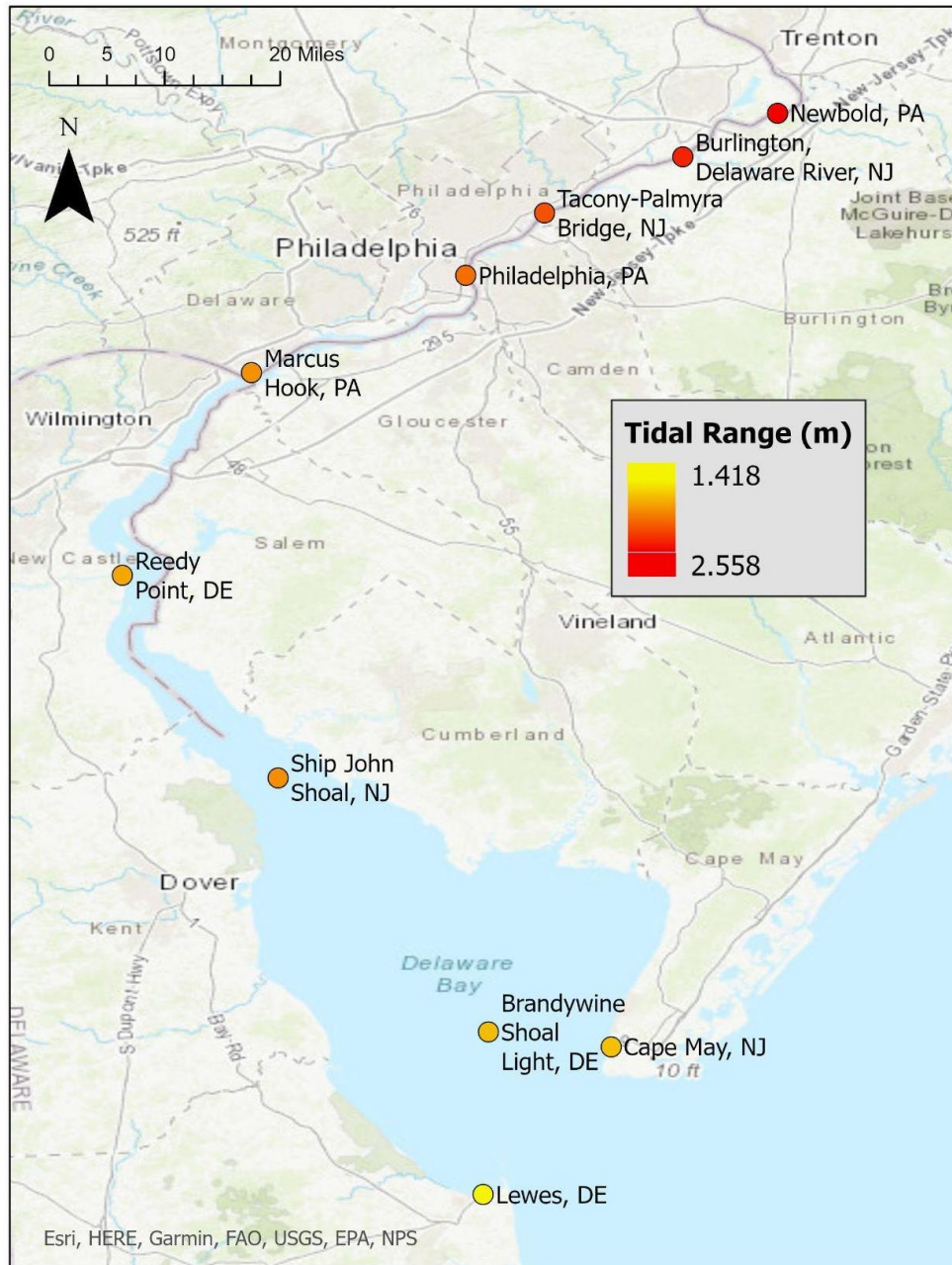


Figure 8. The great diurnal range of tidal height (meters) throughout the current survey area.

3.0 METHODS

All on-water operations were conducted using the NOAA-owned research vessel (*RV*) *Tornado* (Figure 9), a 7.6-m (25-ft) pilothouse-style boat manufactured by Parker that has a lifting capability up to 135 kg. Operations consisted of deploying a calibrated ADCP in an appropriate platform at each station location and recovering it after the planned station occupation period (Table A1 and Table B1). For each station deployment and recovery, the water depth from the vessel’s fathometer was recorded, and a CTD vertical profile was taken using a YSI CastAway® CTD to ascertain physical properties of the seawater such as the actual speed of sound in the water—which is used to double-check the speed of sound used by the acoustic instrument—at the approximate location of each station. All station metadata were recorded on station log sheets. For

each station, the ADCP instrument's internal compass was calibrated after the batteries were installed. Calibrations were performed to manufacturers' specifications before the deployment for bottom-mounted ADCPs or after the instrument was mounted to the side of a U.S. Coast Guard (USCG) ATON for mounted ADCPs. No compass calibration was conducted on the side-looking ADCP, as it collects data relative to the direction of the instrument (X-Axis, Y-Axis, and Z-Axis) and not in Earth directional coordinates (East, North, Up [ENU]). However, detailed looking directional measurements were made to determine the orientation of the side-looking ADCP relative to Earth.



Figure 9. The NOAA *R/V Tornado* (7.6-meter [25-foot] Parker) equipped with a davit used for operations in the Delaware Bay and River.

3.1 Description of Instrumentation and Platforms

At each station, the ADCP was mounted in either a bottom-mounted platform for upward-facing measurements, on a surface platform (i.e., ATON or CURBY) for downward-facing measurements, or attached to a fixed structure for side-looking (horizontal) measurements (Figures 10-12; Table B1).

Currents were measured at each station using an ADCP with a platform configuration determined by factors such as station depth, seafloor composition, expected maritime activities, anticipated currents, and available instrument and platform inventory. All stations were equipped with one of the following: a Teledyne RD Instruments (TRDI) Workhorse Sentinel with frequencies of 600 kHz or 1200 kHz, or a Nortek Aquadopp (AqD) with frequencies of 600 kHz, 1000 kHz, or 2000 kHz (Table B1). The maximum distance of an ADCP profile is a function of the instrument frequency, with lower frequency instruments capable of longer profiles. The

instrument frequency for each station was therefore determined primarily by calculating the distance within the water in which current measurements were desired. For vertical profiling (i.e., bottom mounts, ATONs, CURBY), this distance is the depth of the water column below the MHHW tidal datum plus an added range buffer to account for uncertainties in depth and potential significant events (Table B1). For side-looking profilers, this distance is intended to reach at least the center of the navigational channel when possible.

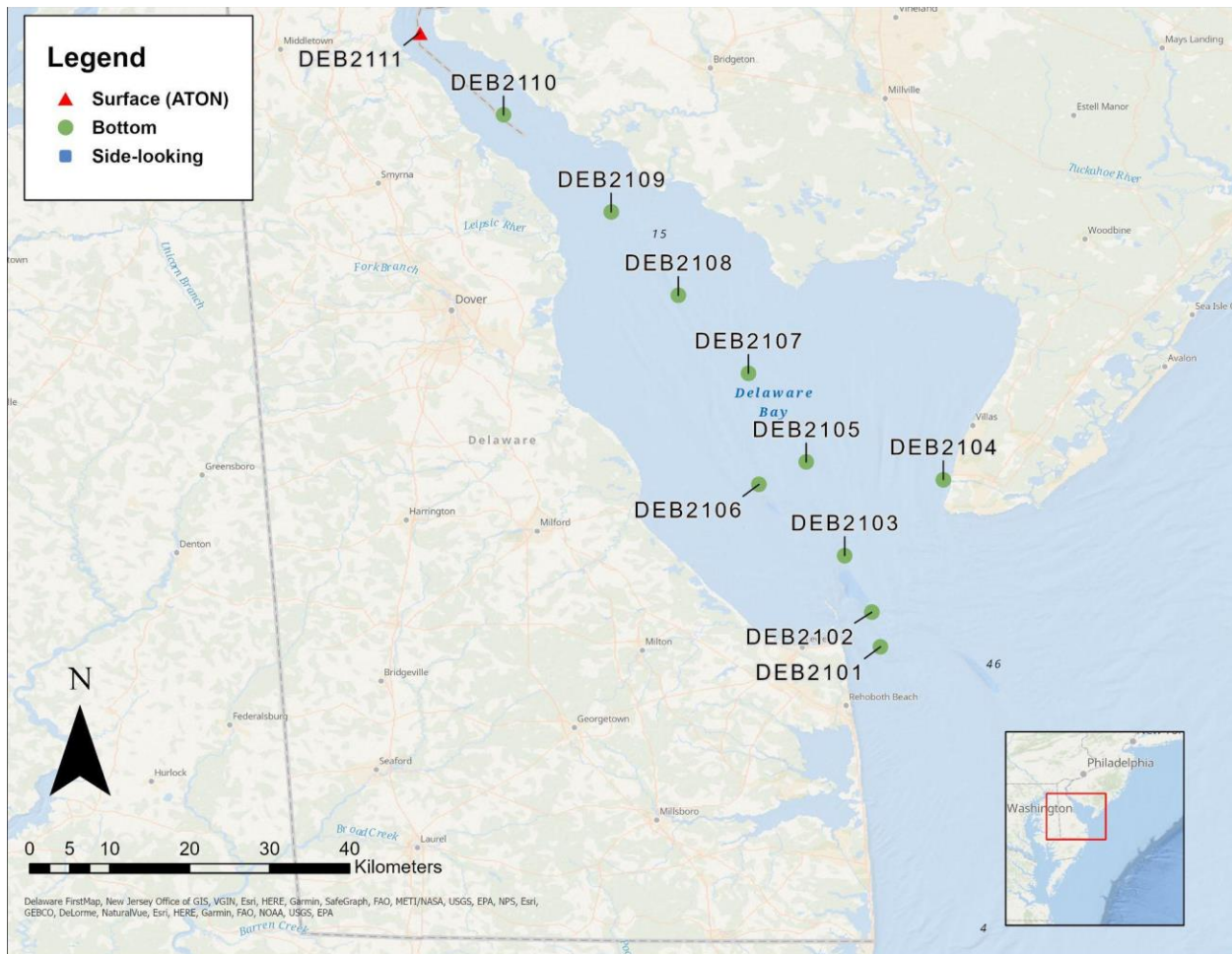


Figure 10. Mount types for stations in the lower Bay: surface (red triangle), bottom (green circle), and side-looking (blue square).

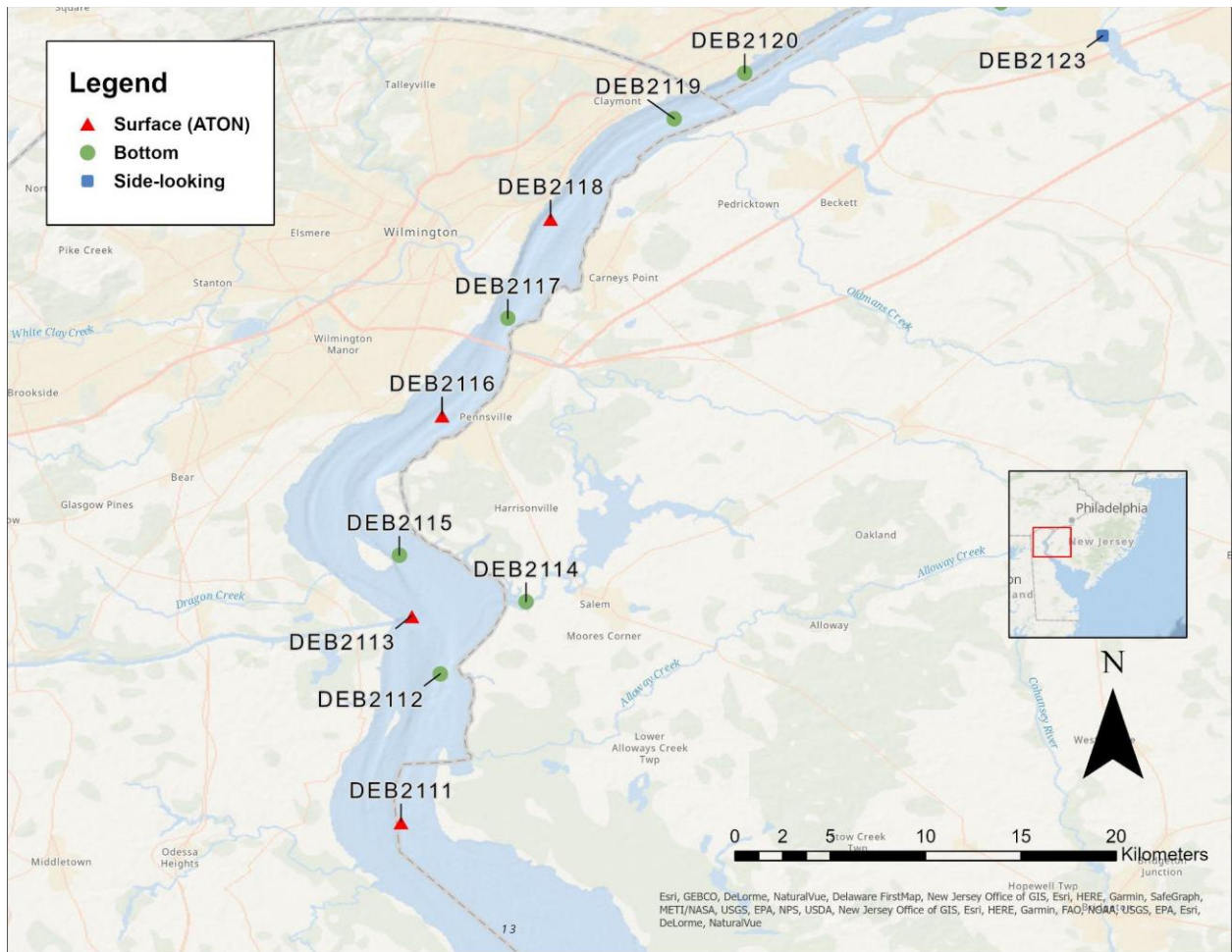


Figure 11. Mount type for stations in the lower River: surface (red triangle), bottom (green circle), and side-looking (blue square).

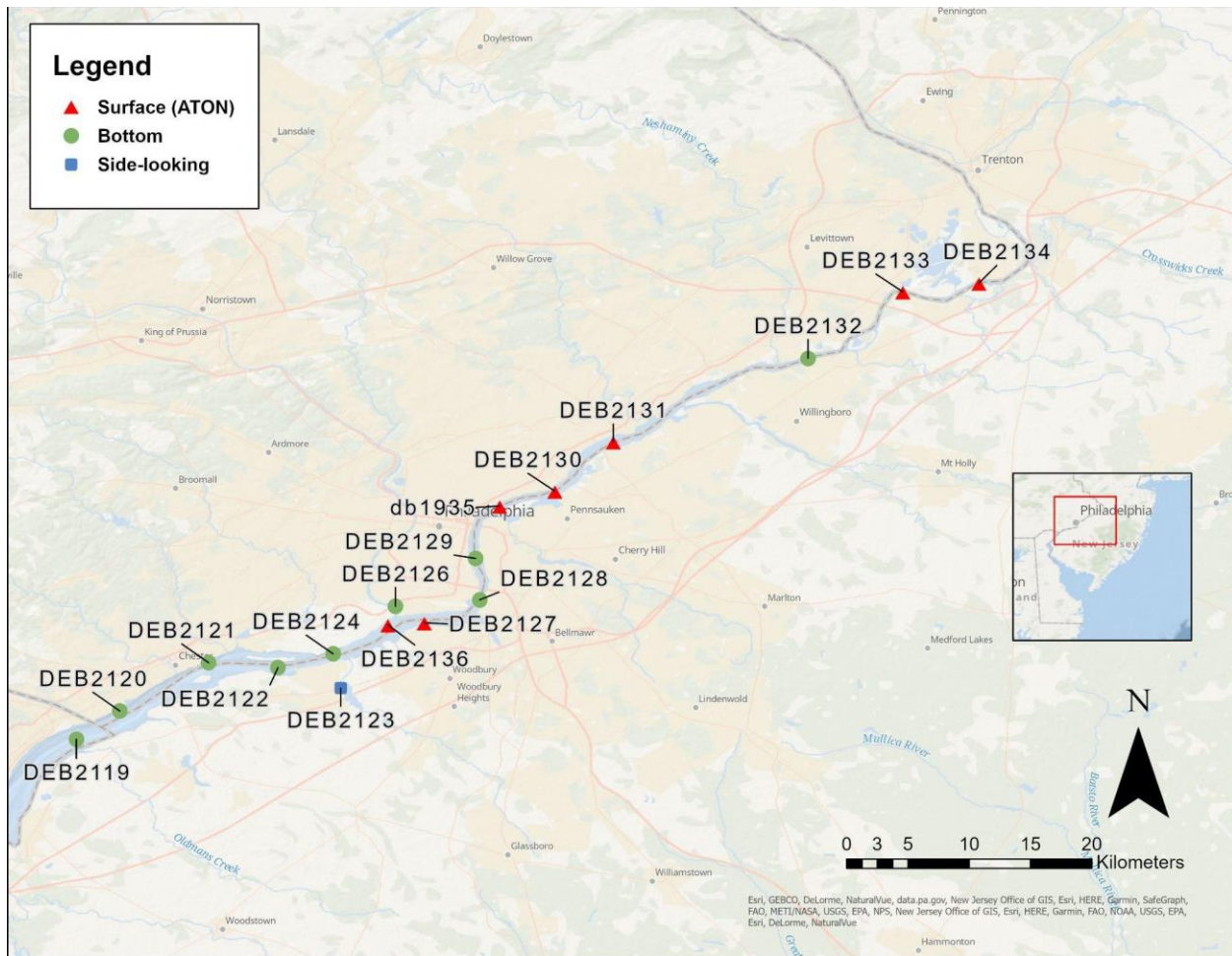


Figure 12. Mount type for stations in the upper River: surface (red triangle), bottom (green circle), and side-looking (blue square).

3.1.1 Bottom Mounts

Bottom mounts are designed to rest on the seafloor and provide a stable platform for an upward-facing ADCP during station occupation. Gimbals are used to keep ADCPs vertical on all bottom mounts except for fiberglass grates. All bottom-mounted platforms were positioned on the seafloor with no surface presence. Stations were recovered by either activating an acoustic release or by a ground dragline. In the event that an equipped acoustic release failed to work properly, a secondary means of recovery (such as dragging) was employed. Bottom-mount platforms used during this project were either manufactured by Mooring Systems, Inc. (MSI) or DeepWater® Buoyancy (previously Flotation Technologies), or they were purpose-built by engineers at NOAA (Figures 13-15).

The SEABY is a subsurface taut-line mooring that allows for the recovery of the anchor that is typically left behind with other acoustic release systems. The ellipsoid buoy holds the upward-facing ADCP and is attached to the acoustic release and anchor system with a taut wire line (Figure 13). The taut wire cable allows for an in-line CTD to be attached, as it was at DEB2101. The first operational deployment of the SEABY occurred in the Delaware Bay in 2021, and it was used at 5 stations. The SEABY is deployed with a quick release and sinks to the bottom. The acoustic release allows for the recovery of the ellipsoid buoy and ADCP first, followed by the anchor tethered to the buoy.



Figure 13. Subsurface ellipsoid acoustic Doppler current profiler (ADCP) buoy (SEABY). The ellipsoid buoy holds the upward-facing ADCP and is attached to the acoustic release and anchor system with a taut wire line.



Figure 14. Mooring Systems, Inc. (MSI) H-TRBM-35 and H-TRBM-48 (formerly GP35 and GP48), which differ in diameter. The bottom mount holds an upward-facing acoustic Doppler current profiler (ADCP) and is lowered to the bottom to deploy and recovered with a grapnel that is dragged to snag the ground line connecting the mount to an anchor. Specifications for the mount of both sizes are here: <https://www.mooringystems.com/mounts.htm> (Image from MSI.)

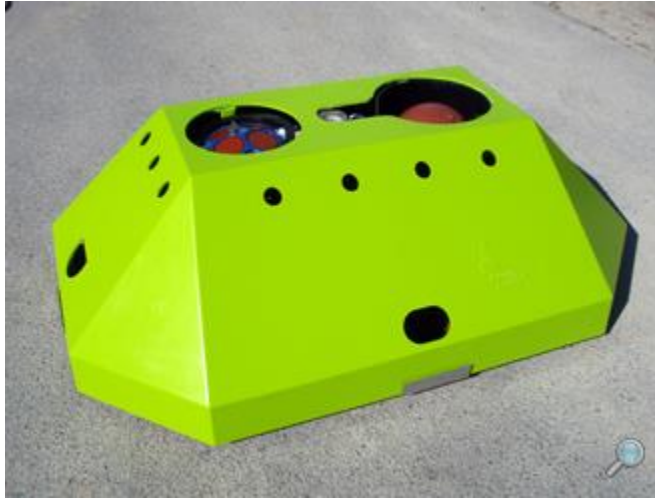


Figure 15. Mooring Systems, Inc. (MSI) GP-TRBM (formerly mTRBM). The bottom mount holds an upward-facing acoustic Doppler current profiler (ADCP) and acoustic release system. The mount is lowered to the bottom for deployment and recovered by acoustically releasing to the surface a float that is tethered to the bottom mount. If the acoustic release fails, a grapnel is used to drag and snag the ground line connecting the mount to an anchor. Specifications for the mount are here <https://www.mooringsystems.com/mounts.htm>. (Image from MSI.)

3.1.2 Horizontal Mount

One station (DEB2123 [Mantua Creek US 44 Bridge Paulsboro]) was occupied using a side-looking ADCP mounted to the bridge cribbing using clamps and a pole (Figure 16). This mount was designed and built by NOAA. The ADCP is held in the mount by a clamp and oriented to collect data across the channel.



Figure 16. Bridge cribbing side-looking mount (left). Side-looking acoustic Doppler current profiler (ADCP) deployed in the bridge cribbing mount (right).

3.1.3 Surface Mounts

ATON-mounted ADCPs can observe currents in or adjacent to navigational channels where bottom mounts are impractical or not allowed. For NCOP operations, an Oceanscience Clamparatus (Bosley et al. 2005) without a topside electronics enclosure was mounted to the USCG buoy through an eye bolt, which held a downward-facing ADCP in a tube about 2 m below the surface (Figure 17). A communications cable was attached to the ADCP and fed through the Clamparatus tube for calibration and programming. The cable was left attached and tucked into the tube during the deployment. The ADCP was calibrated on the ATON during deployment to ensure the metal buoy did not interfere with the ADCP compass and magnetic variation. Instruments were configured to collect data internally.



Figure 17. Clamparatus on a green (left) and red (right) aid to navigation (ATON).

The CURBY utilizes a NexSens buoy to mount the downward-facing ADCP near the surface and transmits the data in realtime (Figure 18). A CTD is mounted below the buoy in the bridle cage. This buoy was designed to be easily deployable from a small vessel while providing near-surface real-time currents data. The initial design of the CURBY was deployed in the Delaware River in 2019 at Petty Island (db1935) as the first operational deployment. Fiorentino et al. (2022) analyzed the CURBY performance with comparison to a bottom-mounted ADCP used as a reference. Since 2019, the CURBY design has been upgraded to include meteorological sensors as described in Fiorentino et al. (2022).

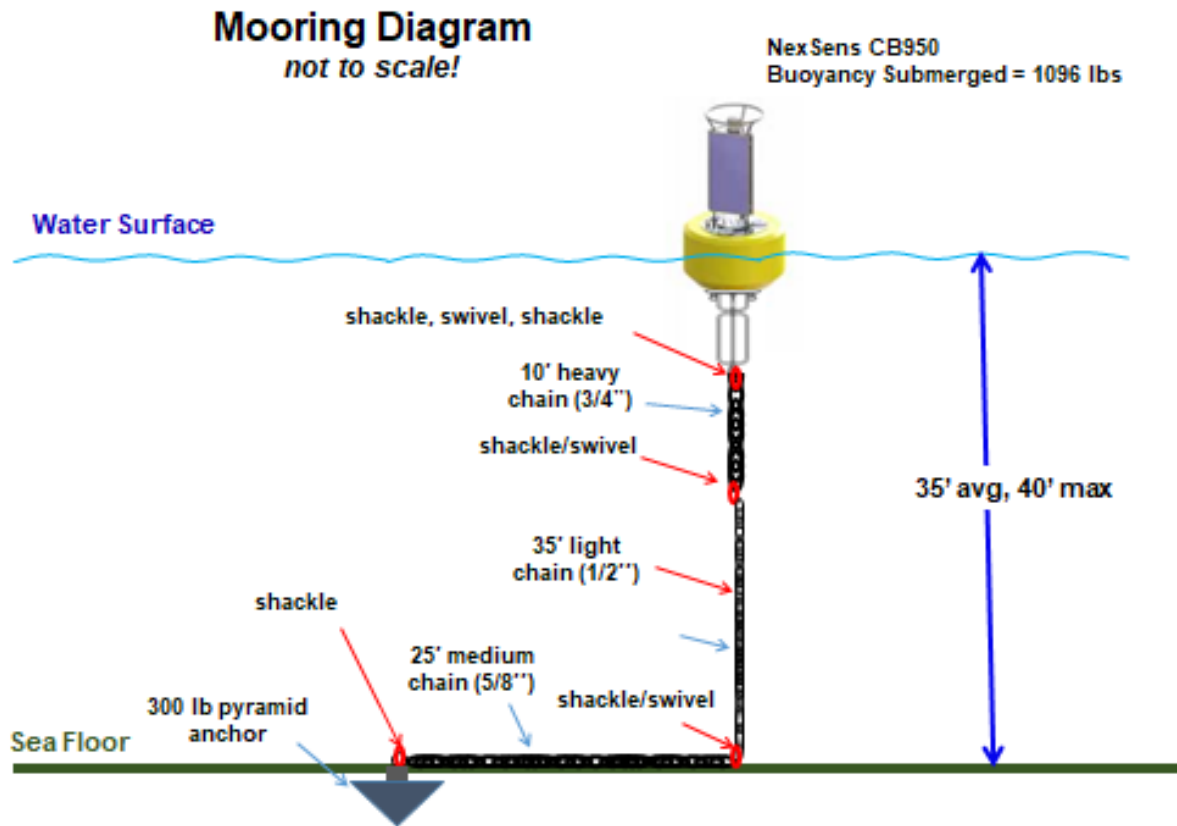


Figure 18. Mooring diagram (not to scale) of the Currents Real Time Buoy (CURBY).

3.2 ADCP Setup and Data Collection

ADCPs compute water velocity by sending out a series of acoustic pulses, or pings, and measuring each acoustic ping's return signal for Doppler shift. Unlike single-point current meters, ADCPs are generally configured to measure a profile of the water column. Profiles are created from many discrete bins of data collected in the water directly away from the acoustic heads of the ADCP. Bins are determined from the timing of acoustic returns of the unique signal (ping) sent from the instrument transducer using the speed of sound in water to calculate the 2-way travel time over the distance traveled. Water velocity is calculated by measuring the Doppler shift of each ping after reflection off microscopic bubbles or particulate matter suspended in the water averaged across each bin of the profile.

Bins therefore represent spatially averaged subdivisions along the profile. Optimal bin size is a compromise between higher spatial resolution along the profile (i.e., smaller bins) and lower standard deviation of the velocity ensemble (i.e., larger bin size increases the number of returning pings to calculate the spatial average). Bin size, like profile distance, is also a function of ADCP frequency. Higher frequency instruments measure smaller bins than low frequency instruments with the same standard deviation; however, lower frequency instruments can measure longer profiles and thus are used at deeper stations.

Velocity profiles can be collected either vertically (upward- and downward-facing ADCPs) or horizontally (side-looking ADCPs). Because the ADCP is measuring either a 3-dimensional (bottom and surface platforms) or 2-dimensional (side-looking) flow field, the acoustic transducer heads are set at an angle with respect to the instrument's measurement profile. For the upward-facing ADCPs used in this survey, the angle is either 20 degrees or 25 degrees. For 3-dimensional

flow measurements, a minimum of 3 acoustic transducers are necessary. The Doppler-shifted velocities along each beam can then be transformed mathematically into any orthogonal coordinate system, such as an ENU orientation (with the help of a compass).

Each ADCP was configured to collect profiles of data in 6-min averages (called ensembles) of acoustic pulses (pings). The number of pings per ensemble (the number of transmitted acoustic pulses whose returns as described above are averaged in time to form a single velocity measurement for each bin) should minimize the theoretical standard deviation of expected velocity within an ensemble with respect to the engineering constraints of the system. NCOP uses manufacturer-supplied software which calculates the ensemble standard deviation, battery usage, and memory usage for the anticipated duration of the deployment for a specified number of pings per ensemble, number of bins, and bin size. All these factors affect battery life.

The optimal number of pings is a compromise between reducing the ensemble standard deviation and choosing an appropriate bin size and number of bins to ensure sufficient battery life and data storage for the expected conditions at each station. TRDI Workhorses and Nortek AqDs are self-contained ADCPs with internal data storage and battery packs. For this project, stations were configured to minimize standard deviation by maximizing pings per ensemble while still ensuring sufficient battery life to complete the planned deployment duration.

There are some additional constraints on velocity profiles from ADCPs. Because of the angled beams, a portion of the water column near the water surface (or bottom) will be lost to side-lobe interference (approximately 5-10% of the profile depth depending upon beam angle). Transducer ringing, the result of the noise of the transmit pulse on the co-located transducer and receiver, leads to the loss of part of the profile nearest the ADCP head. Blanking distance accounts for this and varies as a function of ADCP frequency and transducer properties. The manufacturer's recommended default settings for blanking distance were used on both TRDI and Nortek instruments.

In bottom-mounted platforms, the ADCPs have an upward orientation; thus, bin 1 is the bin closest to the ADCP near the seafloor, and the profile extends to the surface. Conversely, in surface mounts, the ADCP has a downward orientation where bin 1 is near the surface and increases in number toward the bottom. In horizontal mounts, bin 1 is near the ADCP, which is typically mounted on an existing structure (e.g., bridge cribbing, pier), and the bins increase horizontally outward toward the channel.

The following ancillary measurements were collected and used as data quality assurance parameters: water temperature, pressure (depth), and instrument tilt collected at the sensor. For TRDI ADCPs only, beam echo intensity and correlation magnitude were also collected for each transducer head at each bin of the profile.

ADCPs were calibrated and tested for proper operation using built-in internal testing algorithms. Upon completion of these procedures, a unique configuration file was uploaded to each instrument based upon settings derived from the manufacturers' software. A unique, 5-character deployment name and the time to start pinging were also programmed. For all instruments that were redeployed for the second half of the survey, an examination of the ADCP's performance was conducted, and new settings were configured based upon the new location.

3.3 Description of Data Processing and Quality Control

The sampling rate for the ADCP data was 10 times per hour (centered every 6 min from the top of the hour through 54 min past the hour). Each sample was an average of a minimum of 180 up to 360 evenly timed pings based on the ADCP type, setup, and frequency. Even though the shortest tidal constituent period is about 2 hours, 6-minute samples enable a high-resolution estimation of the maximum and minimum tidal currents with the ability to capture short duration,

non-tidal events. This rate also provides a statistically sound time series in which erroneous records are less likely to influence the longer series.

Quality control measures were used to mark each record as bad, good, or questionable based on best practices implemented by CO-OPS (Paternostro et al. 2005) and based on the community-accepted Quality Assurance/Quality Control of Real-Time Oceanographic Data (QARTOD) standards and recommendations (U.S. Integrated Ocean Observing System 2019, 2020). Quality control applied to the measurements consist of threshold checks (for speed, tilt [pitch and roll], echo amplitude, and correlation magnitude) and rate of change checks (for speed, pitch, roll, and heading). An automated algorithm flagged the records that failed any of these checks. Questionable data were reviewed by an experienced analyst and marked as either bad or good. Only good data are disseminated to the public and used for harmonic analysis.

The principal flow (currents) direction is calculated by maximizing the direction of variance. This calculation enables an orthogonal transformation from an east-north coordinate system to major and minor flow direction axes (generally along- and cross-channel, respectively). Representing the currents in the major and minor axes components is especially beneficial in coastal and estuarine areas, which exhibit a rectilinear reversing flow rather than a rotary flow. In these cases, a significant majority of energy is along the major axis, and we can effectively represent the tidal currents with a single variable (major axis current speed).

All ADCP data collected were analyzed to separate the harmonic or tidal part of the signal from the residual or non-tidal flow (Parker 2007). Data were extracted from the binary instrument output into columnar ASCII data and then were processed further by NOAA's harmonic analysis routines (Zervas 1999). Harmonic analyses were then performed upon the current velocity time series in the major and minor flow directions.

The accepted analysis method for tidal current data is an optimization technique called Least Squares Harmonic Analysis (LSQHA; Parker 2007). The least squares technique allows for the presence of data gaps and can be used on time series of varying lengths. Amplitudes and phases of a given set of tidal constituents are resolved by using this method. The frequencies and number of the tidal constituents used in the analysis for each station are determined by the length of the time series (i.e., longer time series allow for more constituents to be resolved and, consequently, for more precise predictions). LSQHA was used to calculate harmonic constituents at all stations that had sufficiently long periods of good data. NOAA typically collects at least 33 days of data to ensure that most tidal energy can be adequately resolved by the least squares analysis.

Predictions provided online by CO-OPS are generated directly from harmonic constituents to meet USCG vessel carriage requirements.

3.4 CTD and Pressure Sensors

CTD sensors manufactured by Sea-Bird Scientific (model SBE 37 MicroCAT) were deployed co-located with ADCPs at the following locations: DEB2101 (Delaware Bay Entrance Channel), DEB2105 (0.5 nm west of Brandywine Shoal Light, 0.5 nm west of), DEB2107 (Brandywine Range at Miah Maull Range), and DEB2117 (Deepwater Point, 0.5 nm NW of). An In-Situ Aqua TROLL 200 CTD was also deployed at DEB2119 (Marcus Hook Bar [north]) as an ongoing test of the sensor, which performed well. These locations were chosen in collaboration with both the CO-OPS modeling team to help resolve the salinity gradient at the mouth of the Bay and the USGS modeling team to support the development of the new Delaware Bay model that will be used in helping determine the salinity of drinking water farther upriver. CTD results are discussed in Section 6.3.

An external pressure sensor (Onset Hobo U20-001-03) was deployed on the anchor of the SEABY at DEB2102 (Cape Henlopen, 2 mi NE of) in order to compare the pressure to the pressure

sensor in the ADCP to better understand the subsurface buoy motion. This is an effort to assess the mooring design and determine if buoy suppression and buoyancy are within acceptable ranges, especially during strong current conditions.

4.0 DATA ACQUIRED

Data were acquired at 35 stations occupied during the summer of 2021, with the exception of the CURBY deployment in 2019 (db1935 [Petty Island]). Due to a recreational vessel allision with the USCG ATON, 1 ADCP and the Clamparatus mount it was secured in were lost. However, the station was reoccupied during the second half of the survey, and data was collected. Analysis revealed that data from 1 station (DEB2125 [Schuylkill River Entrance]) was unusable due to a corrupted compass matrix, and overall, 4 stations collected an insufficient length of data to generate reliable tidal current predictions. The tables in Appendices A and B describe station data and metadata used in the analysis. Additionally, all stations have CTD data from vertical profile casts taken at deployment and recovery.

The estimated depth of the current profiler platform and the measurement bin depths are given in meters relative to an approximation of MLLW. This estimated MLLW depth is calculated statistically from the known height of the platform above the bottom in combination with the time series from the ADCP's pressure sensor. Error in the MLLW calculated at a given current station is the result of both the length of time of observations and uncertainties in the observed station depth. Station depth uncertainty is affected by any pressure sensor errors (such as drift and offset errors) and platform instability. Swanson (1974) calculated MLLW sigma errors of ± 0.4 to 0.3 m for tide observations with a time series of 30-90 days. Calculated depth is therefore a best approximation. This MLLW approximation can be compared to the station depth, which is logged using the boat's fathometer during deployment and recovery and entered into the database.

Stations in Table A1 of the appendix are listed with position, depth as recorded at deployment, and station occupation start and end dates.

5.0 STATION RESULTS

A brief, quantitative description of a subset of survey stations is provided in this section. These include stations that exhibit characteristics of different flow regimes.

For each station in this section, a description of the mean maximum flood current (MFC) and mean maximum ebb current (MEC) is given for the station's near-surface depth bin which is represented in the official NOAA tidal current predictions (TCP). For some stations, up to 2 additional depths are available in the TCP. For ADCPs, "bin 1" refers to the depth closest to the instrument's head (bottom-most for bottom mounted, upper-most for ATON mounted, and closest to the structure for side-looking); the bin number increases with distance from the instrument. The principal flood direction is the predominant axis of flow as described in Section 3.3. Directions are provided in degrees from true north. The variance along this axis is provided to give an indication of how confined the flow is along the axis; a high percentage variance implies a rectilinear flow. Seven stations are described in this section. These stations were selected based on spatial representation and/or scientific interest. The results presented below are a small subset of the full analyses conducted on the data sets. Defant ratios for the near-surface bin in the water column or the bin closest to the ship channel are provided to indicate tide type. For each of the 7 stations described, there are 5 figures that include the following:

1. A scatter plot of the north versus east velocity component of the entire data set at the near-surface depth bin.
2. Two plots of a subset of the velocity time series at the near-surface depth bin. The upper plot shows a comparison of observed (green dots) major-axis velocity and calculated (red line) tidal predicted velocity. The ADCP pressure sensor data is shown as magenta dots indicating the approximate water depth; the lower plot shows the residual flow (the difference between observed and predicted velocity).
3. A vertical profile of the mean velocity along the major (red vectors) and minor (blue vectors) axis of the water column. The vectors are scaled to the speed of the mean current. This represents the approximate mean residual (non-tidal) circulation throughout the water column. The surface level is estimated (shown as gray triangles).
4. A vertical profile plot showing the timing (red) and speed (blue) of the MEC throughout the water column.
5. A vertical profile plot showing the timing (red) and speed (blue) of the MFC throughout the water column

5.1 db1935 - Petty Island

This was the first operational deployment of the CURBY spanning nearly 99 days from July 9, 2019, to October 17, 2019. This station is located to the northwest of Petty Island in the main channel of the Delaware River, approximately 1.2 nm upriver of the Benjamin Franklin Bridge. The CURBY station used a NexSens CB950 buoy hull equipped with a downward-facing Nortek Z-Cell ADCP that sampled at 1 Hz. The analysis of the Z-Cell failed in NOAA's harmonic analysis software (Paternostro et al. 2005), which is being addressed for future surveys. Bins 2-11 are marked as having good data. Quality Control (QC) passed good data, and LSQHA solved 25 harmonic constituents over the 3-month deployment period. The last day of deployment was removed with QC to avoid suspect data likely due to increased winds. The low echo amplitude period from October 14-October 15 wasn't fully removed with QC in the surface bins, leading to observations that don't match the predictions and slightly larger residuals during this time. Slack Greenwich Interval (GI) timing occurs earlier at depth than at the surface for SBF (10.2 min), SBE (3.6 min), and MEC (36.6 min). MFC occurs 5.4 min later at depth than at the surface. Speeds are fastest at the surface in bins 3 (91.6 cm/s, 1.78 knots [kn], ebb) and 4 (104.4 cm/s, 2.03 kn, flood). The historic station (ACT4431) is located 0.04 nm SW of db1935. Comparing the historic prediction bin (7.3 m) with CURBY bin 7 (7.0 m), the CURBY has slightly faster MFC and slightly slower MEC speeds with similar directions (within 12 degrees). As for the GI values compared to the historic station, db1935 SBF is 18.2 min earlier, MFC is 4.6 min earlier, SBE is 5.2 min later, and MEC is 18.2 min later.

For an extended data analysis and mooring design assessment, see Fiorentino et al. (2022), which also includes comparison of the CURBY data with the DBOFS nowcast output and the historic station tidal current predictions.

Julian Days: 190.75-289.62

Velocity North/East - "db1935-Bin-3"

Orientation: down

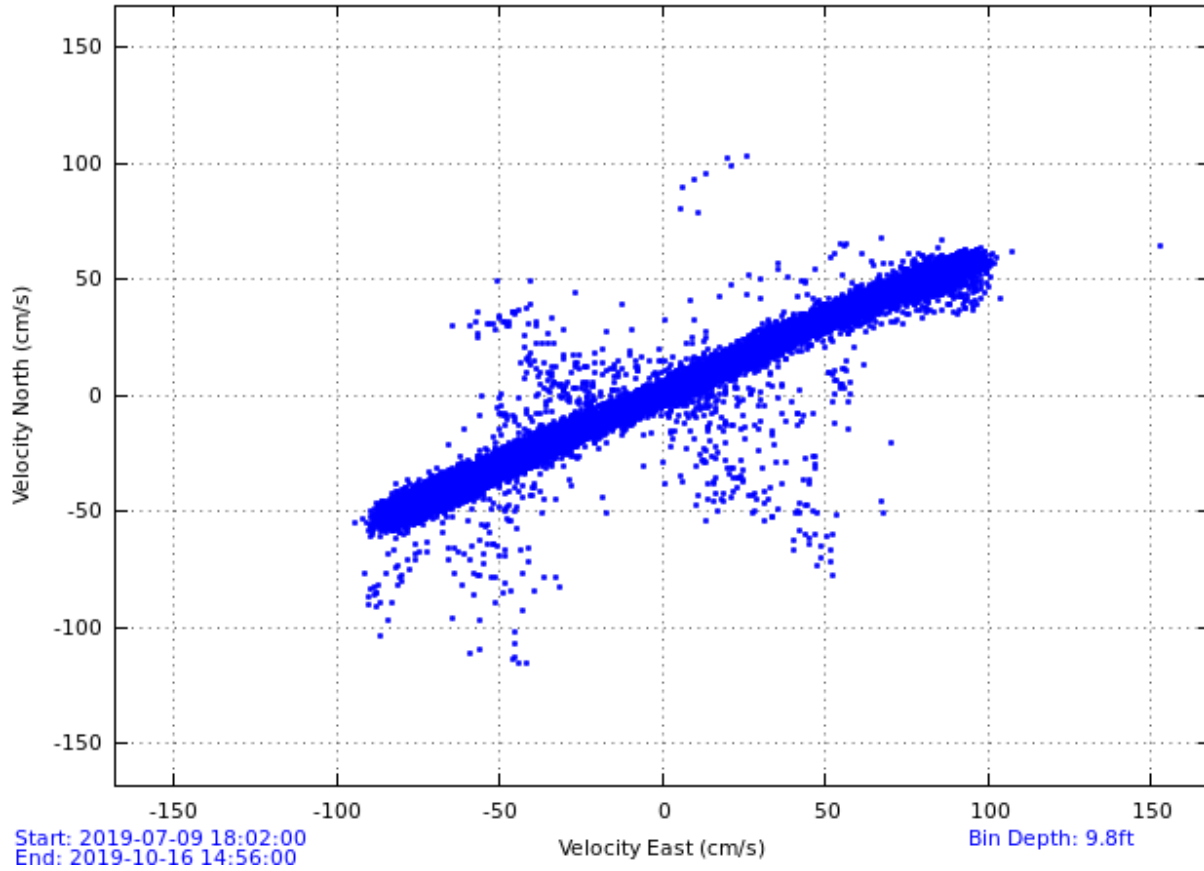


Figure 19. Scatter plot of north-versus-east velocity (cm/s) for station db1935 at the near-surface prediction bin, bin 5 at 3 meters (m) below mean lower low water (MLLW).

Julian Days: 238.22-242.40

Orientation: down

Analysis: LSQHA

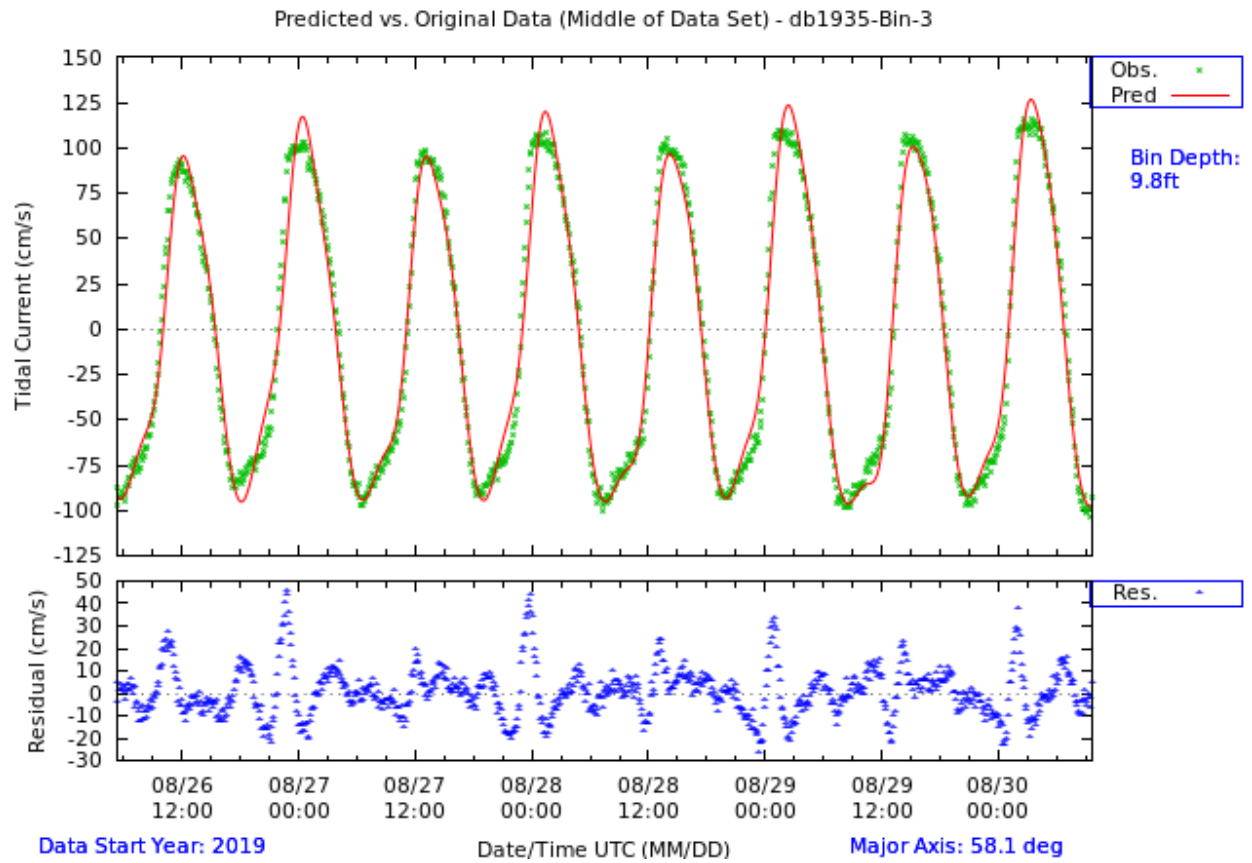


Figure 20. Comparison of observed major axis velocity data (green points) to predicted tidal velocity (red line) along the major axis for station db1935. The lower figure shows the non-tidal residual (blue dots), which is the difference between the predicted and observed velocity from the upper panel.

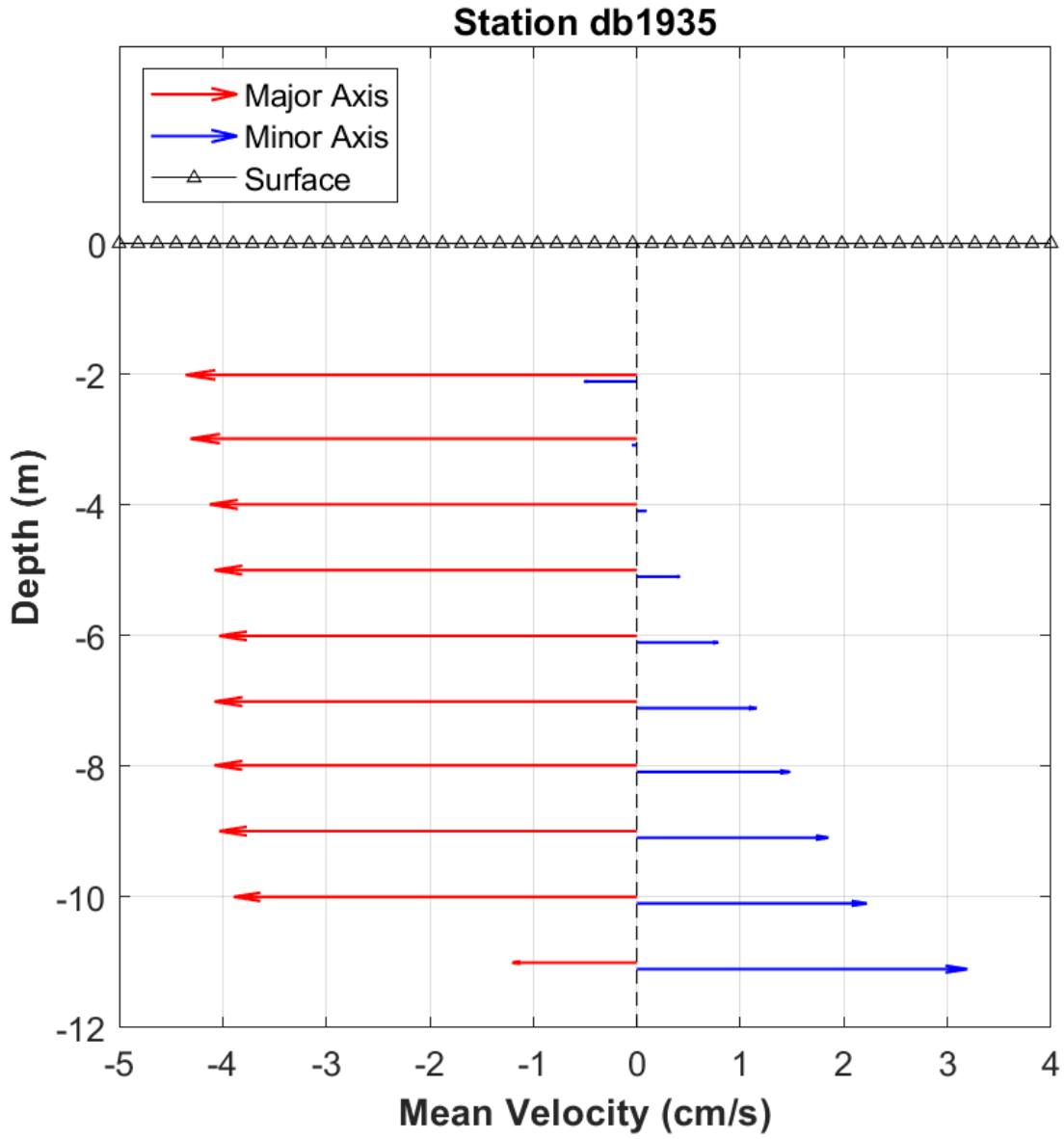


Figure 21. db1935 mean velocity (cm/s) profile along the major axis (red vectors) and minor axis (blue vectors) by depth. Only bins that passed quality control criteria are shown. This station was configured to collect 1-m bins.

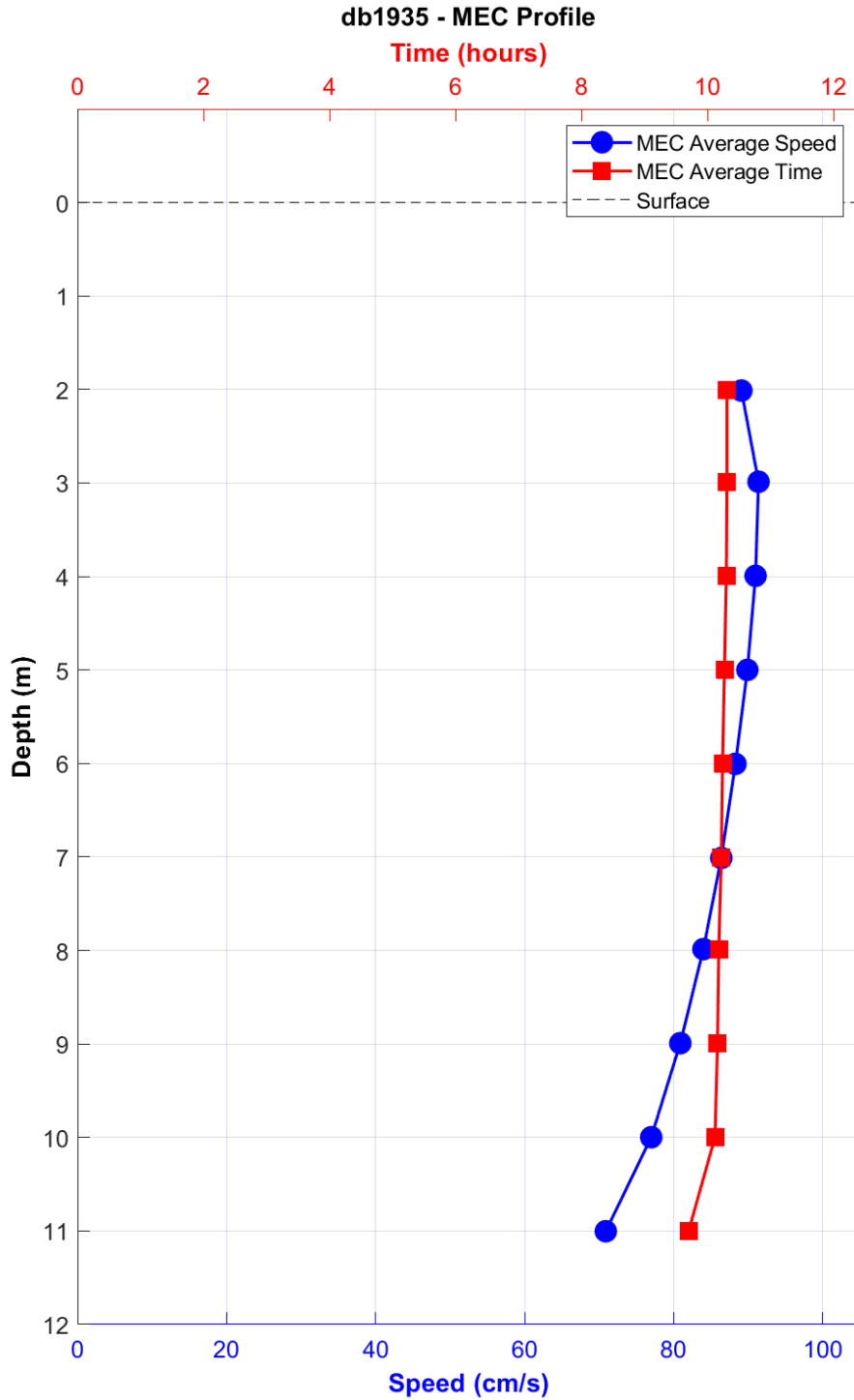


Figure 22. db1935 maximum ebb current (MEC) timing (Greenwich Intervals [GI], red squares, upper x-axis) and speed (blue circles, lower x-axis) by depth.

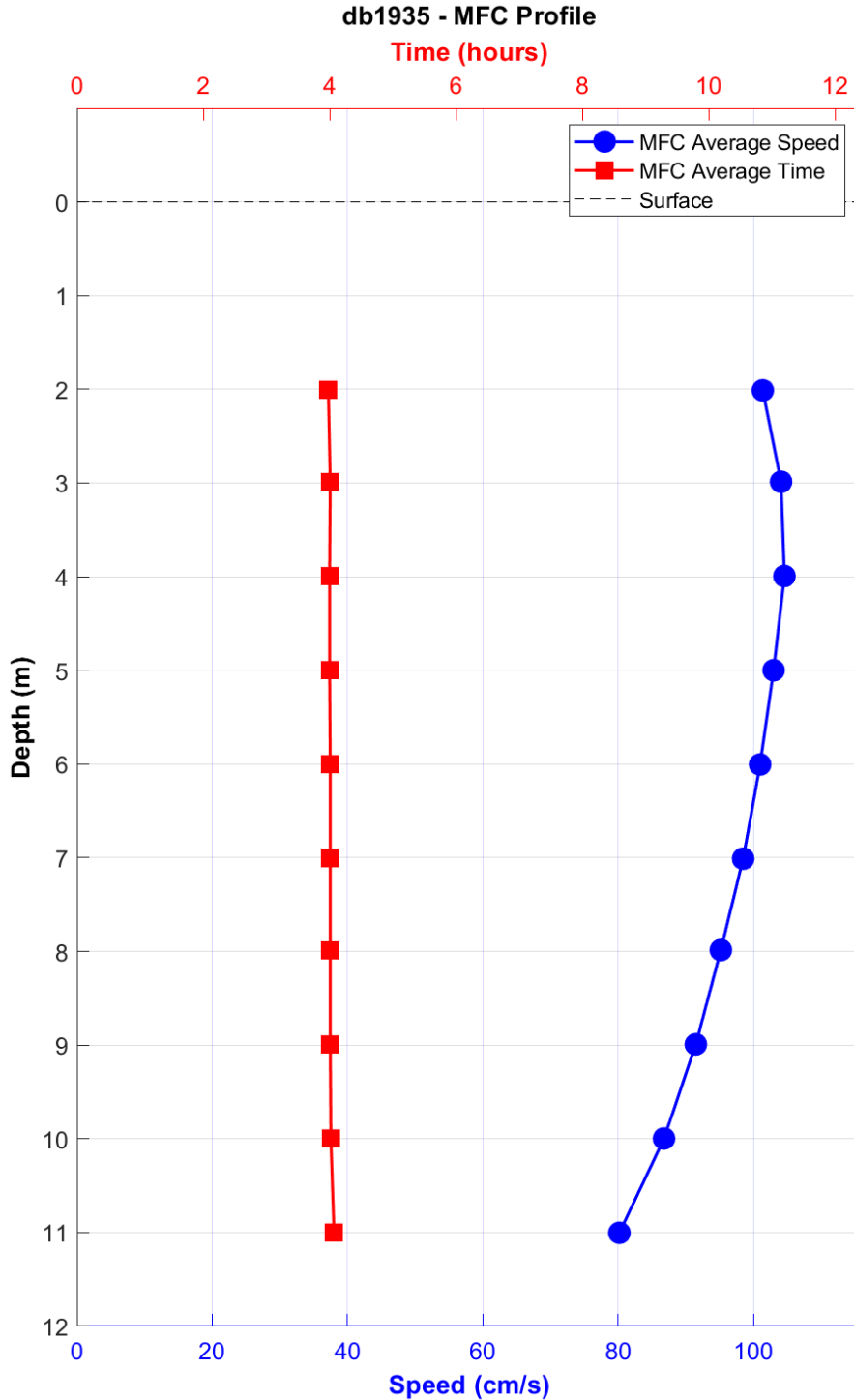


Figure 23. db1935 maximum flood current (MFC) timing (Greenwich Intervals [GI], red squares, upper x-axis) and speed (blue circles, lower x-axis) by depth.

5.2 DEB2101

Station DEB2101 Delaware Bay Entrance was occupied for 87 days from July 15, 2021, to October 11, 2021, with a 600 kHz TRDI ADCP in a SEABY mount about 2.9 m above the bottom. This station is located in the Atlantic Ocean, approximately 2.5 nm southeast of Cape Henlopen. Data are good up to the point where the mount broke free of its mooring on October 11,

2021. The mount was later found which allowed all data to be recovered. A Seabird CTD was moored with this instrument. Depths from the ADCP pressure sensor match the depths observed by the CTD (the CTD was mounted ~1.5 m below the ADCP). Pitch and roll vary between -15 degrees and 5 degrees, consistent with this type of mount and within the accepted range of -20 degrees to 20 degrees. Bins 1-13 passed all QC checks.

This station is mostly rectilinear with major axis variance >95% in all good bins; however, there is some sign of rotary flow in the velocity plots. This station is ebb dominant with a strong ebb directed mean flow that increases from 10.3 cm/s (0.2 kn) near bottom to almost 41 cm/s (0.8 kn) near the surface. As a result, MEC are 144 cm/s (2.8 kn) in the near surface bins while floods are ~67 cm/s (1.3 kn). Maximum ebb currents occur in bin 12 and maximum floods in bin 8. This station is strongly semidiurnal in all good bins. LSQHA solving for 25 harmonics explains >96 % of energy in all good bins with a low residual variance (<4%).

This station superseded the nearby historic station ACT4071, which is located 1.15 nm to the west. Flood magnitude compares well with the historic station and is 15 min later. Ebb is significantly stronger and later than the historical station: twice as fast at approximately 134 cm/s (2.6 kn) and a full hour later (5:55 vs 4:55). Slack before flood is also about an hour after the historical station.

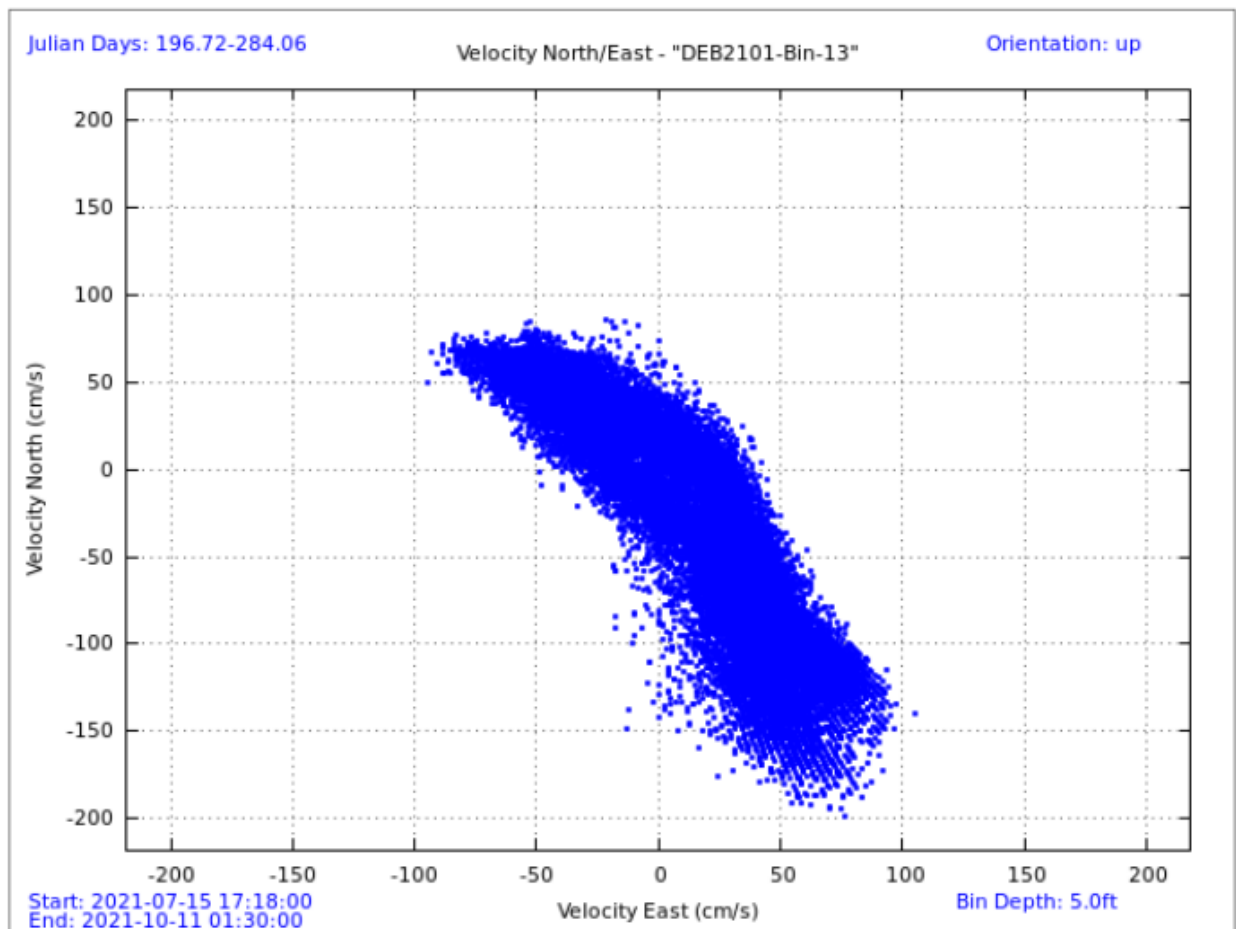


Figure 24. Scatter plot of north-versus-east velocity (cm/s) for station DEB2101 at the near-surface prediction bin, bin 13 at 1.5 meters below mean lower low water (MLLW).

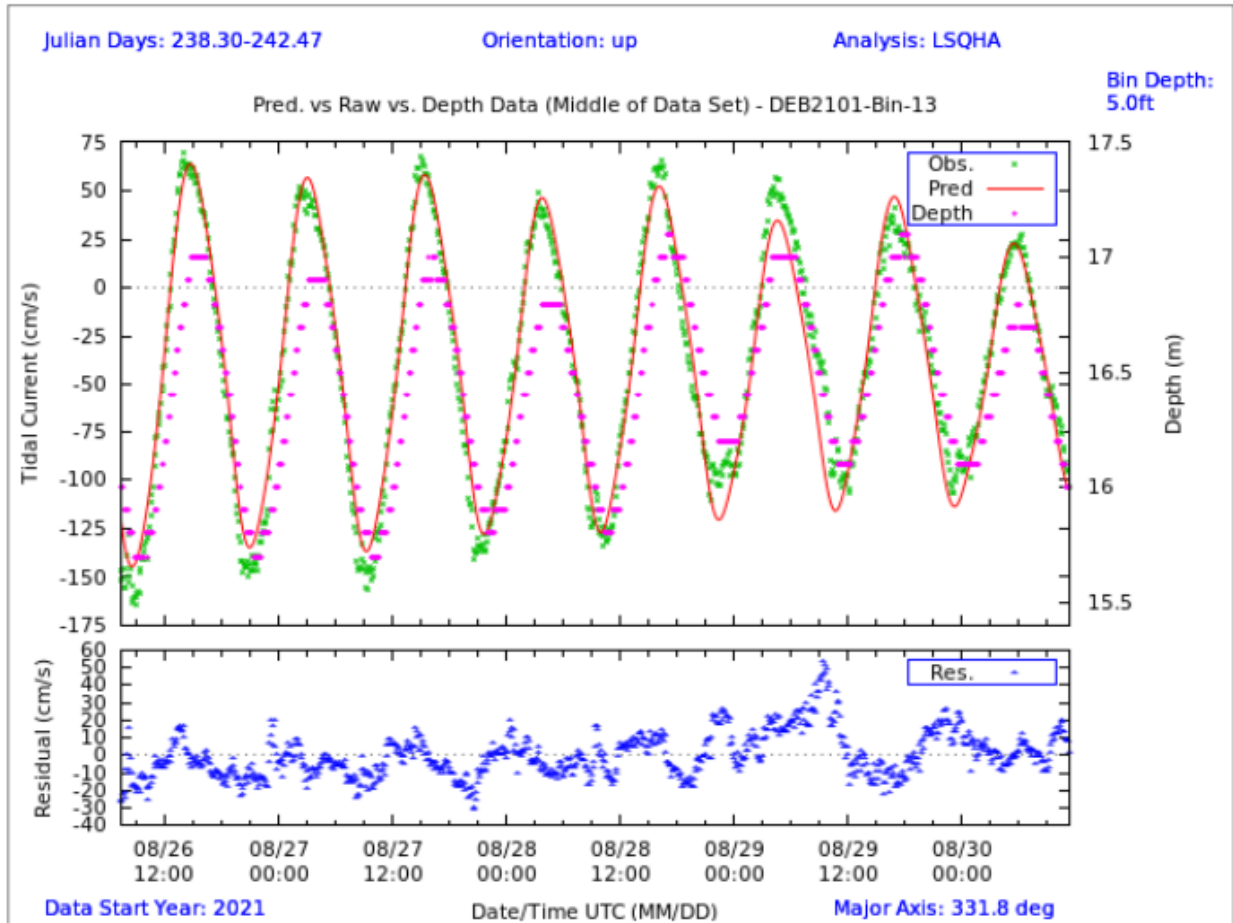


Figure 25. Comparison of observed major axis velocity data (green points) to predicted tidal velocity (red line) along the major axis for station DEB2101. The sensor depth (magenta dots) is measured using the acoustic Doppler current profiler (ADCP) pressure sensor and shows the tidally-induced water level changes over time. The lower figure shows the non-tidal residual (blue dots), which is the difference between the predicted and observed velocity from the upper panel.

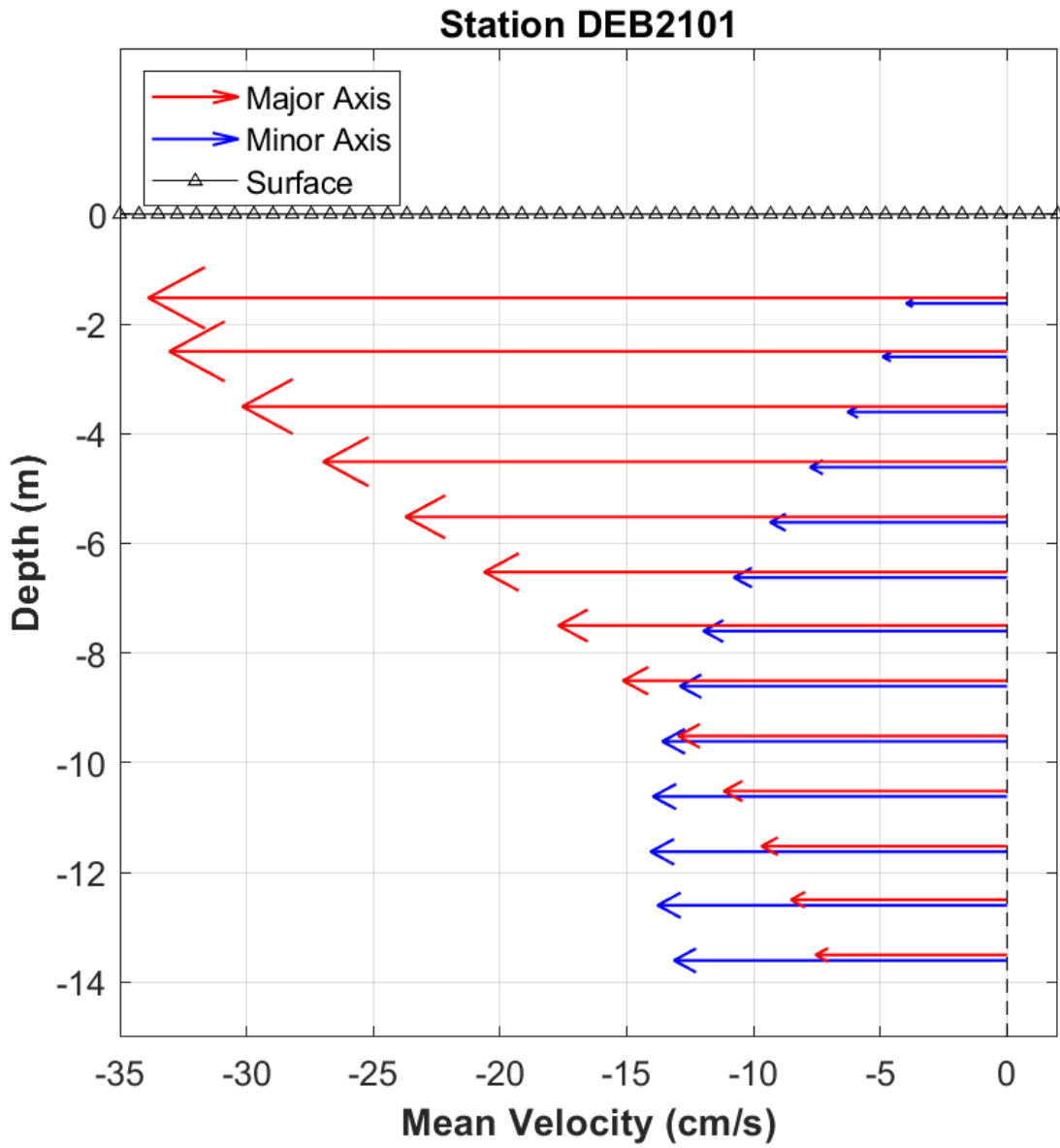


Figure 26. DEB2101 mean velocity (cm/s) profile along the major axis (red vectors) and minor axis (blue vectors) by depth. Only bins that passed quality control criteria are shown. This station was configured to collect 1-m bins.

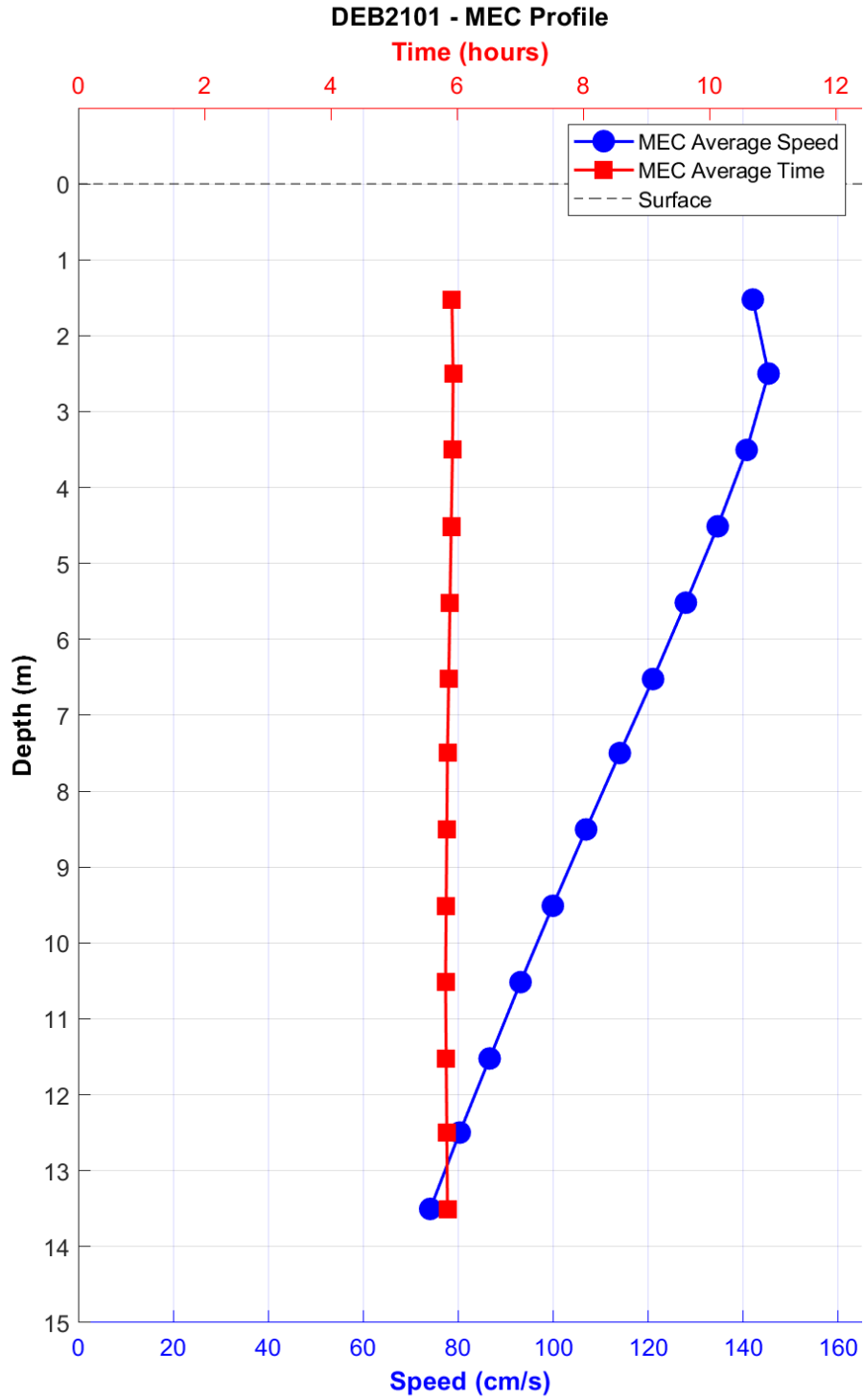


Figure 27. DEB2101 maximum ebb current (MEC) timing (Greenwich Intervals [GI], red squares, upper x-axis) and speed (blue circles, lower x-axis) by depth.

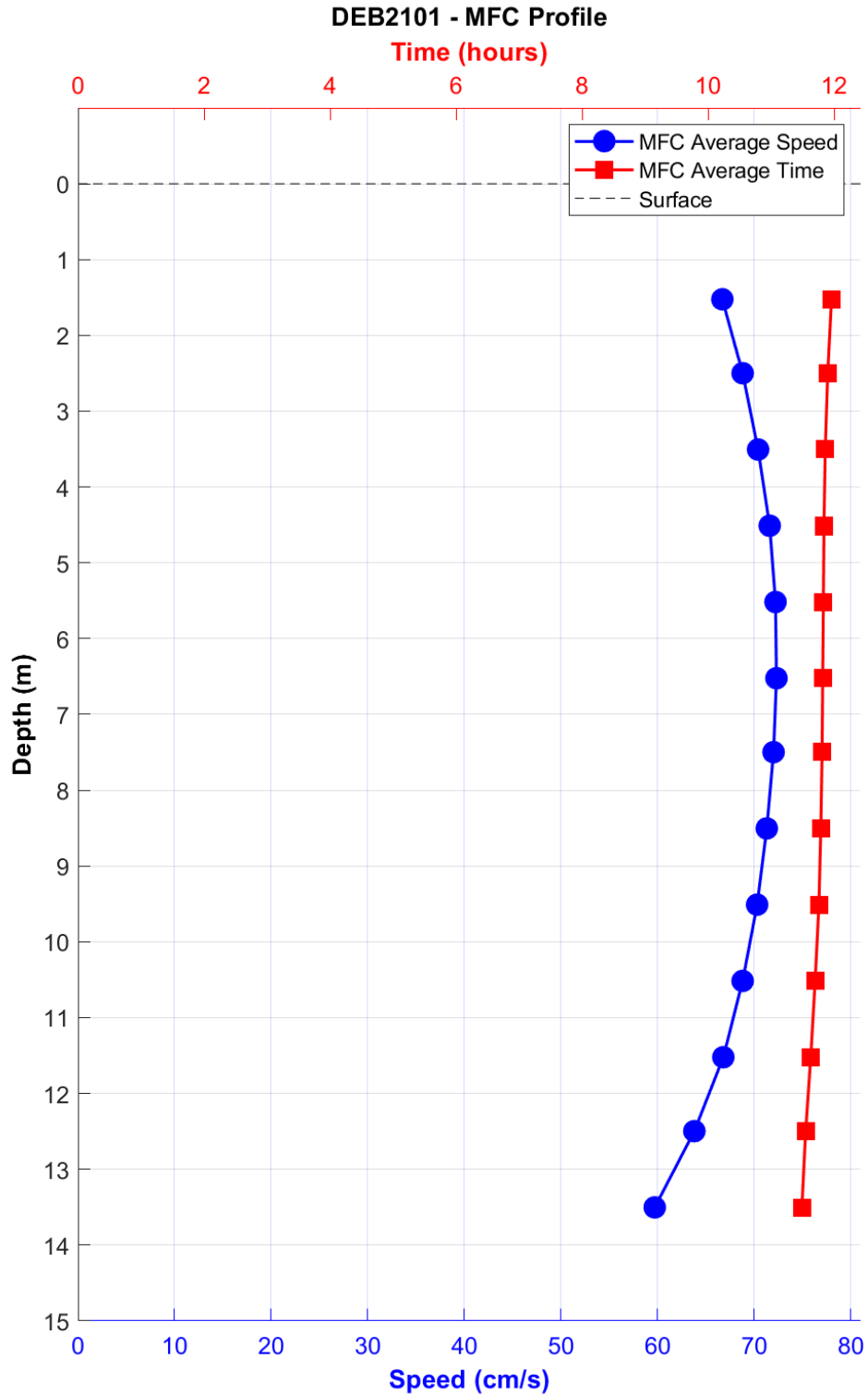


Figure 28. DEB2101 maximum flood current (MFC) timing (Greenwich Intervals [GI], red squares, upper x-axis) and speed (blue circles, lower x-axis) by depth.

5.3 DEB2105

DEB2105 (Brandywine Shoal Light, 0.5 nm west of) was equipped with a bottom-mounted (upward-facing) TRDI Workhorse Sentinel 1200 kHz ADCP mounted in a mTRBM. The sensor at this location was deployed on September 14, 2021, and recovered on November 3, 2021. This

station is in the center of Delaware Bay between Brandywine Shoal and the navigational channel. There is an indication of movement observed on 3 occasions (data on around October 22 and October 27, 2021, show changes in pitch and roll, and on 9/24 in heading). These slight movements don't seem to affect the data, possibly because the sensor used an ENU coordinate system, and the onboard processing of the ~1 second raw data uses the observed values of pitch, roll, and heading to correct the averaged ENU data. Custom QC was used to trim outliers in echo intensity and correlation magnitude for all good bins.

Data was collected for about 50 days, of which bins 1-13 are set to have good data in C-MIST. Currents at this location are semidiurnal and strongly tidal; up to 97% of the total current energy was accounted for by the 25 terms in the harmonic analysis (LSHQA-25). There is also a strong rectilinear signature observed with the major axis variance reaching as much as 98.8%. Bins 1 (12.4 m), 9 (4.5 m), and 12 (1.4 m) are suggested as prediction bins to capture the slow bottom currents, 4.6 m navigational depth (also historical prediction depth), and the maximum speeds, respectively.

Floods are slightly faster than the ebbs throughout the water column, resulting in a permanent mean flood throughout the water column reaching up to over 7.7 cm/s (0.15 kn). The maximum observed MFC is 84.9 cm/s (1.65 kn) and MEC is 68.9 cm/s (1.34 kn), both at bin 12 (1.4 m) slightly below the surface. The GI timing occurs slightly earlier for ebbs at the surface and slightly earlier for floods at depth.

This station is recommended to supersede historic station ACT4136 (Brandywine Range, DE [off Brandywine Shoal North]) located approximately 1.27 nm away. This historic station collected data for 28 days at depths of 4.6 m and 12.2 m in 1985. Historic stations observation (4.6 m) compares well with DEB2105 bin 9 (4.5 m). The new observation registers later flood and ebb GI timing by about 11 and 6 min, respectively. Both MFC and MEC speeds are faster in the new observations. The data collected at this station may have had a problem with 1 or more transducers, as the automated onboard processing showed there were more 3-beam solutions rather than full solutions than there should have been in all bins. Despite that, the data appears to be good. This shows the advantage of a 4-beam instrument over a 3-beam instrument. Since only 3 beams are necessary to resolve a 3-dimensional system, the fourth beam allows for good data even if 1 beam (transducer or receiver) is malfunctioning.

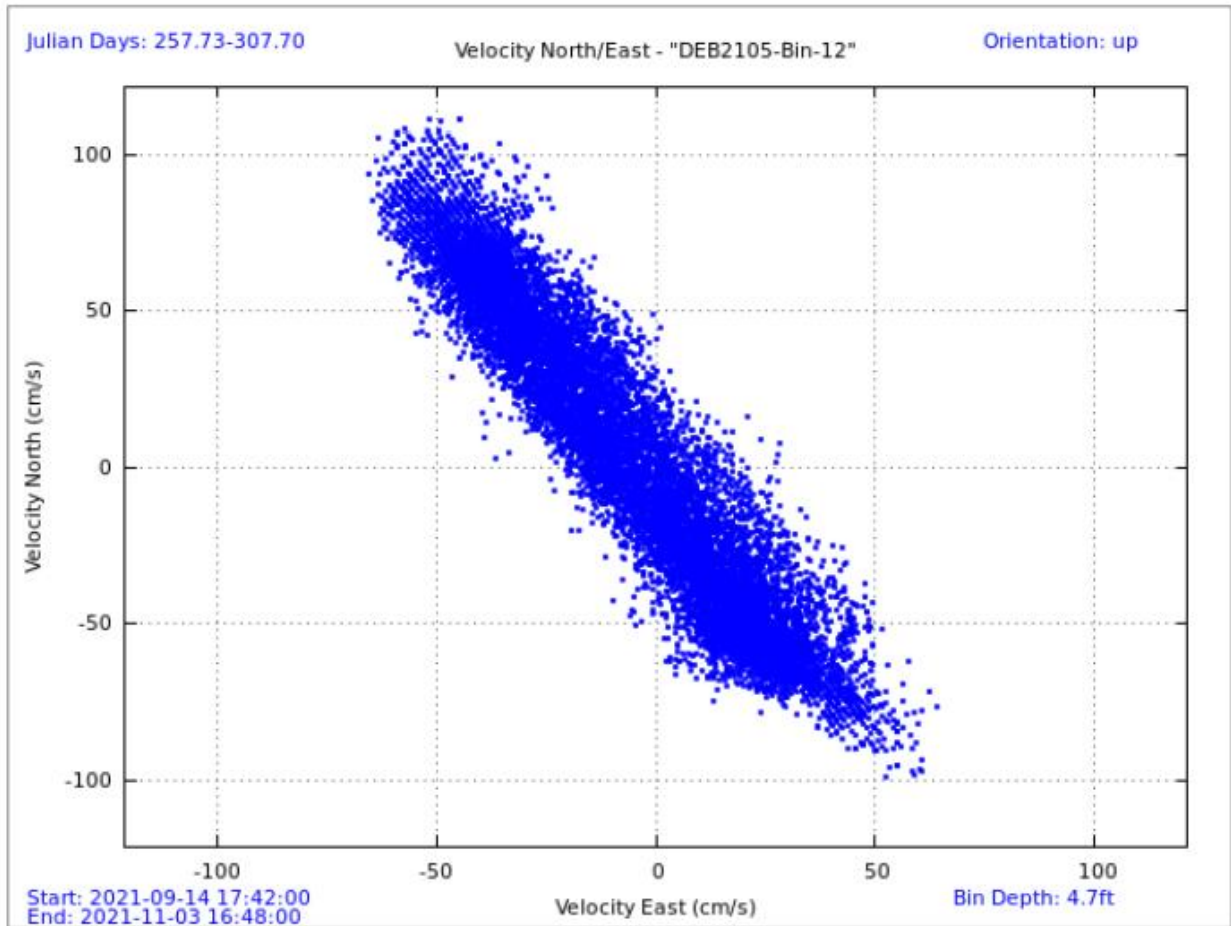


Figure 29. Scatter plot of north-versus-east velocity (cm/s) for station DEB2105 at the near-surface prediction bin, bin 12 at 1.4 m below mean lower low water (MLLW).

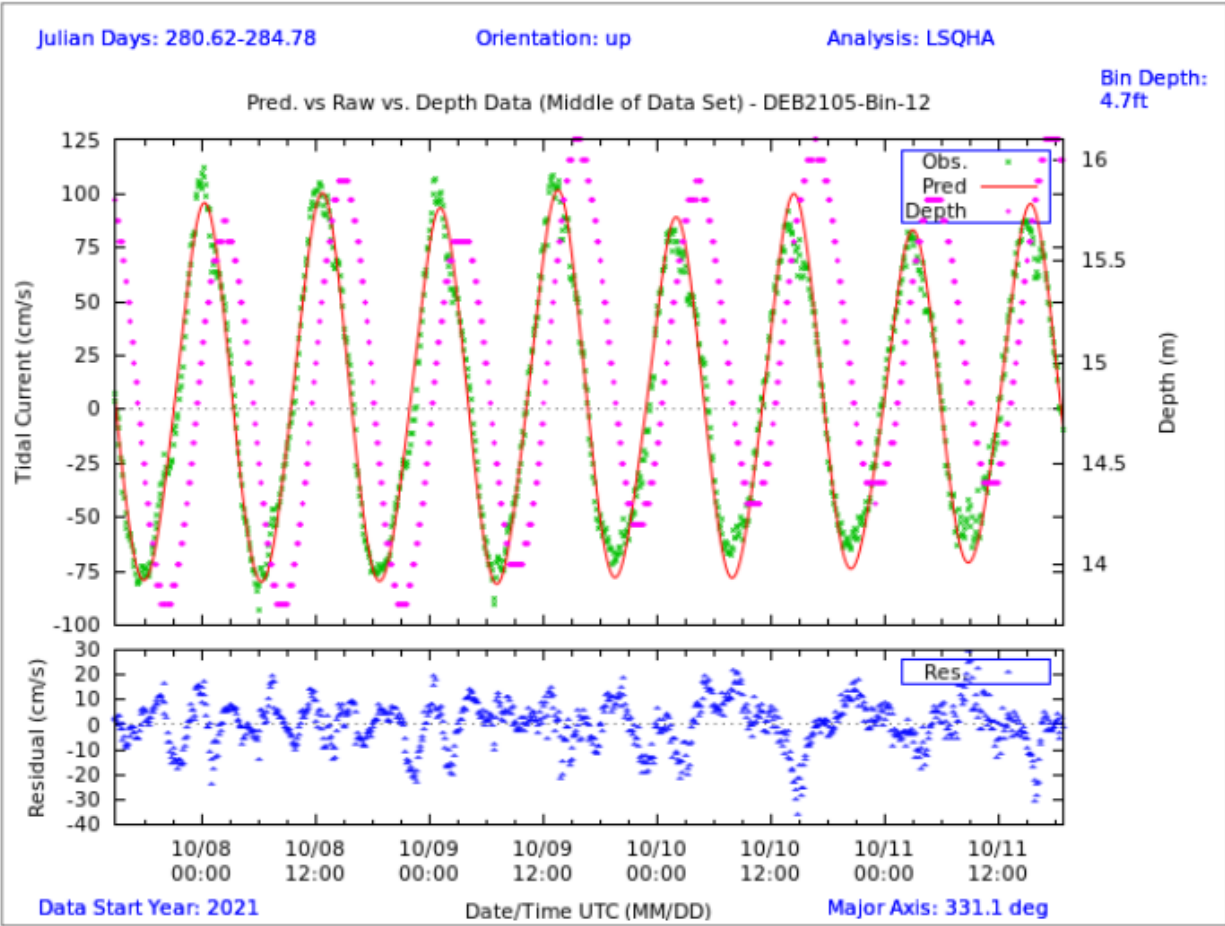


Figure 30. Comparison of observed major axis velocity data (green points) to predicted tidal velocity (red line) along the major axis for station DEB2105. The sensor depth (magenta dots) is measured using the acoustic Doppler current profiler (ADCP) pressure sensor and shows the tidally-induced water level changes over time. The lower figure shows the non-tidal residual (blue dots), which is the difference between the predicted and observed velocity from the upper panel.

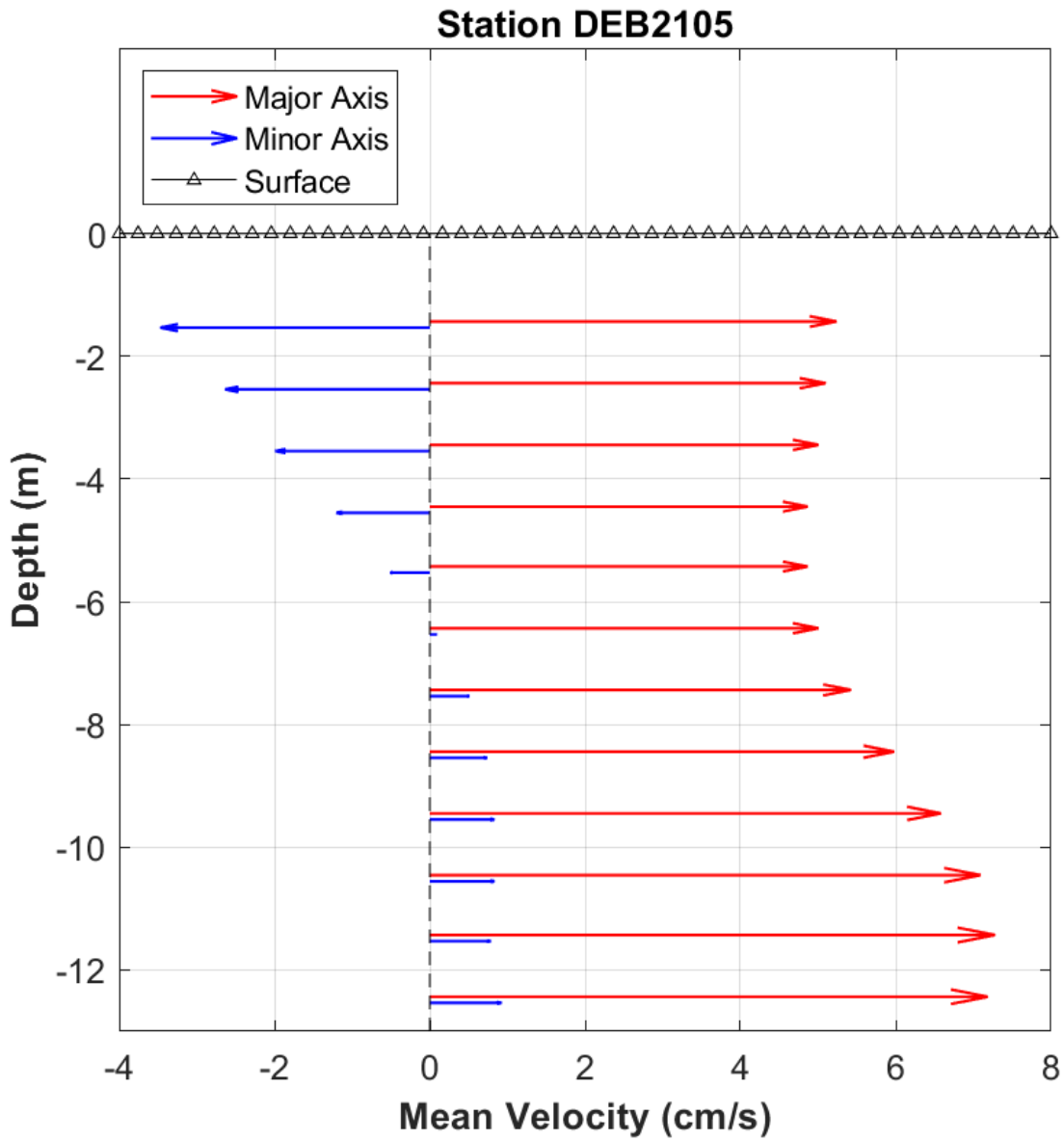


Figure 31. DEB2105 mean velocity (cm/s) profile along the major axis (red vectors) and minor axis (blue vectors) by depth. Only bins that passed quality control criteria are shown. This station was configured to collect 1-m bins.

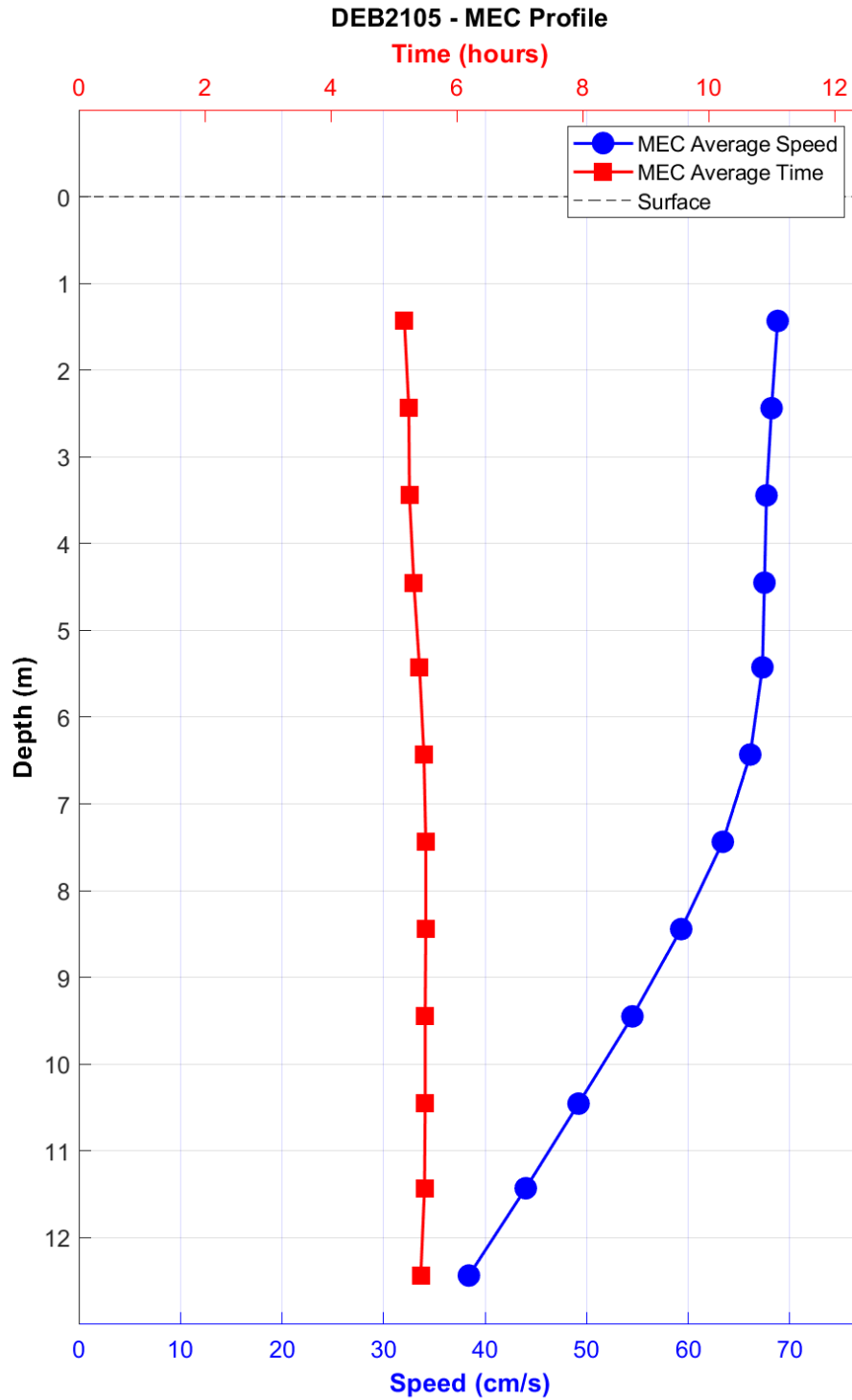


Figure 32. DEB2105 maximum ebb current (MEC) timing (Greenwich Intervals [GI], red squares, upper x-axis) and speed (blue circles, lower x-axis) by depth.

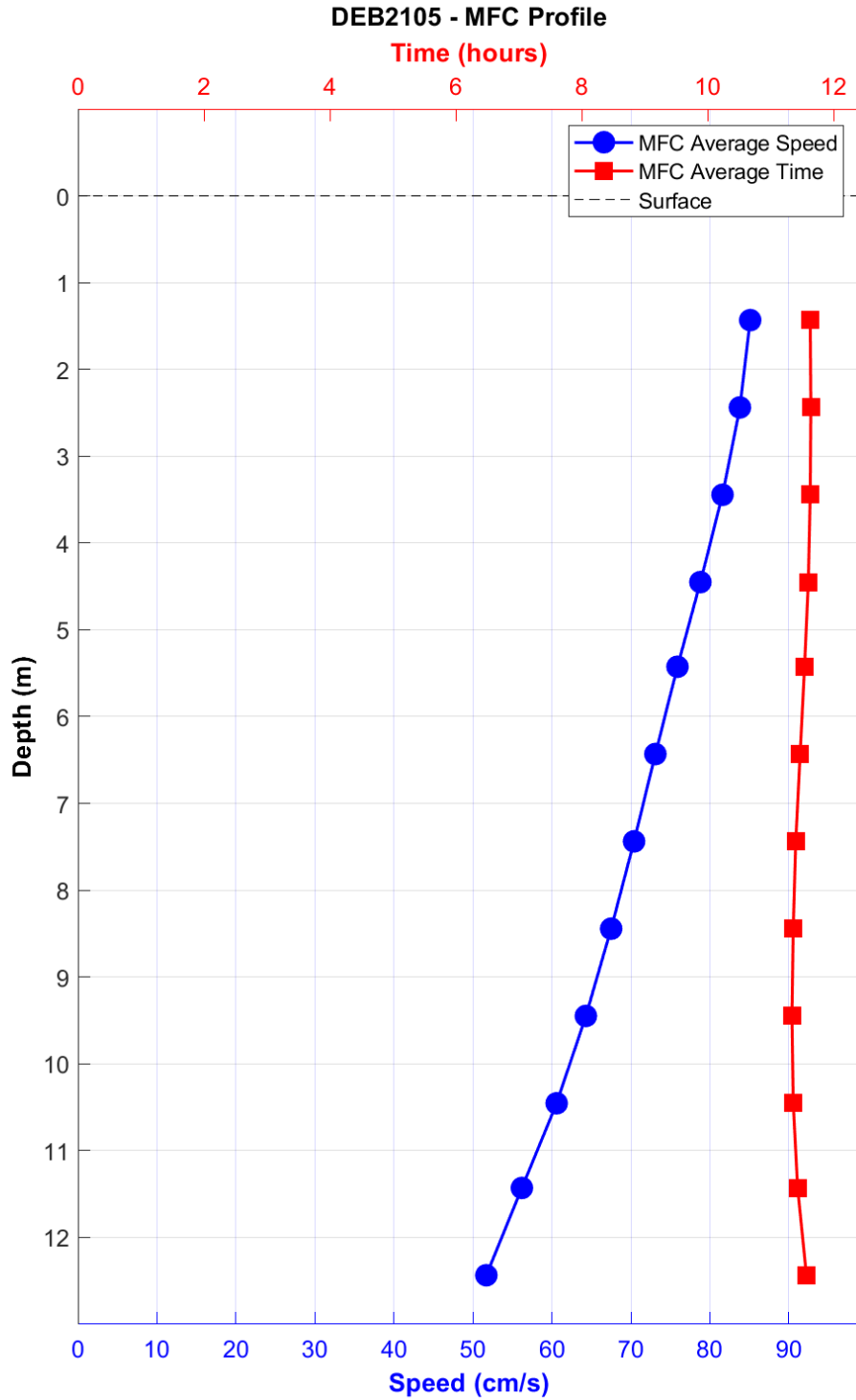


Figure 33. DEB2105 maximum flood current (MFC) timing (Greenwich Intervals [GI], red squares, upper x-axis) and speed (blue circles, lower x-axis) by depth.

5.4 DEB2117

Station DEB2117 was occupied for 106 days from July 21, 2021, to November 5, 2021, with a 600 kHz TRDI workhorse in an mTRBM bottom mount. This station is just upriver of the Delaware Memorial Bridge on the Delaware river at Deepwater Point. The pressure sensor and

surface echo matched, and the calculated statistical MLLW is 16.93 m. Metadata including pitch and roll look good, and data for this station is of high quality. Bins 1-14 are good.

This station is strongly semidiurnal in all good bins. A 29-term LSQHA explains more than 97% of the energy in all bins. The station is also highly rectilinear, with a major variance percent of 99% or more in all bins. Floods are stronger than ebbs at all depths and both are stronger near the surface than at depth. There is about a 5.1 cm/s (0.1 kn) mean flow in the ebb direction near the surface. Ebbs near the surface are about 102.9 cm/s (2 kn), and floods are about 131.2 cm/s (2.55 kn).

In comparison to the historic station, MFC is slower by 20.6 cm/s (0.4 kn) and earlier by 17 minutes, MEC is also slower by ~25.7 cm/s (0.5 kn) and earlier by 11 minutes. SBE is earlier by 8 minutes. MFC direction of 23 degrees is 4 degrees north of the historical station, and MEC direction of 208 degrees is 7 degrees less than historic. The direction (azimuth [AZI]) of 25 degrees (very close to flood direction) reinforces the observation that this station is rectilinear. Evidence of Hurricane Ida is seen in the velocity data around September 2, 2021, as well as the smaller magnitude flooding event later on October 29, 2021, leading to larger than normal residual flow.

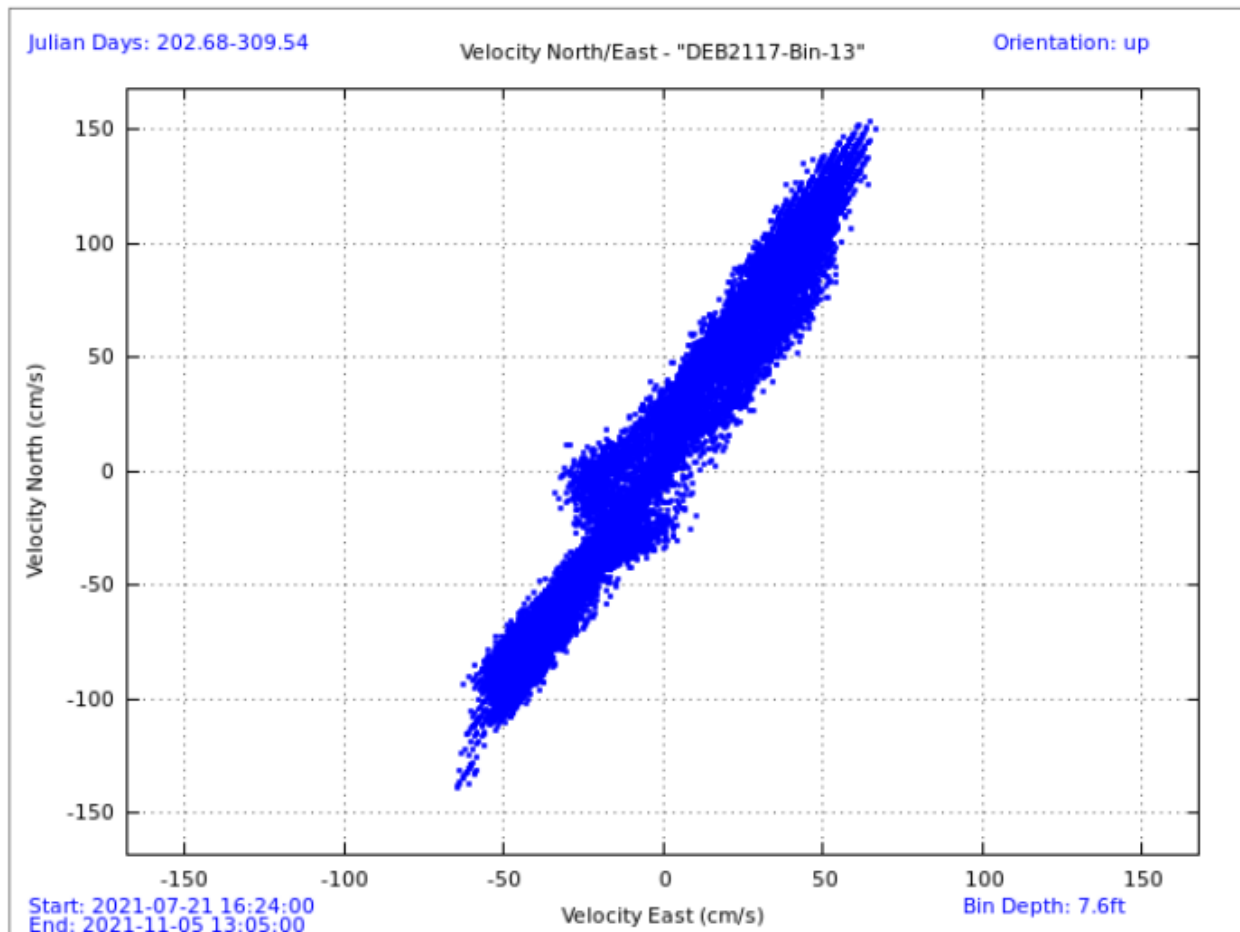


Figure 34. Scatter plot of north-versus-east velocity (cm/s) for station DEB2117 at the near-surface prediction bin, bin 13 at 2.3 m below mean lower low water (MLLW).

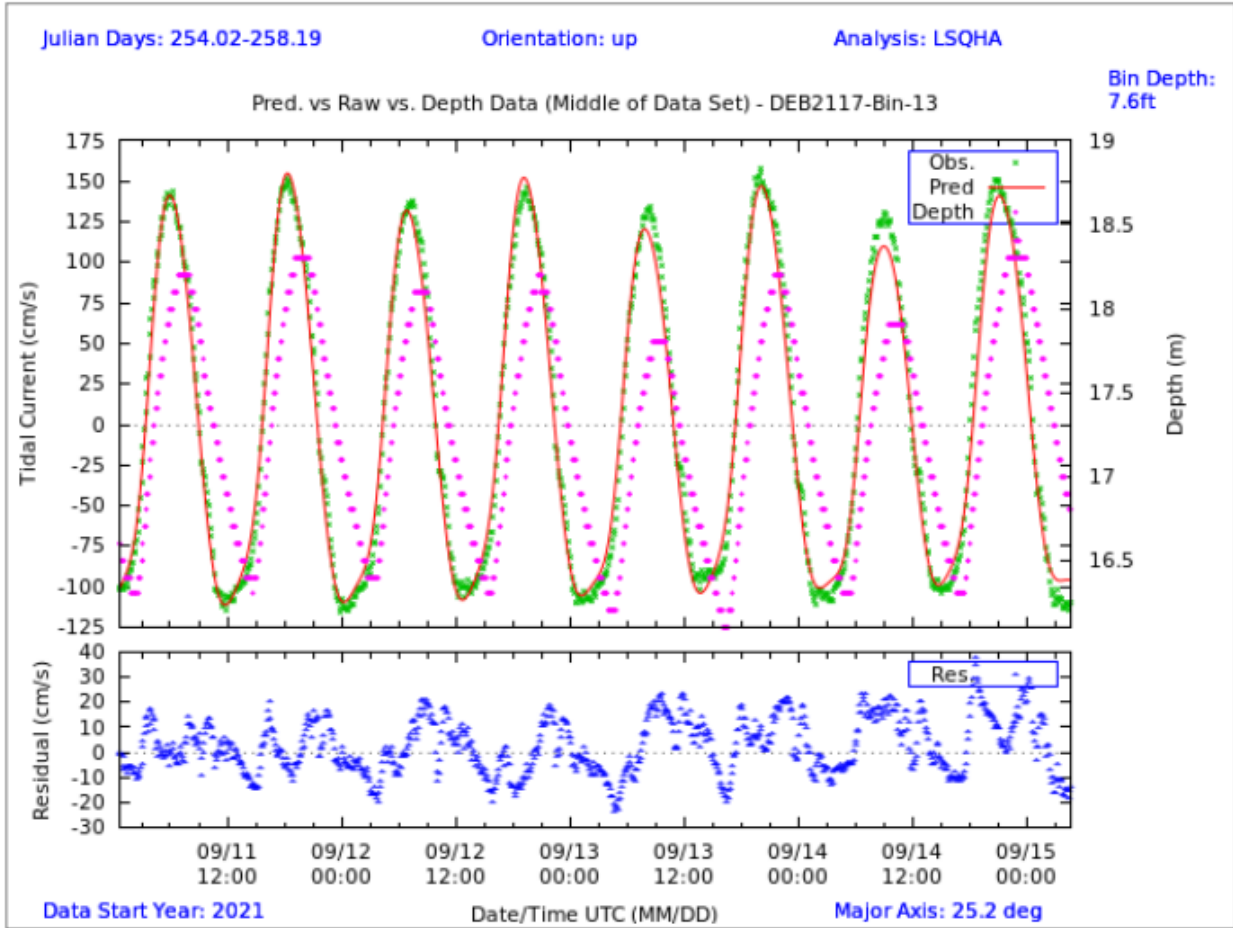


Figure 35. Comparison of observed major axis velocity data (green points) to predicted tidal velocity (red line) along the major axis for station DEB2117. The sensor depth (magenta dots) is measured using the acoustic Doppler current profiler (ADCP) pressure sensor and shows the tidally-induced water level changes over time. The lower figure shows the non-tidal residual (blue dots), which is the difference between the predicted and observed velocity from the upper panel.

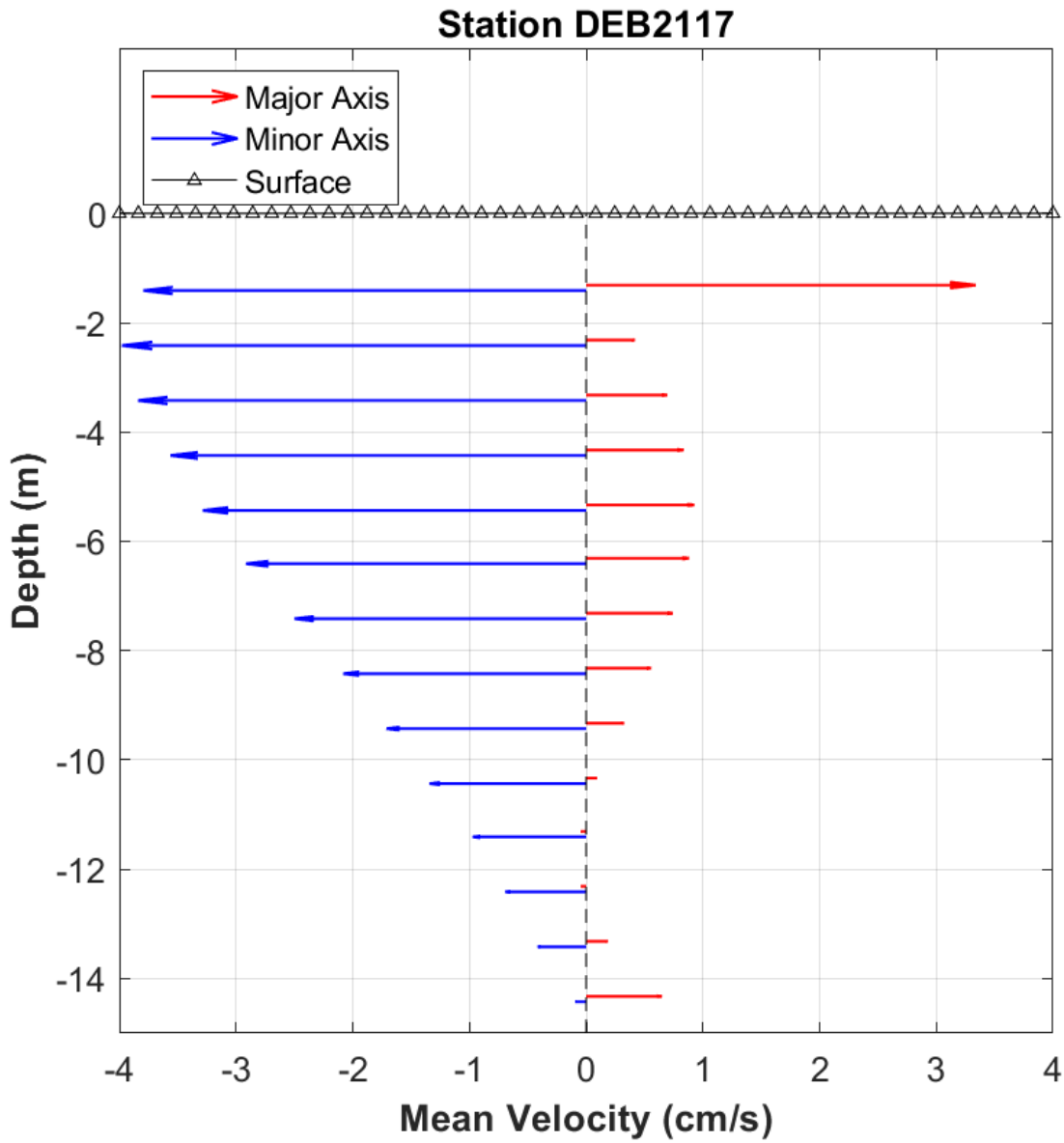


Figure 36. DEB2117 mean velocity (cm/s) profile along the major axis (red vectors) and minor axis (blue vectors) by depth. Only bins that passed quality control criteria are shown. This station was configured to collect 1-m bins.

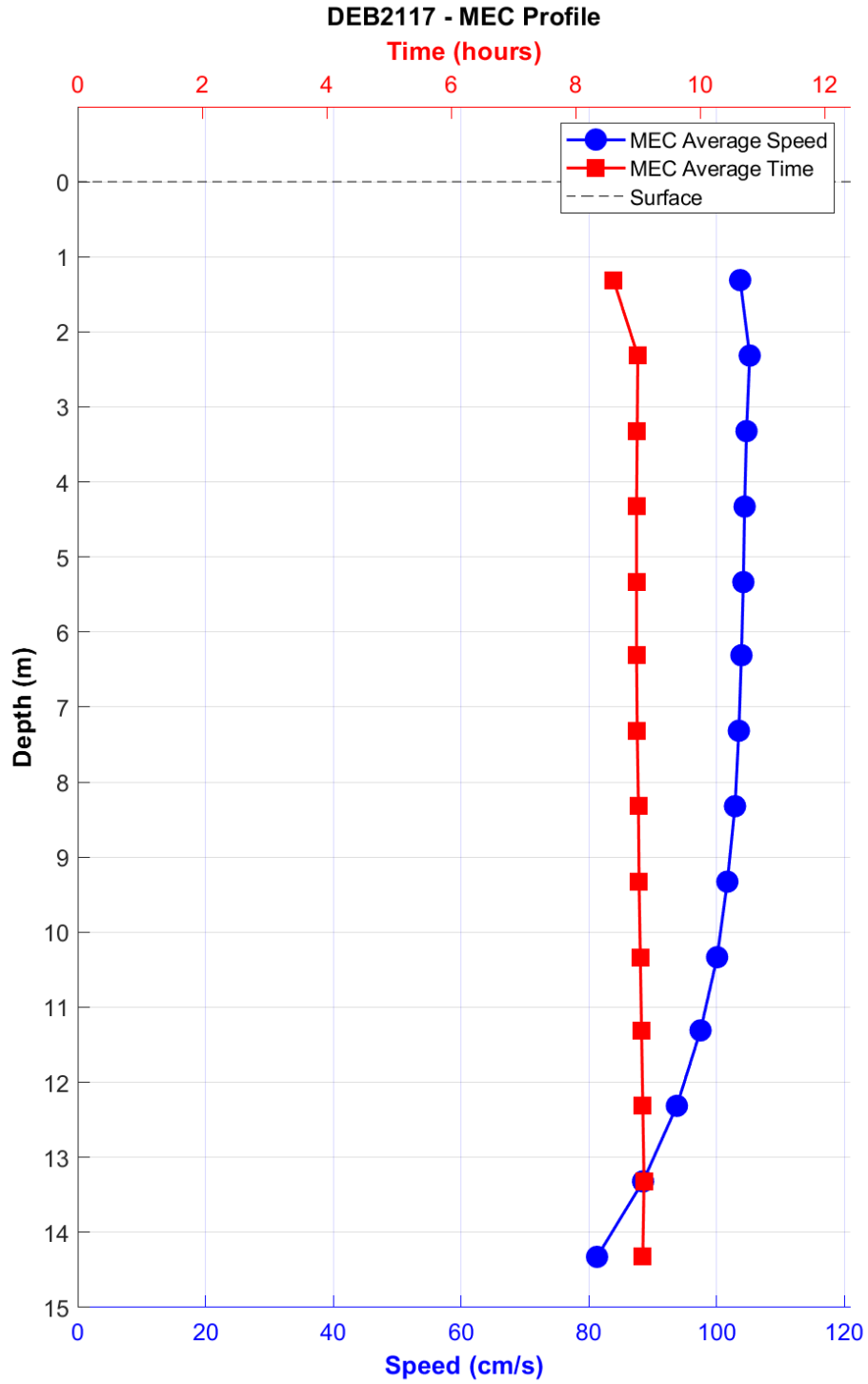


Figure 37. DEB2117 maximum ebb current (MEC) timing (Greenwich Intervals [GI], red squares, upper x-axis) and speed (blue circles, lower x-axis) by depth.

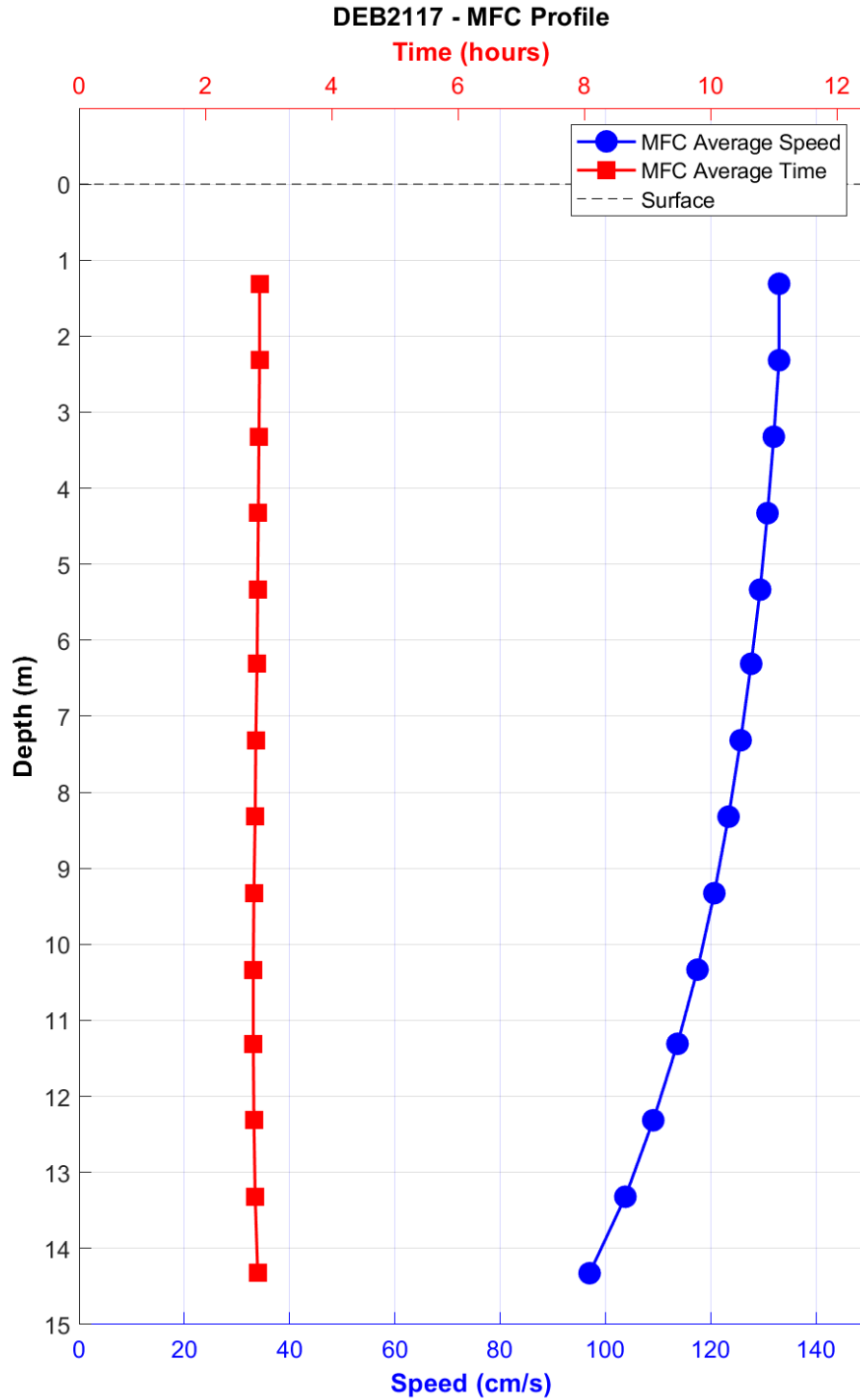


Figure 38. DEB2117 maximum flood current (MFC) timing (Greenwich Intervals [GI], red squares, upper x-axis) and speed (blue circles, lower x-axis) by depth.

5.5 DEB2119

DEB2119 Marcus Hook Bar (north) was equipped with a 1000 kHz Nortek ADP mounted in mTRBM in 9.7 m depth. With an upward orientation, the sensor was deployed between July 23, 2021, and November 9, 2021, for almost 109 days. LSQHA analysis was run (25 constituents)

with custom QC due to some outliers. This station was in the Delaware River, south of the navigational channel and just upriver from where Oldmans Creek enters.

The currents are semidiurnal and pretty tidal (97%). Since the station is located in the river, the currents follow its orientation, and they are rectilinear. The ebbs are a bit stronger than the floods, and they are both stronger near the surface versus speeds at the bottom. The fastest speeds occur near the surface in bin 6 (1.9 m): MEC speeds reached 102.4 cm/s (1.99 kn), and MFC speeds reached 90.5 cm/s (1.76 kn). The AZI are steady at 67 degrees in all bins. Bins 1-6 have good data, and bins 1 (6.9 m), 3 (4.9 m), and 6 (1.9 m) are recommended for prediction bins. They represent strongest speeds near the surface, close to 4.6 m depth speeds, and bottom speeds. Bin 7 also doesn't look bad, but it is noisier: more noise on echo intensity plots and more scattered on the N/E velocity scatter plots.

Hurricane Ida can be seen on the raw data speed/direction plots near September 2, 2021 (speeds increased).

Predictions look very good and in agreement with observed data. This station supersedes historic station "Marcus Hook Bar (North)," ACT4366, which was occupied in 1985 for 4 days, and it was very close to DEB2119. Comparing bin 6 (1.9 m) to the historic observations, the historic MFC and MEC speeds were a little slower at 98.8 cm/s (1.92 kn) and 90.5 cm/s (1.76 kn) versus new observations at 102.4 cm/s (1.99 kn) and 88.5 cm/s (1.72 kn), respectively, but the historic ones were measured at 15 ft. The new flood direction is 67 degrees versus historic 59 degrees. The historic MFC and MEC GI timing was close to recent observations, and the historical MEC/MFC was occurring about 4-12 min earlier. This difference is really minimal.

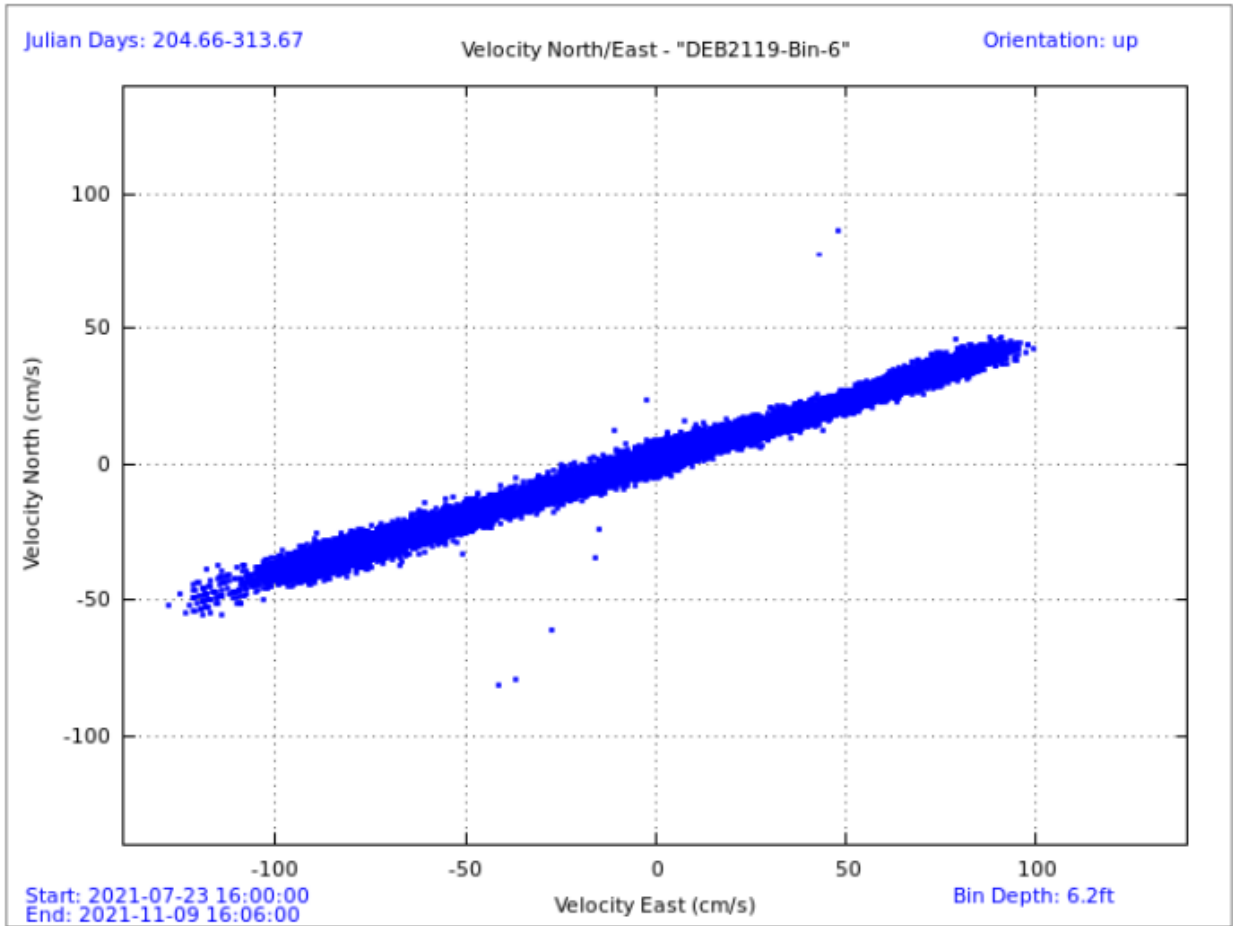


Figure 39. Scatter plot of north-versus-east velocity (cm/s) for station DEB2119 at the near-surface prediction bin, bin 6 at 1.9 m below mean lower low water (MLLW).

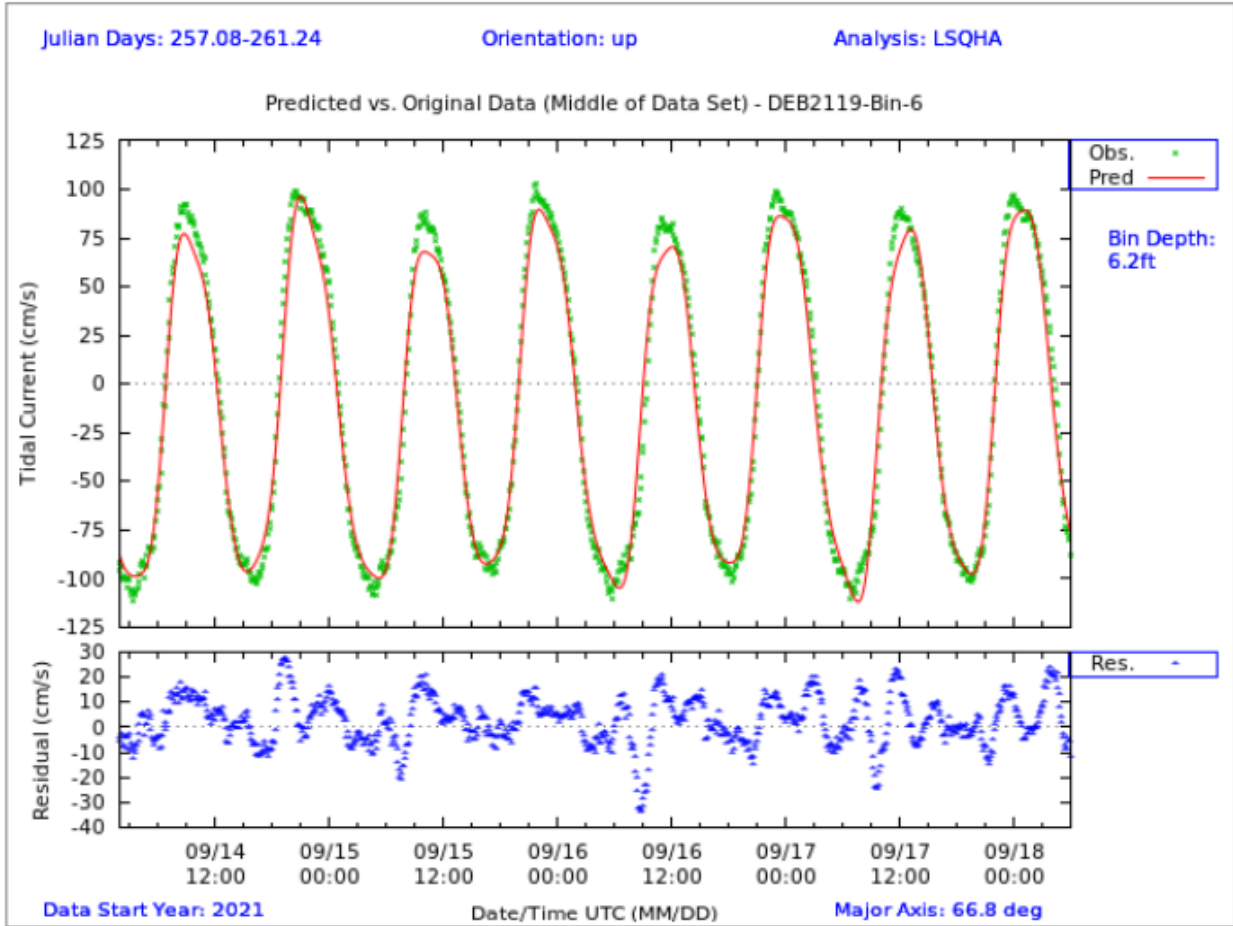


Figure 40. Comparison of observed major axis velocity data (green points) to predicted tidal velocity (red line) along the major axis for station DEB2119. The lower figure shows the non-tidal residual (blue dots), which is the difference between the predicted and observed velocity from the upper panel.

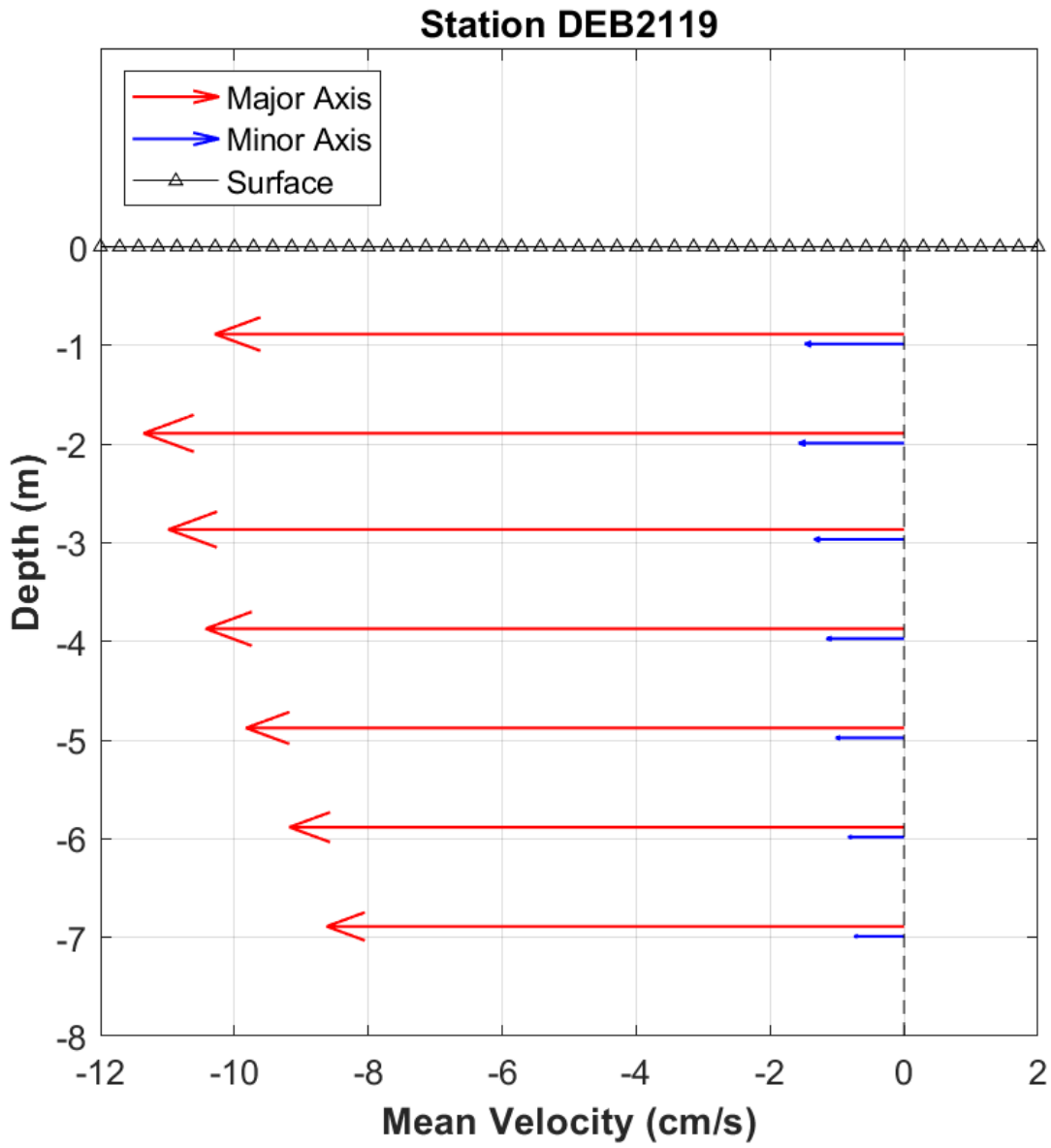


Figure 41. DEB2119 mean velocity (cm/s) profile along the major axis (red vectors) and minor axis (blue vectors) by depth. Only bins that passed quality control criteria are shown. This station was configured to collect 1-m bins.

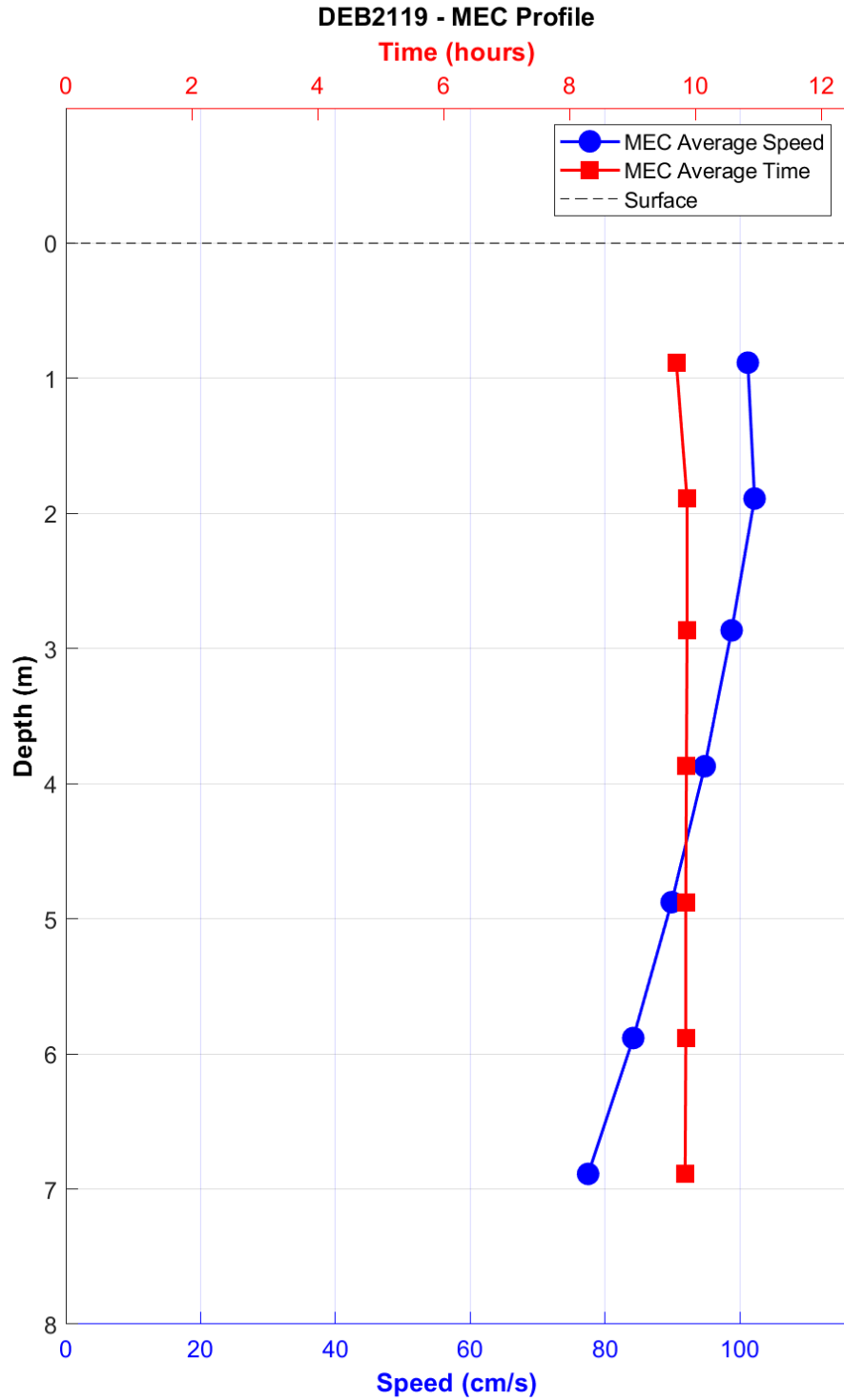


Figure 42. DEB2119 maximum ebb current (MEC) timing (Greenwich Intervals [GI], red squares, upper x-axis) and speed (blue circles, lower x-axis) by depth.

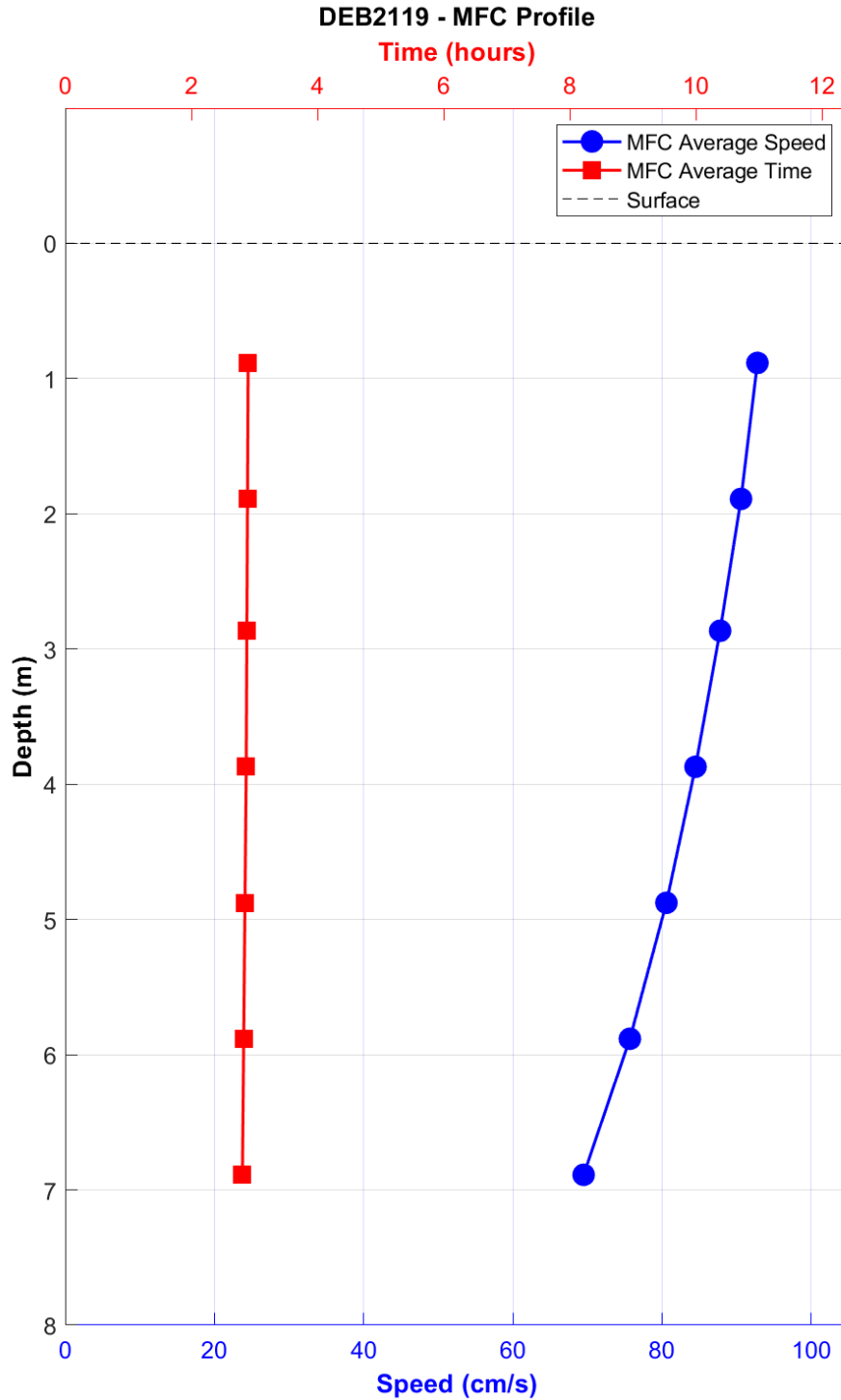


Figure 43. DEB2119 maximum flood current (MFC) timing (Greenwich Intervals [GI], red squares, upper x-axis) and speed (blue circles, lower x-axis) by depth.

5.6 DEB2128

DEB2128 (Gloucester Point) was equipped with an upward-facing 1200 kHz Workhorse ADCP. It was deployed at 15.9 m. The sensor collected 199.12 days of data from July 20, 2021, to November 16, 2021. This station is located in a bend in the Delaware River approximately 0.5 nm south of the Walt Whitman Bridge. There was indication of movement observed 3 times during

deployment from changes in the pitch, roll, and heading: around July 28-August 5, August 14-August 28, and November 9-November 16. The movements did not seem to affect the data.

Bins 1-12 are good. Currents at this location are semidiurnal and strongly tidal with 96% of the total current energy solved by LSQHA-25. The location is also strongly rectilinear with the major axis variance reaching up to 99.9%. The velocity scatter plot shows a northeast/southwest orientation as expected based on the curve of the Delaware River Channel at the location. There is a permanent ebb along the major and minor axis at depth (bins 1-10).

The flood current speeds are slightly faster than the ebbs at all depths. The fastest speeds are observed near the surface where MFC was 100.8 cm/s (1.96 kn) and MEC was 87.97 cm/s (1.71 kn). Bins 1 (13.5 m), 10 (4.5 m), and 12 (2.5 m) are recommended for prediction bins to capture the slower speeds at depth, 4.6 m navigation depth, and fastest currents at the surface.

This station is recommended to supersede the nearest historic stations, ACT4416 (Greenwich Point, northeast of, Delaware River) and ACT4411 (Gloucester, Delaware River), which are located 0.71 nm to the northeast and 0.45 nm to the south of the new station, respectively. Both of the historic stations collected 3 days of observations in May 1947 and recorded the mean of 2.1 m (7 ft) and 5.5 m (18 ft) depths. The data was mostly similar when comparing the historic station data to the surface bin (4.5 m), of the new station. The flood at the northern historic station was 20 degrees less than at the new station, and the ebb was 14 degrees less, but this might be due to the location of the ACT4416 on the eastern side of the river or its proximity to the mouth of Newtown Creek.

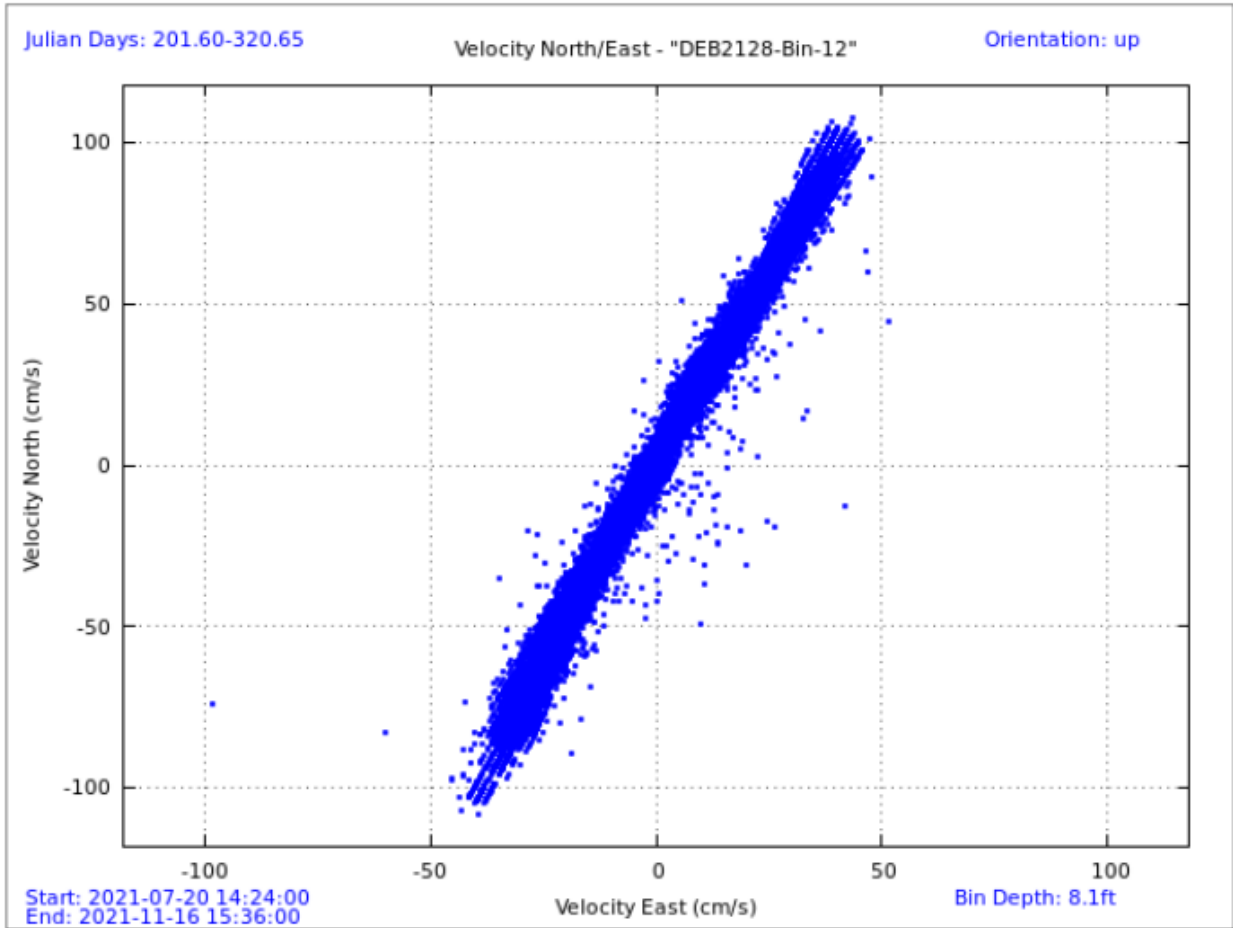


Figure 44. Scatter plot of north-versus-east velocity (cm/s) for station DEB2128 at the near-surface prediction bin, bin 12 at 2.5 meters (m) below mean lower low water (MLLW).

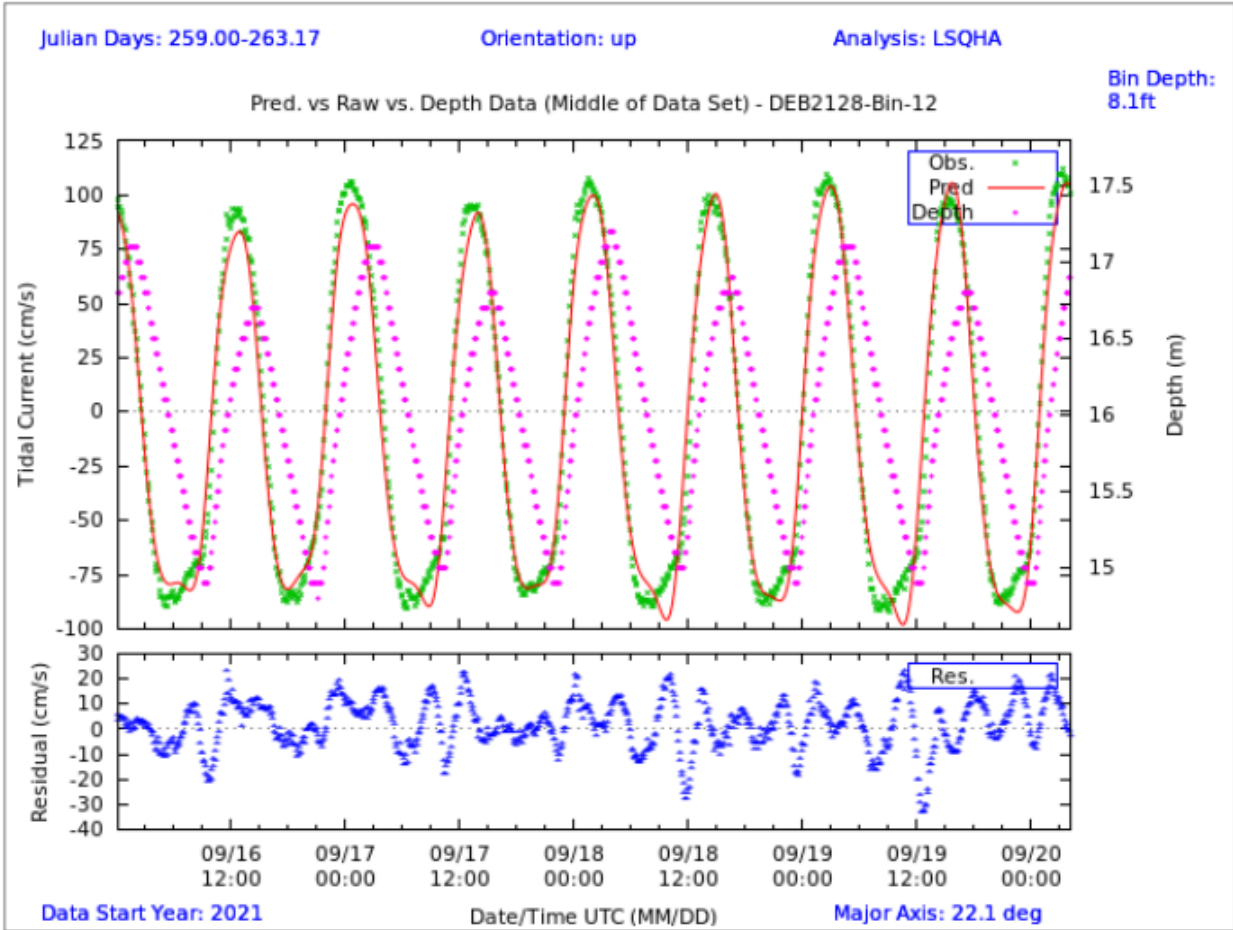


Figure 45. Comparison of observed major axis velocity data (green points) to predicted tidal velocity (red line) along the major axis for station DEB2128. The sensor depth (magenta dots) is measured using the acoustic Doppler current profiler (ADCP) pressure sensor and shows the tidally induced water level changes over time. The lower figure shows the non-tidal residual (blue dots), which is the difference between the predicted and observed velocity from the upper panel.

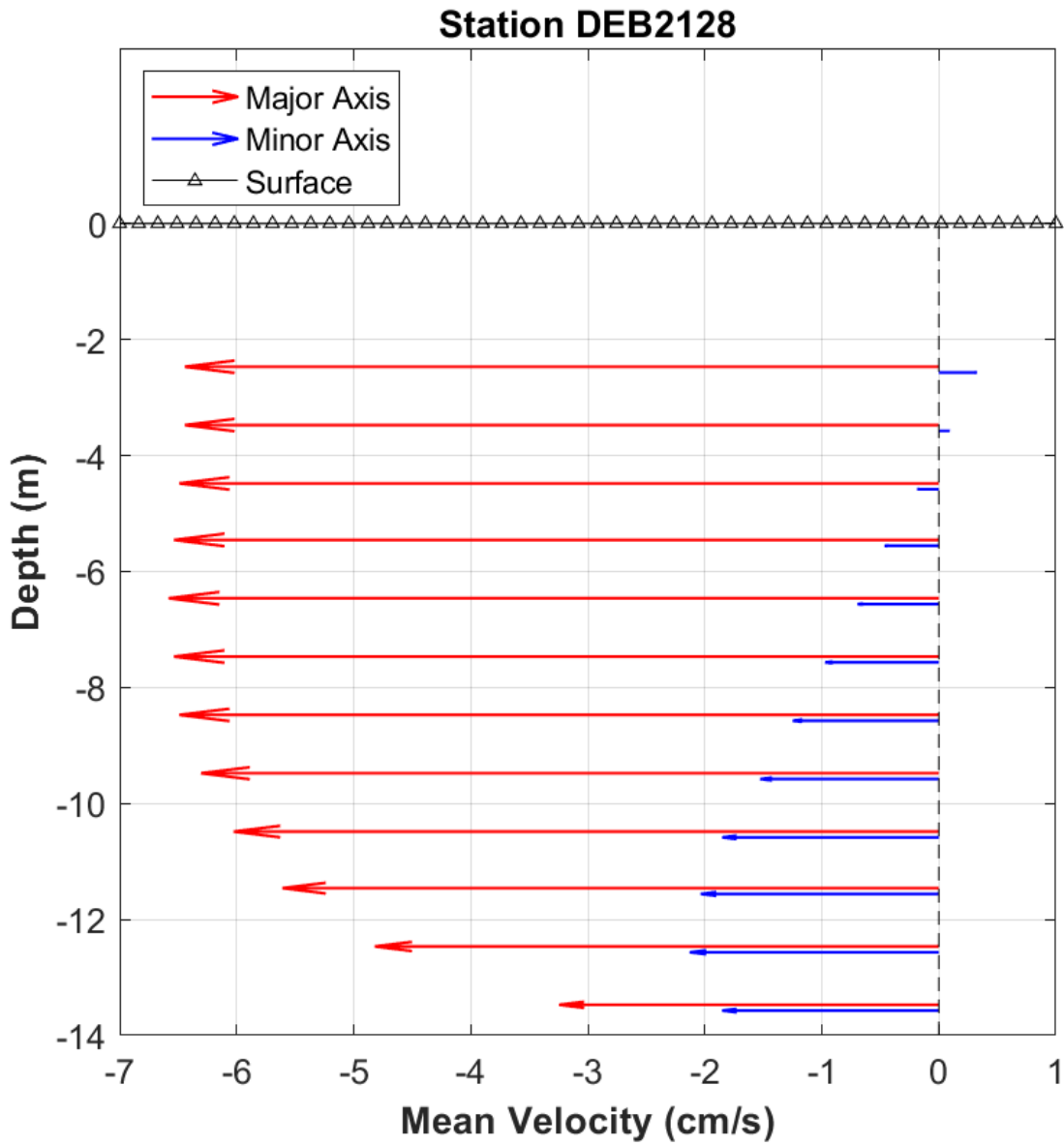


Figure 46. DEB2128 mean velocity (cm/s) profile along the major axis (red vectors) and minor axis (blue vectors) by depth. Only bins that passed quality control criteria are shown. This station was configured to collect 1-m bins.

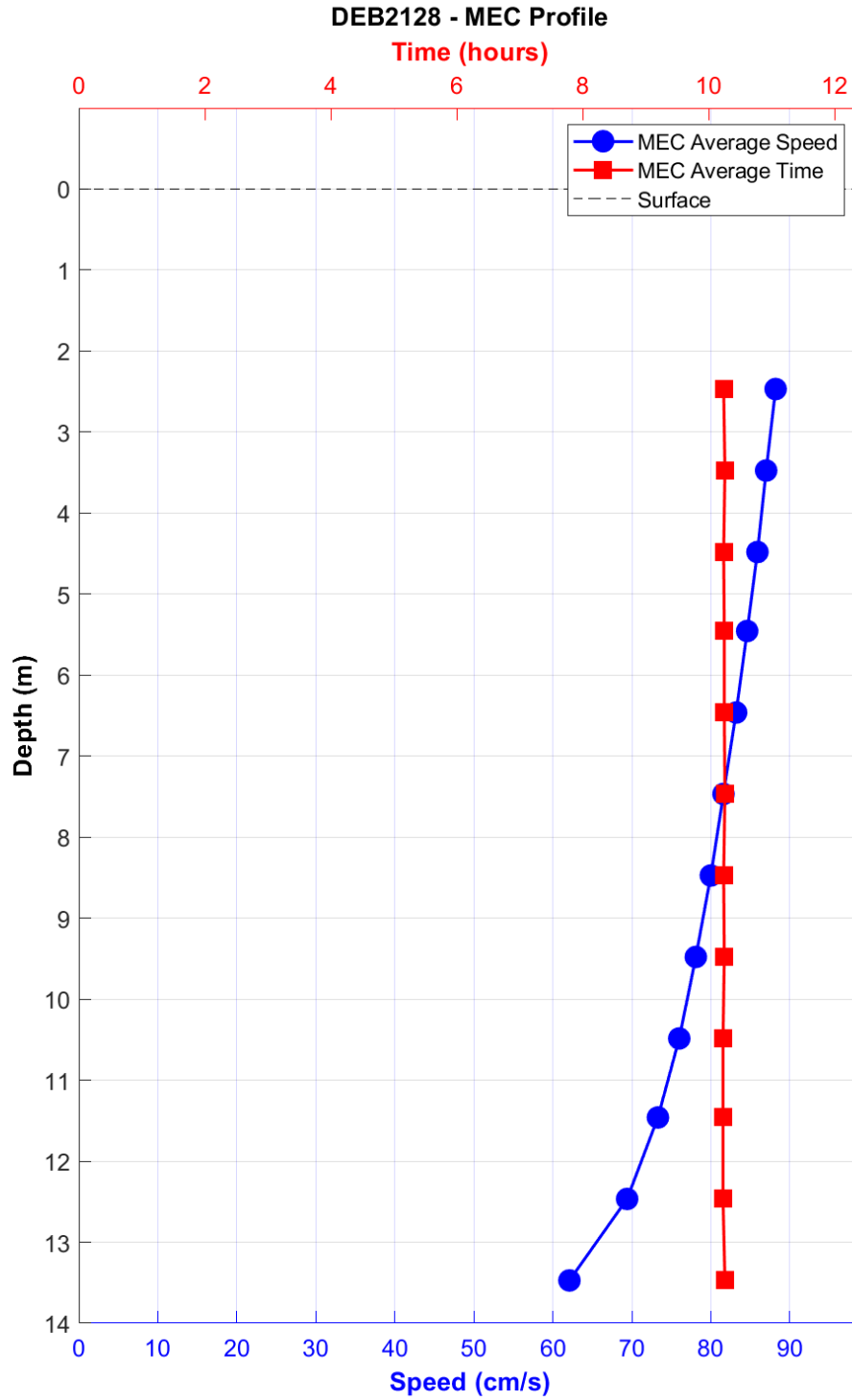


Figure 47. DEB2128 maximum ebb current (MEC) timing (Greenwich Intervals [GI], red squares, upper x-axis) and speed (blue circles, lower x-axis) by depth.

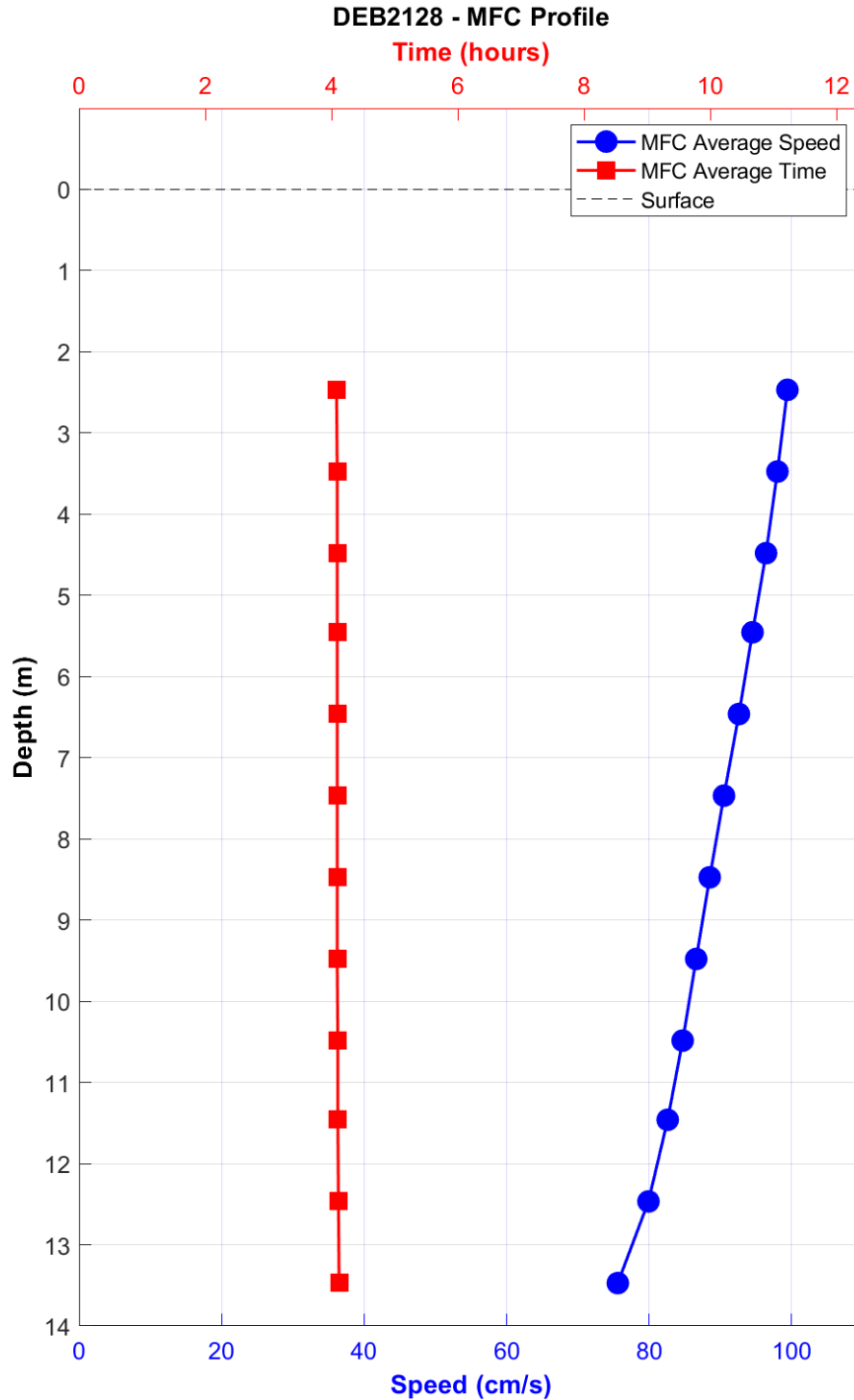


Figure 48. DEB2128 maximum flood current (MFC) timing (Greenwich Intervals [GI], red squares, upper x-axis) and speed (blue circles, lower x-axis) by depth.

5.7 DEB2132

DEB2132, Edgewater Range at Devlin Range, collected 54 days of data using an upward-facing 600 kHz ADCP mounted in a GP-48 bottom mount. The station was located 0.8 nm downriver from the Burlington-Bristol Bridge. Despite movement of the mount around October 4-October 21, 2021, the data passed all QC checks, and data looks very good. The tidal current

predictions look good most of the time. However, during the time of the movement, predicted floods are often 25-50 cm/s too slow. Detide plots show signs of under-predicting floods again starting November 10, 2021, until the recovery.

This station has an M2 constituent that is dominant (10 times larger than most of the others). The very rectilinear (99.9%), semidiurnal currents follow the channel orientation. LSQHA-24 solves up to 91% of the total current energy. Floods occur slightly earlier at depth while the ebbs occur earlier at surface. There is a strong mean ebb along the major axis reaching over 15.4 cm/s (0.3 kn) near the surface. A flooding event around October 28-October 29, 2021—observed through both the velocity data and echo amplitudes—leads to large residuals. The predictions consistently under-predicted the maximum speeds, especially on the floods. Bins 1-9 have good data. The historic station is based on 16 days of data collected in 1984 at 6.4 m below MLLW. Comparing bin 4 (6.8 m), the historic station observed slower currents (~ 5.1 cm/s or 0.1 kn) at very similar ebb directions. The flood direction varies by ~13 degrees. The flood timing is very similar while the ebb timing recently observed is later than the historic GI timing by about an hour and 15 minutes.

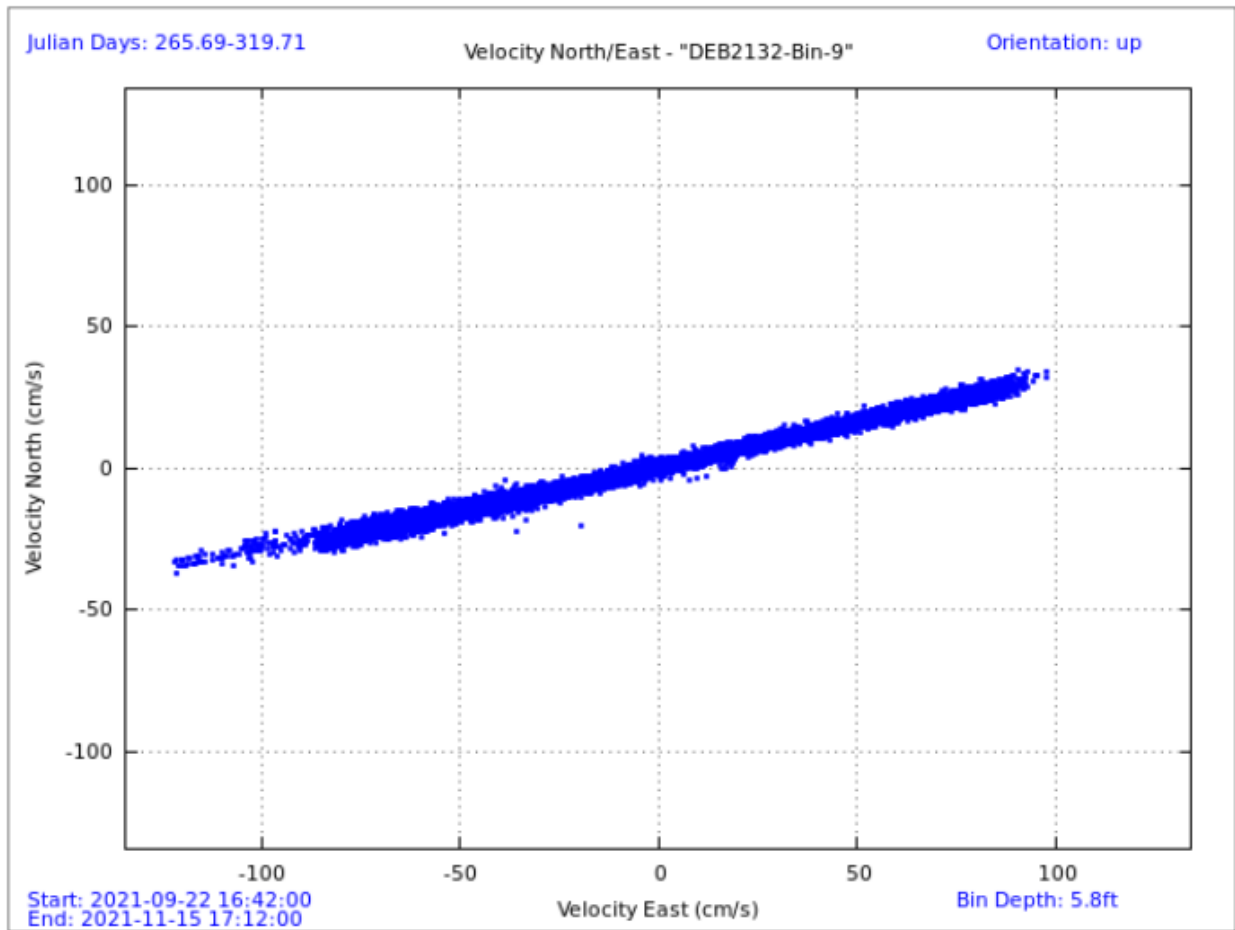


Figure 49. Scatter plot of north-versus-east velocity (cm/s) for station DEB2132 at the near-surface prediction bin, bin 9 at 1.8 meters (m) below mean lower low water (MLLW).

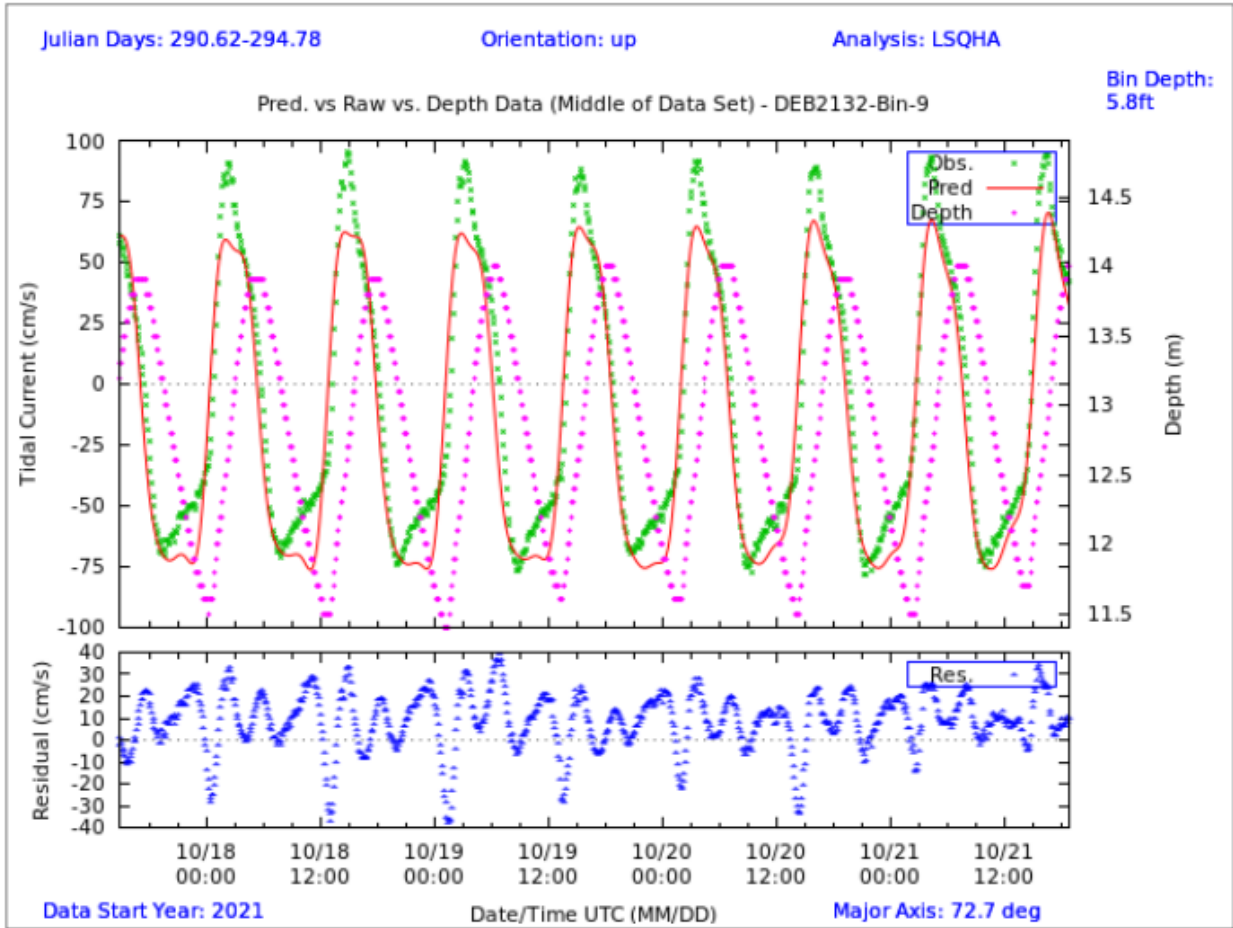


Figure 50. Comparison of observed major axis velocity data (green points) to predicted tidal velocity (red line) along the major axis for station DEB2132. The sensor depth (magenta dots) is measured using the acoustic Doppler current profiler (ADCP) pressure sensor and shows the tidally induced water level changes over time. The lower figure shows the non-tidal residual (blue dots), which is the difference between the predicted and observed velocity from the upper panel.

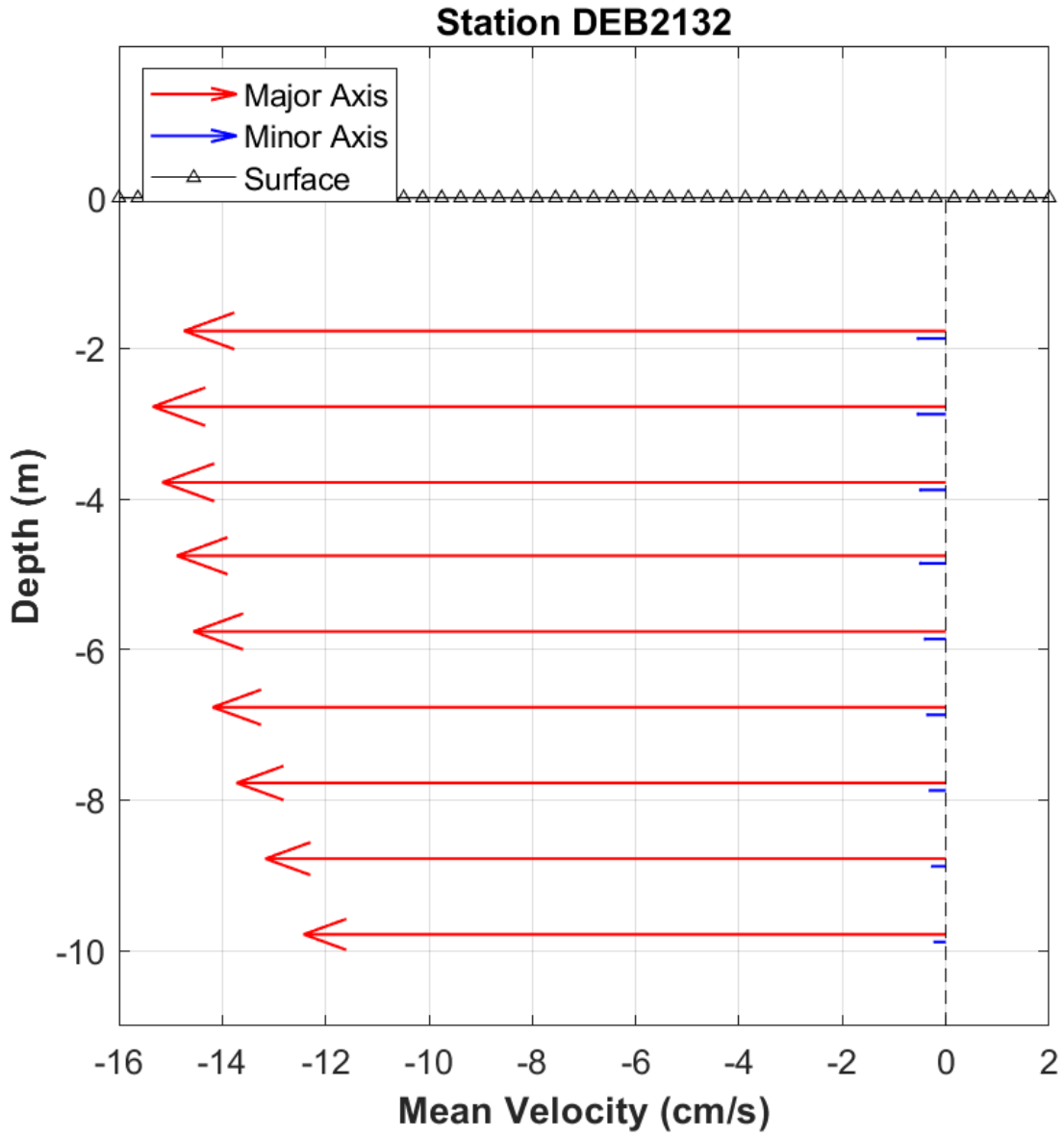


Figure 51. DEB2132 mean velocity (cm/s) profile along the major axis (red vectors) and minor axis (blue vectors) by depth. Only bins that passed quality control criteria are shown. This station was configured to collect 1-m bins.

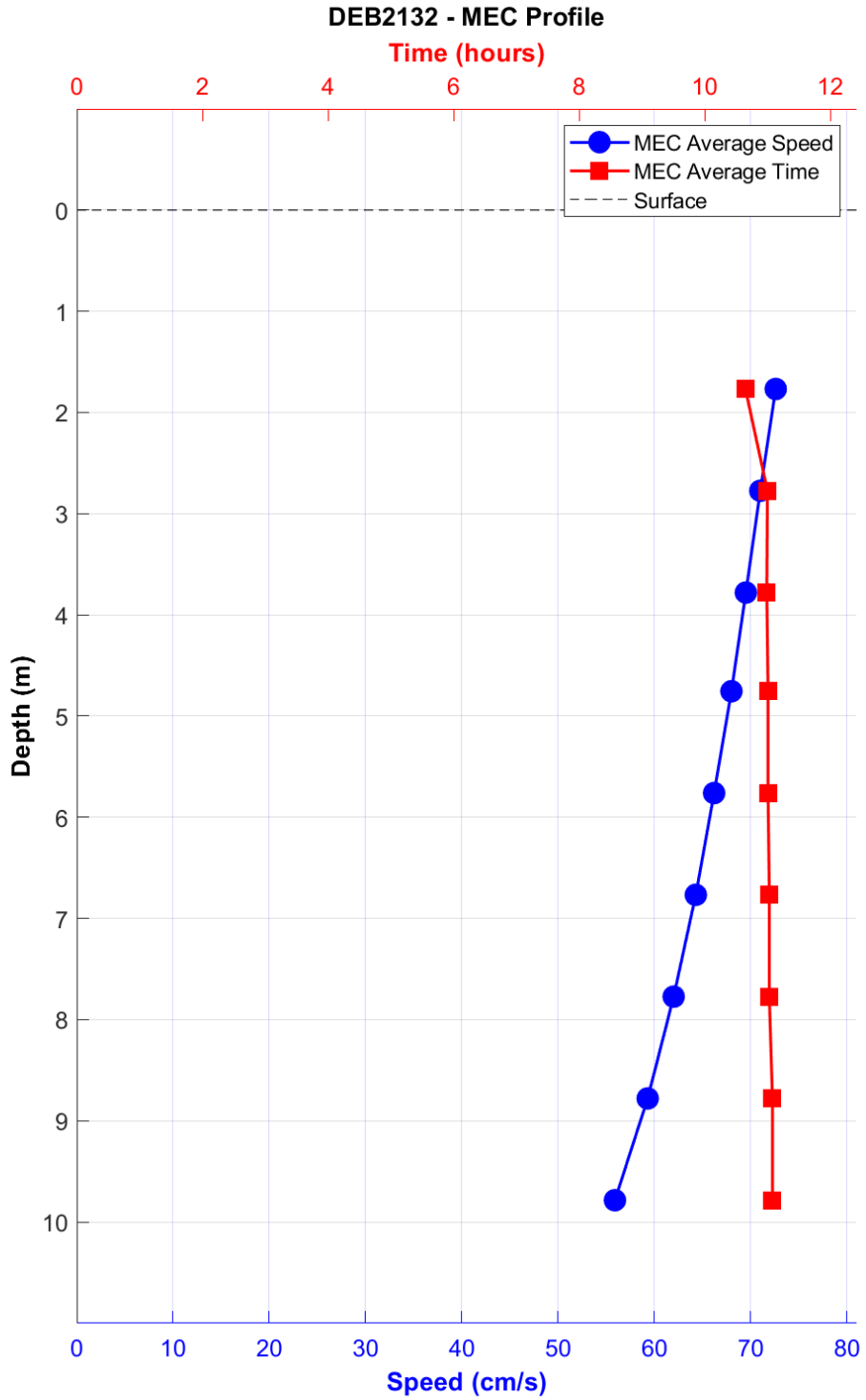


Figure 52. DEB2132 maximum ebb current (MEC) timing (Greenwich Intervals [GI], red squares, upper x-axis) and speed (blue circles, lower x-axis) by depth.

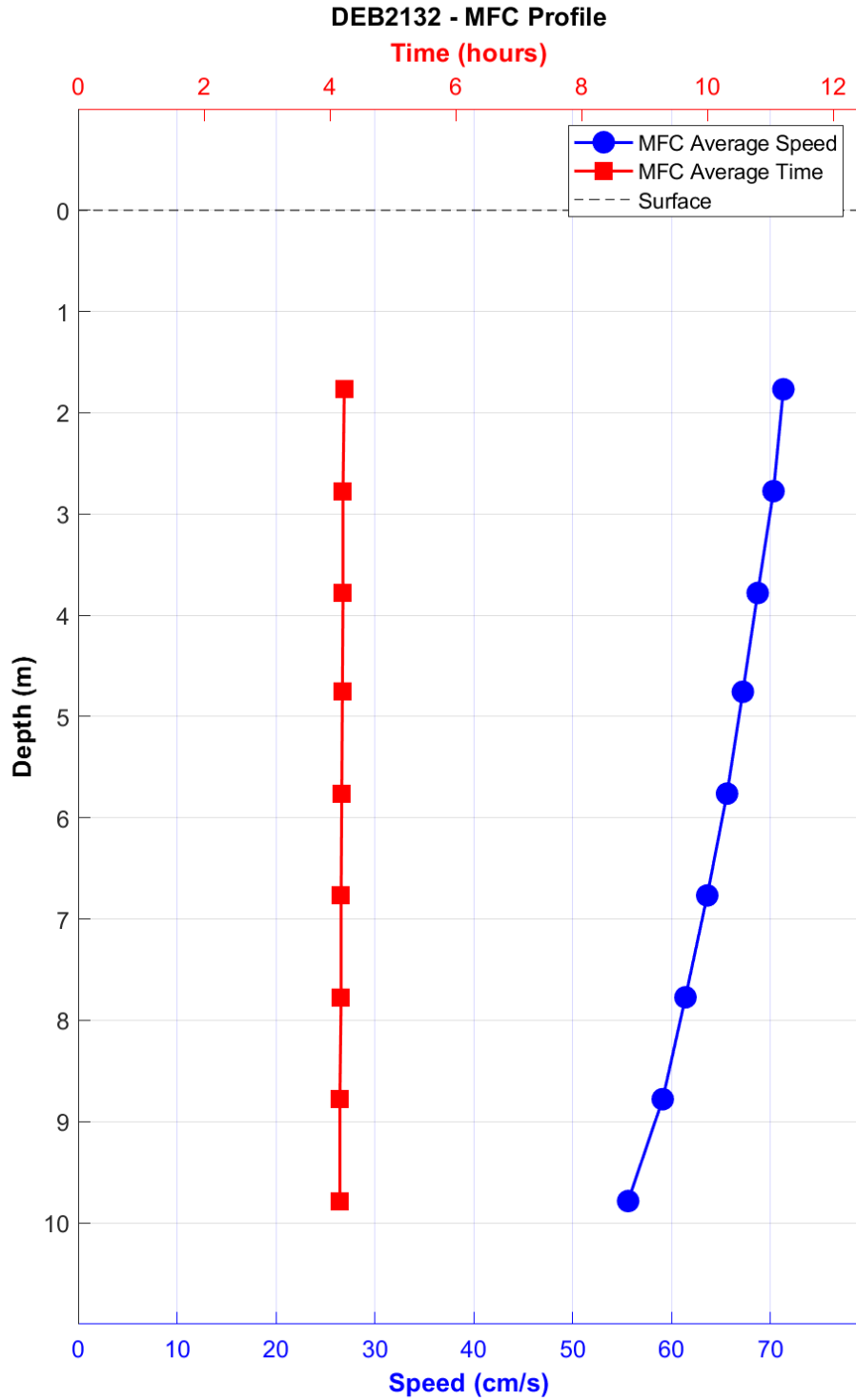


Figure 53. DEB2132 maximum flood current (MFC) timing (Greenwich Intervals [GI], red squares, upper x-axis) and speed (blue circles, lower x-axis) by depth.

6.0 SPATIAL VARIATION

6.1 Harmonic Constituents

Harmonic constituents were generated for all stations in this study using the methods described in Section 3.3. For most stations, tidal harmonic constituents show that the M2 tidal constituent (the principal lunar semidiurnal constituent) is the dominant constituent. This means that tidal characteristics for all stations in the Delaware Bay and River region are predominately semidiurnal. All stations are rectilinear; they exhibit a back-and-forth tidal current motion between flood and ebb, and exhibit no or very limited rotary characteristics. Figures 54-56 show the Defant ratio, which is the ratio of the principal diurnal constituents (O1, K1) to the principal semidiurnal component (M2, S2) of the tides for the major axis at each station.

The spatial distributions of select tidal ellipses of the principal semidiurnal and diurnal constituents are shown in Figures 57-68. The figures clearly show that M2 is the dominant constituent and that bathymetry (particularly the locations of narrow channels) is the driving force behind the relative strength and orientation of the M2 and other constituents, as well as the degree of rectilinearity of the ellipses.

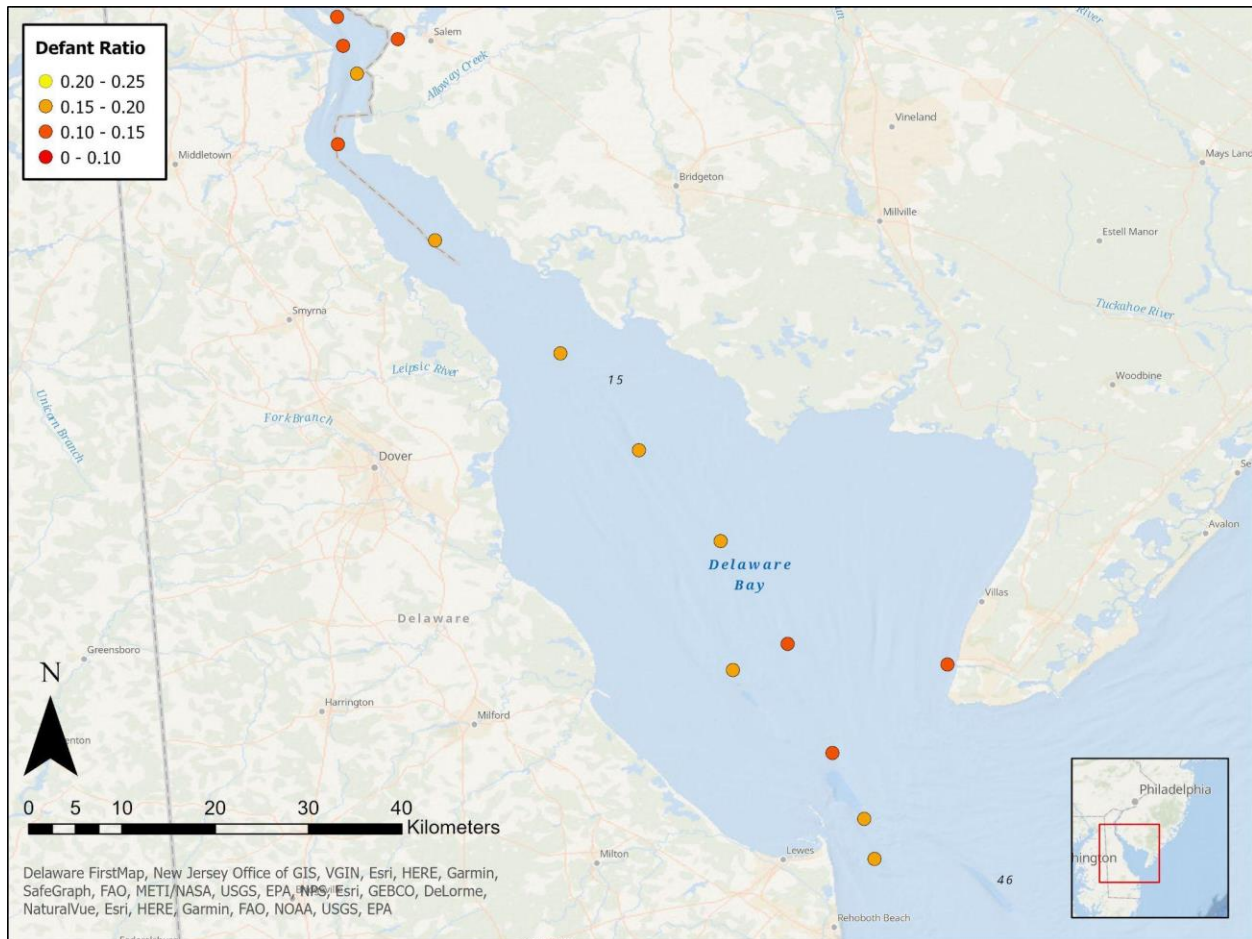


Figure 54. Defant ratios for the lower Bay for the near-surface prediction bin at survey stations. Semidiurnal tides (Defant ratio < 0.25) are observed at all stations.

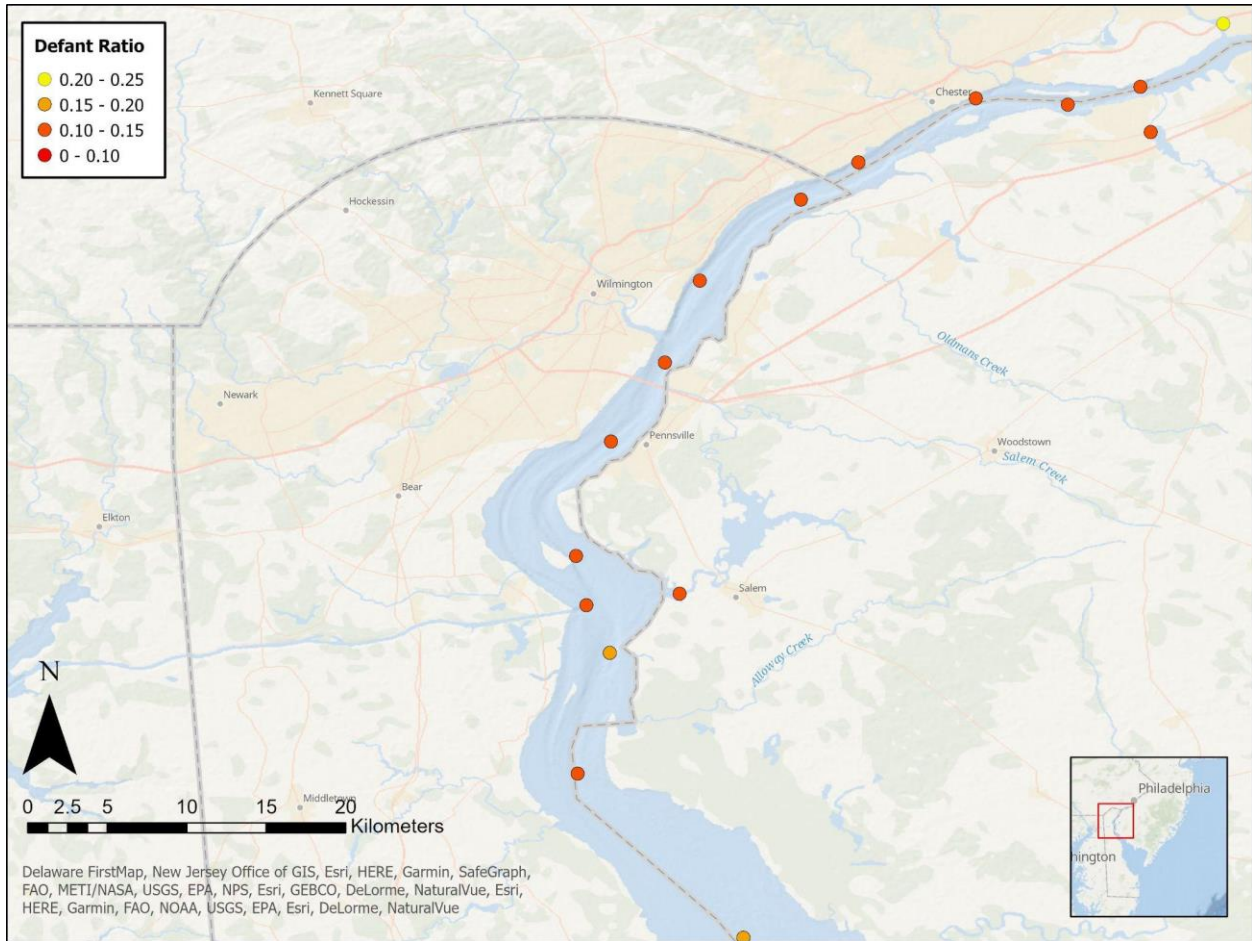


Figure 55. Defant ratios for the lower River for the near-surface prediction bin at survey stations. Semidiurnal tides (Defant ratio < 0.25) are observed at all stations.

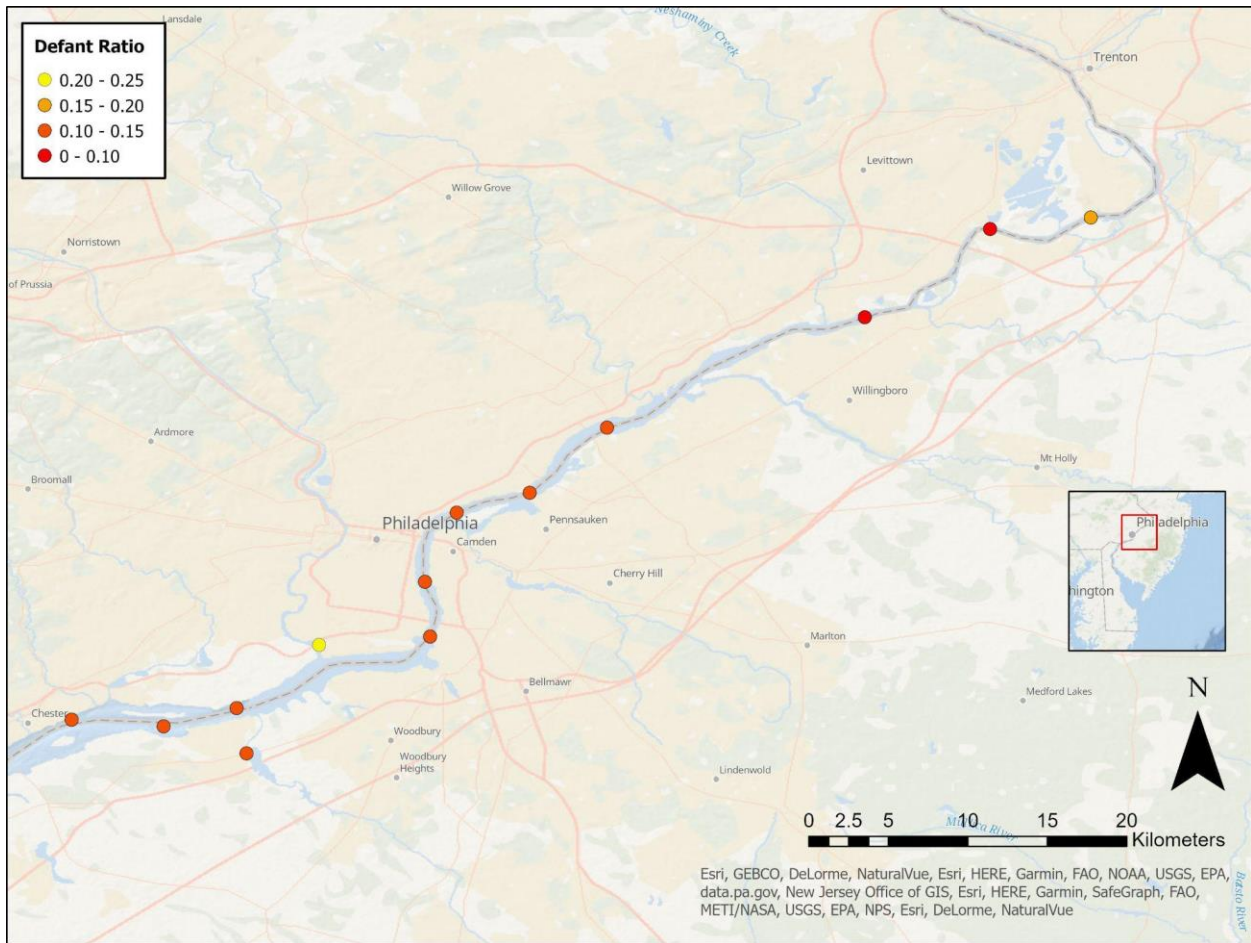


Figure 56. Defant ratios for the upper River for the near-surface prediction bin at survey stations. Semidiurnal tides (Defant ratio < 0.25) are observed at all stations.

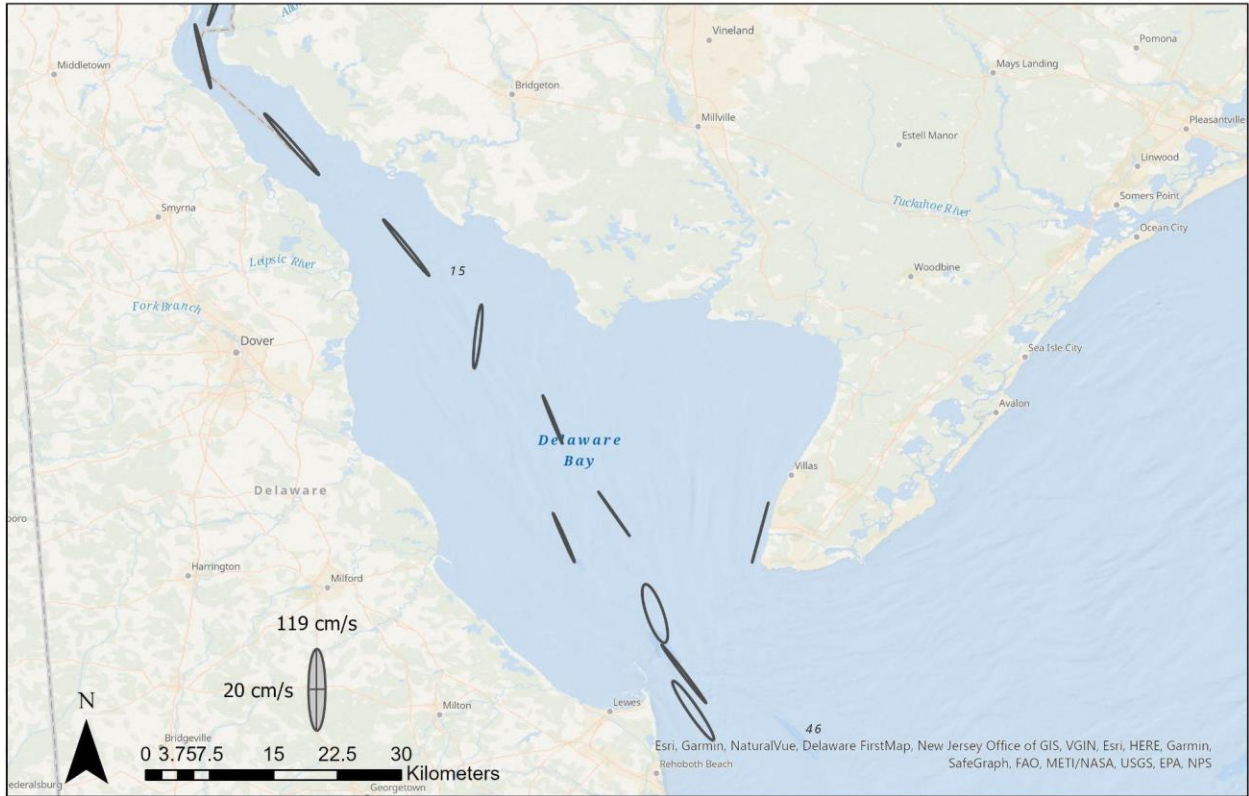


Figure 57. M2 tidal ellipses for prediction stations in Delaware Bay, showing the topographic steering of the ellipses.

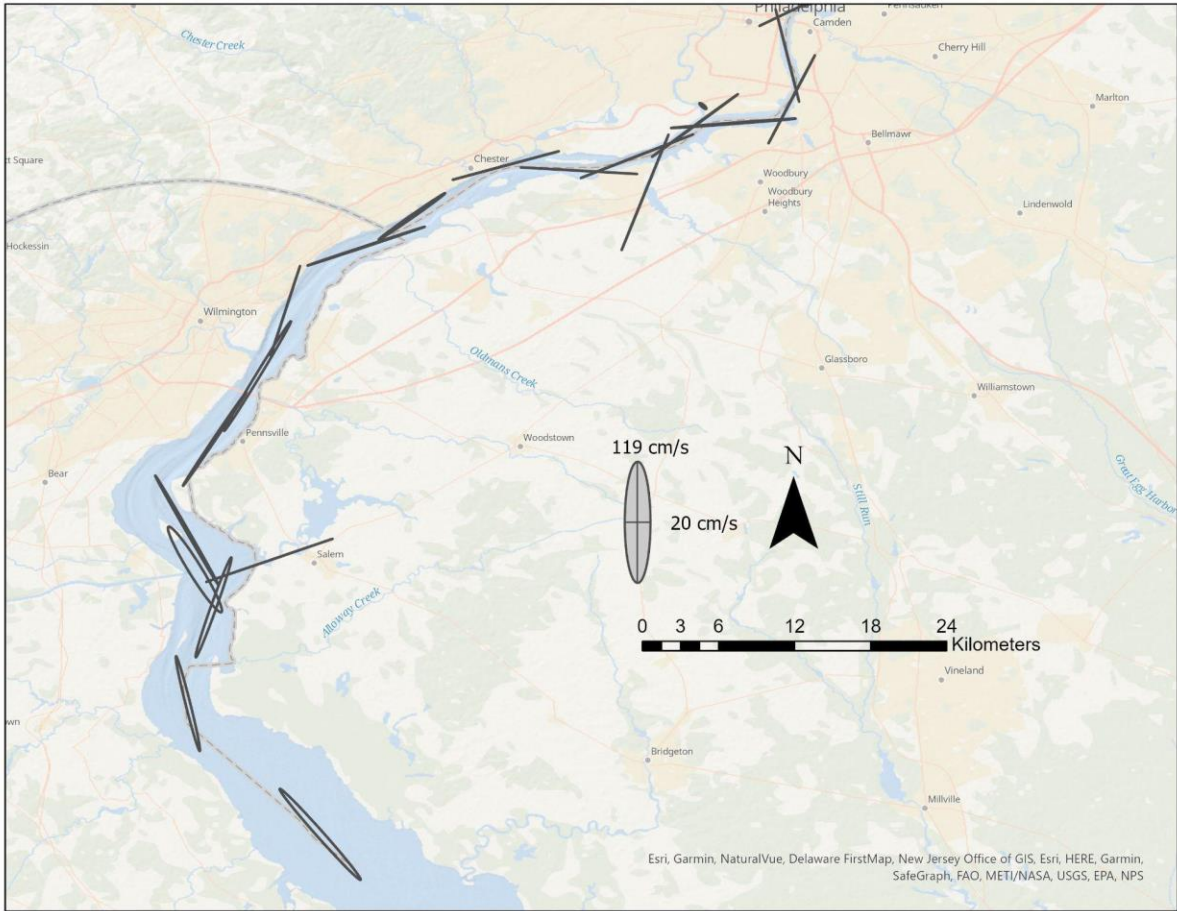


Figure 58. M2 tidal ellipses for prediction stations in the lower Delaware River, showing the topographic steering of the ellipses.

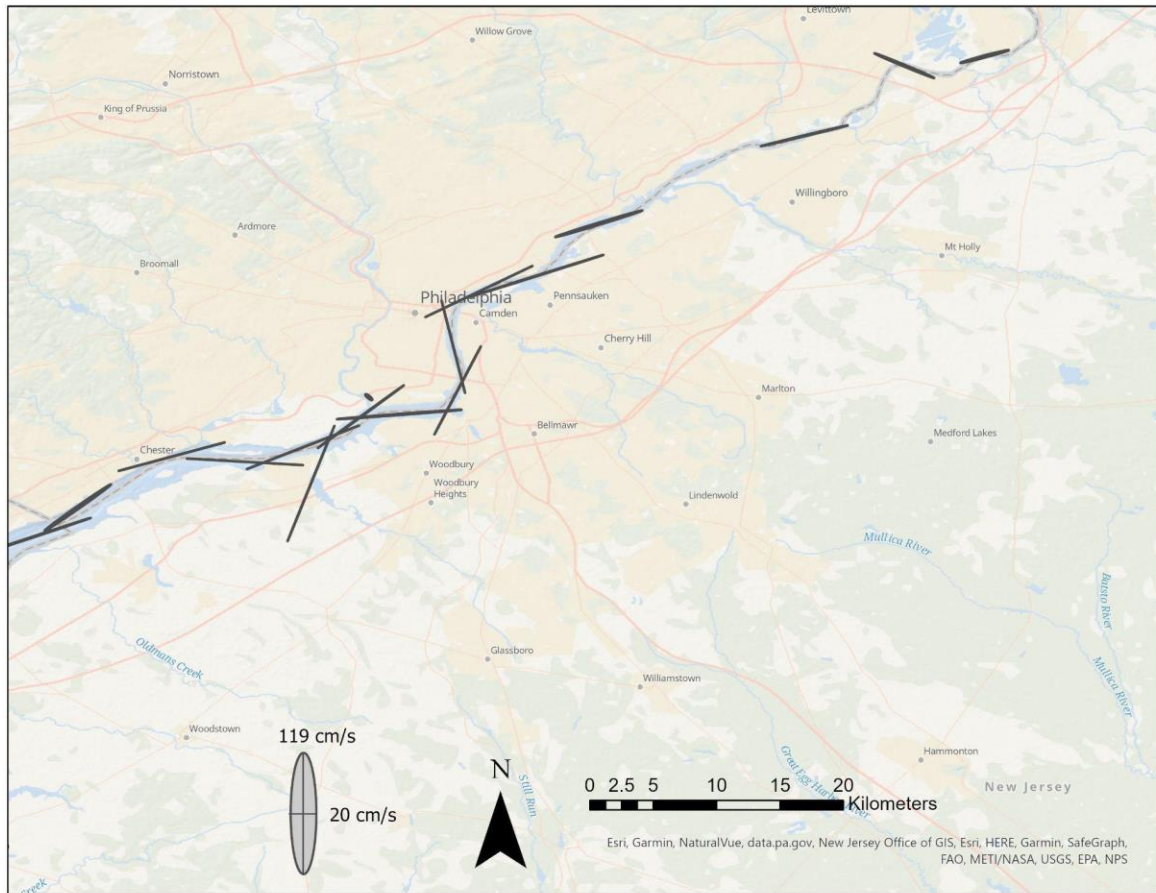


Figure 59. M2 tidal ellipses for prediction stations in upper Delaware River, showing the topographic steering of the ellipses.

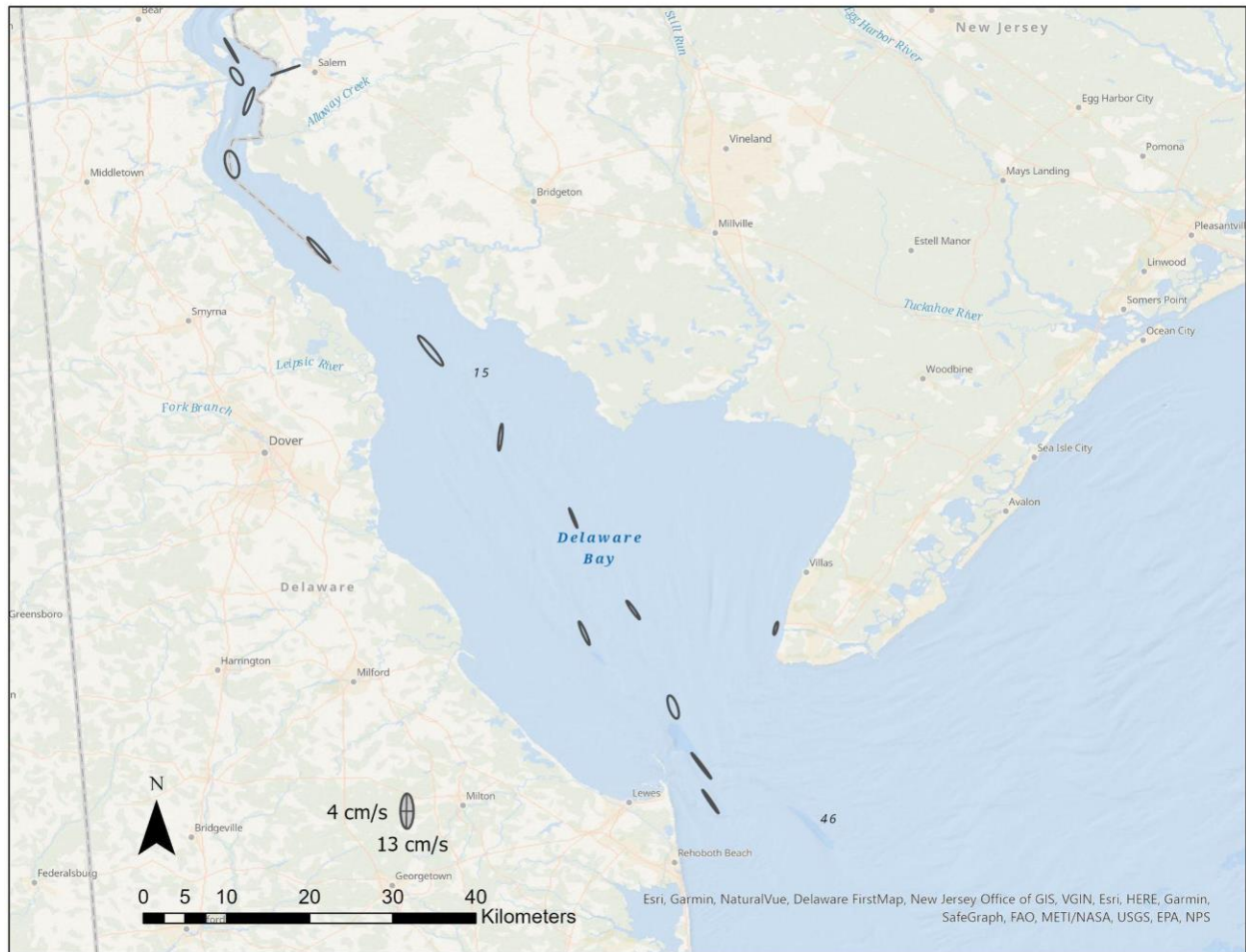


Figure 60. K1 tidal ellipses for prediction stations in Delaware Bay, showing the topographic steering of the ellipses. Note that these are on a different scale than M2 in order to better visualize the ellipses. These data are at about 1/4 the scale of the M2 data.



Figure 61. K1 tidal ellipses for prediction stations in the lower Delaware River, showing the topographic steering of the ellipses. Note that these are on a different scale than M2 in order to better visualize the ellipses. These data are at about 1/4 the scale of the M2 data.

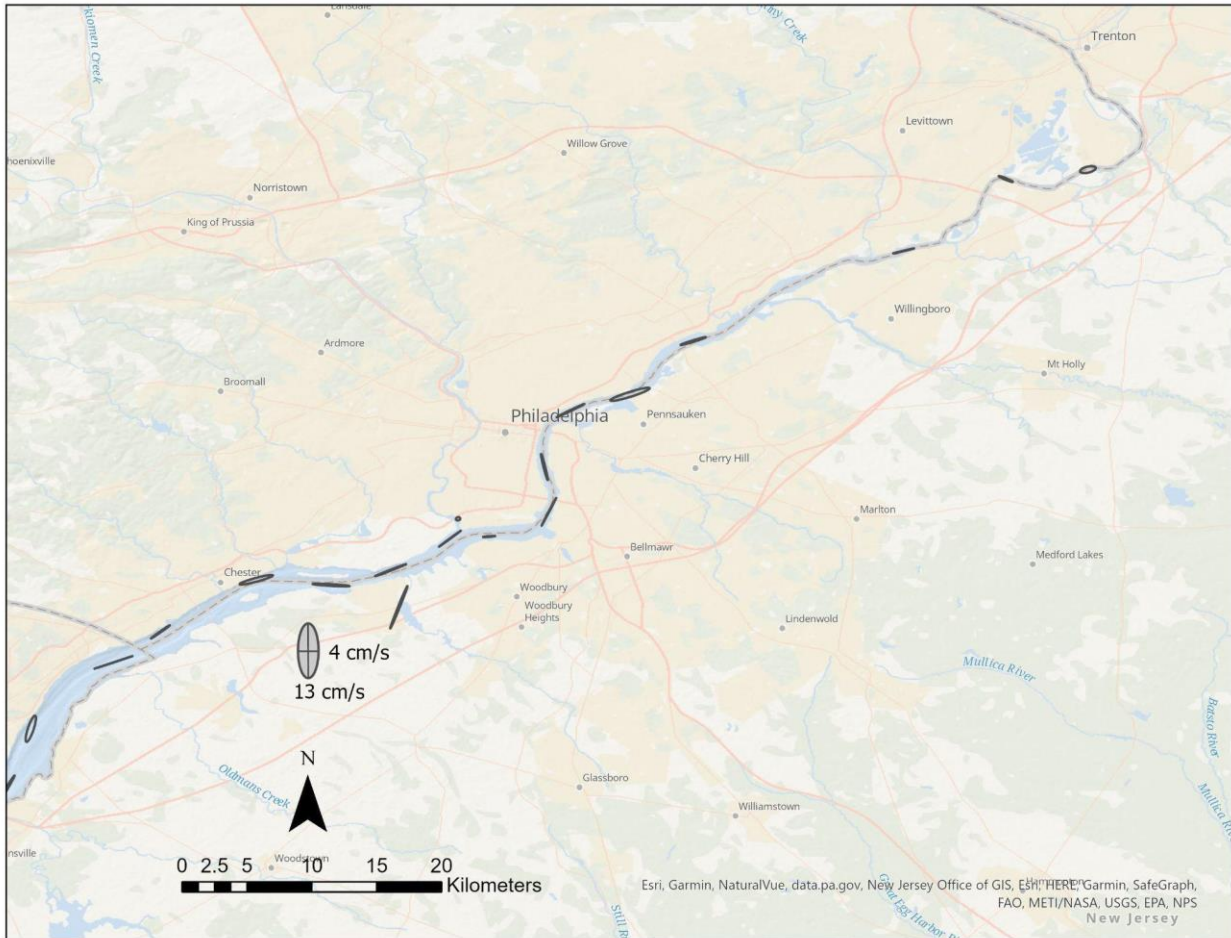


Figure 62. K1 tidal ellipses for prediction stations in the upper Delaware River, showing the topographic steering of the ellipses. Note that these are on a different scale than M2 in order to better visualize the ellipses. These data are at about 1/4 the scale of the M2 data.

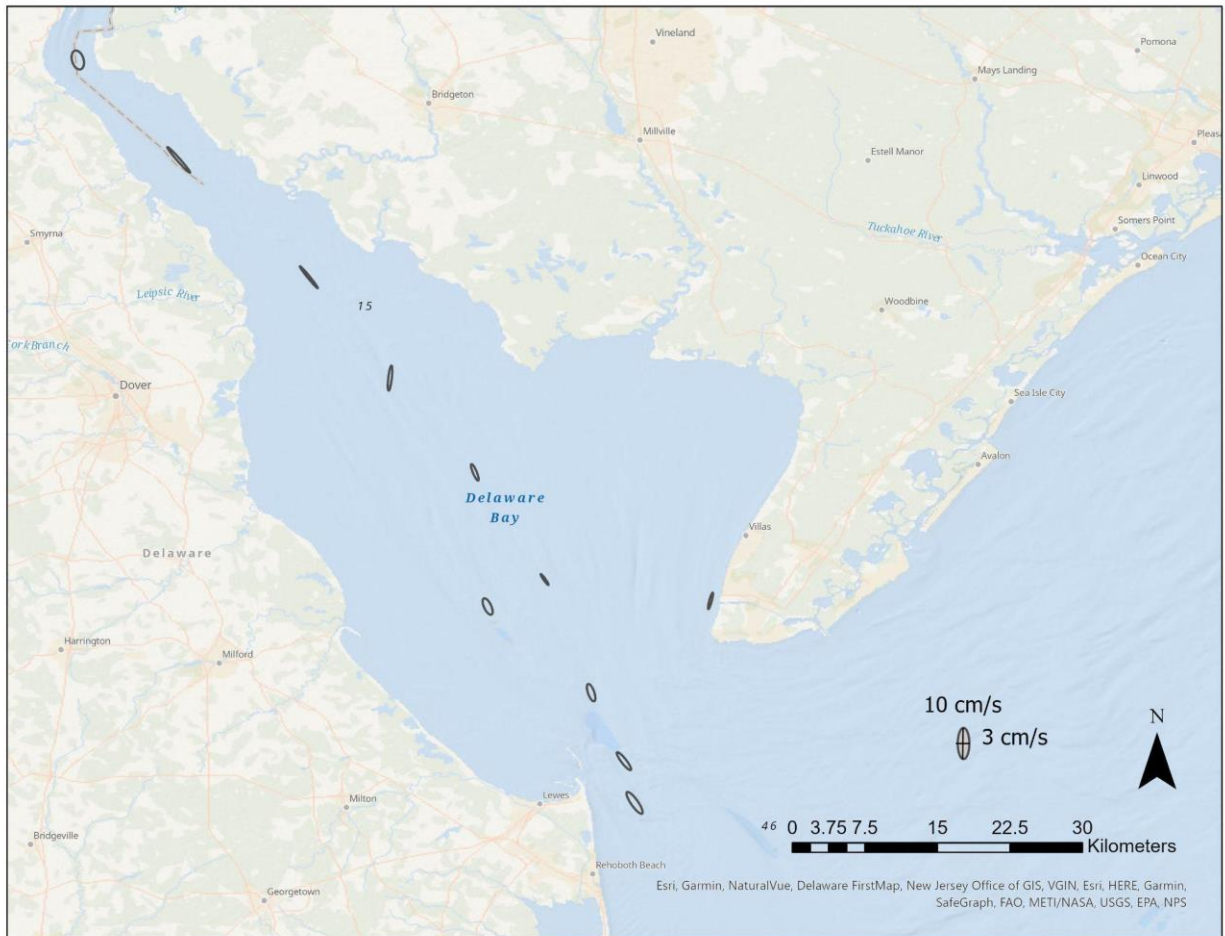


Figure 63. O1 tidal ellipses for prediction stations in Delaware Bay, showing the topographic steering of the ellipses. Note that these are on a different scale than M2 in order to better visualize the ellipses. These data are at about 1/4 the scale of the M2 data.



Figure 64. O1 tidal ellipses for prediction stations in the lower Delaware River, showing the topographic steering of the ellipses. Note that these are on a different scale than M2 in order to better visualize the ellipses. These data are at about 1/4 the scale of the M2 data.

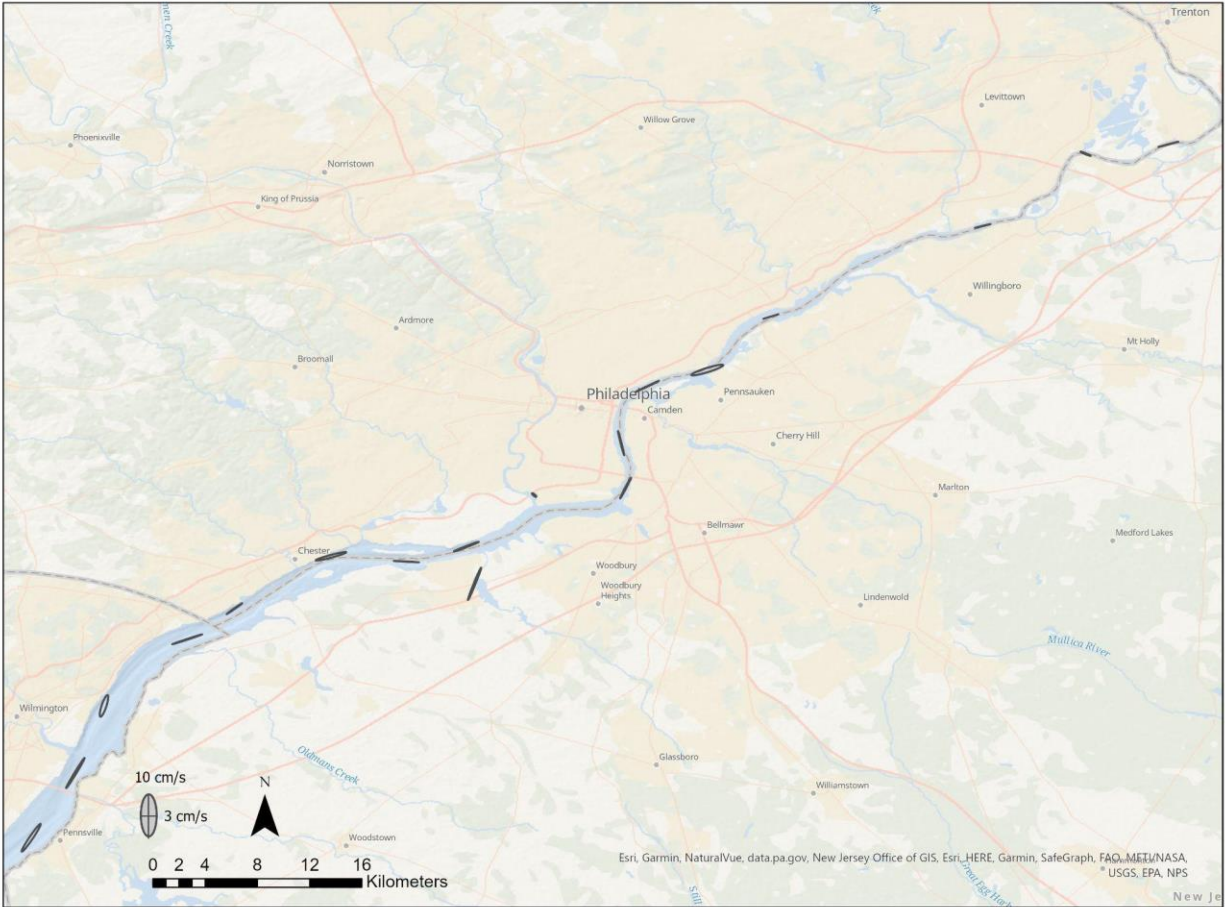


Figure 65. O1 tidal ellipses for prediction stations in the upper Delaware River, showing the topographic steering of the ellipses. Note that these are on a different scale than M2 in order to better visualize the ellipses. These data are at about 1/4 the scale of the M2 data.

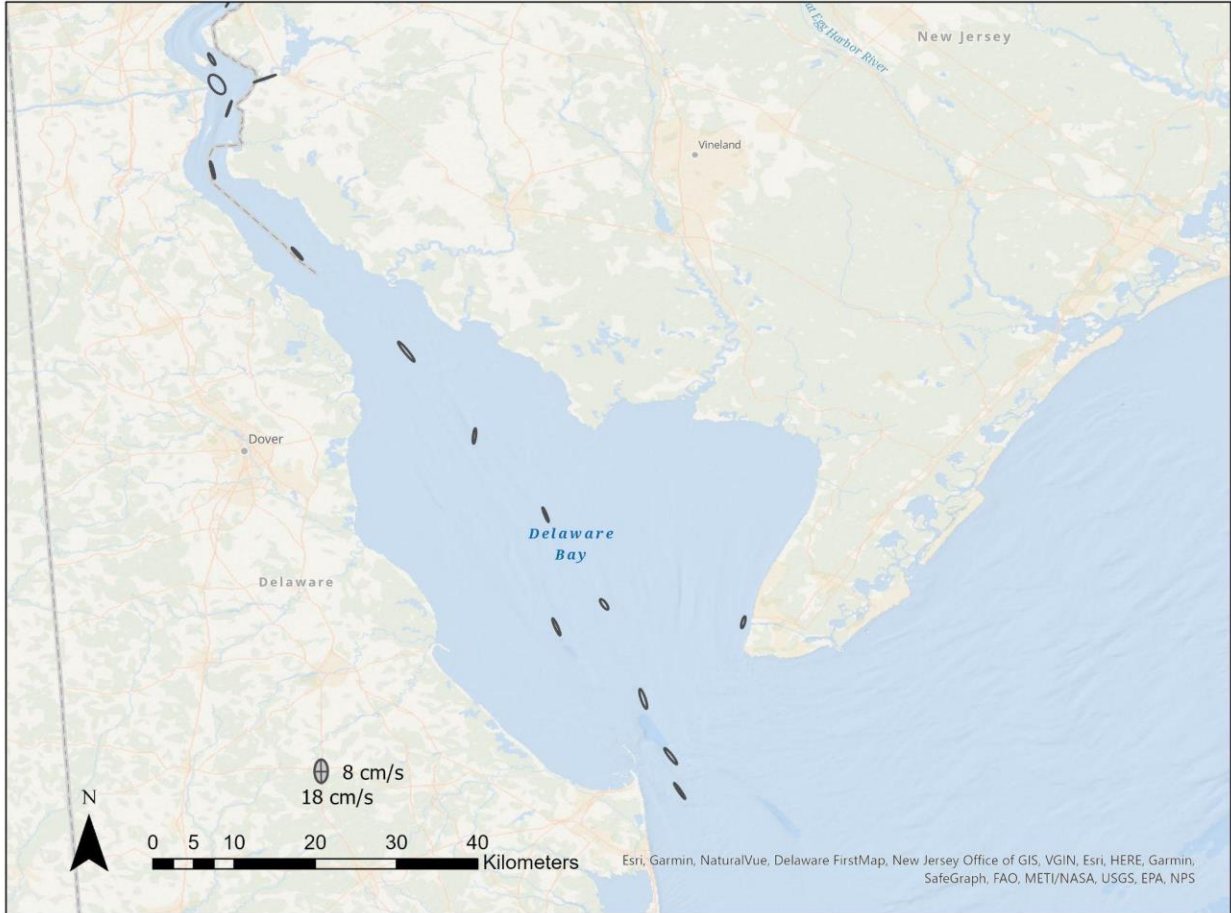


Figure 66. S2 tidal ellipses for prediction stations in Delaware Bay, showing the topographic steering of the ellipses. Note that these are on a different scale than M2 in order to better visualize the ellipses. These data are at about 1/2 the scale of the M2 data.

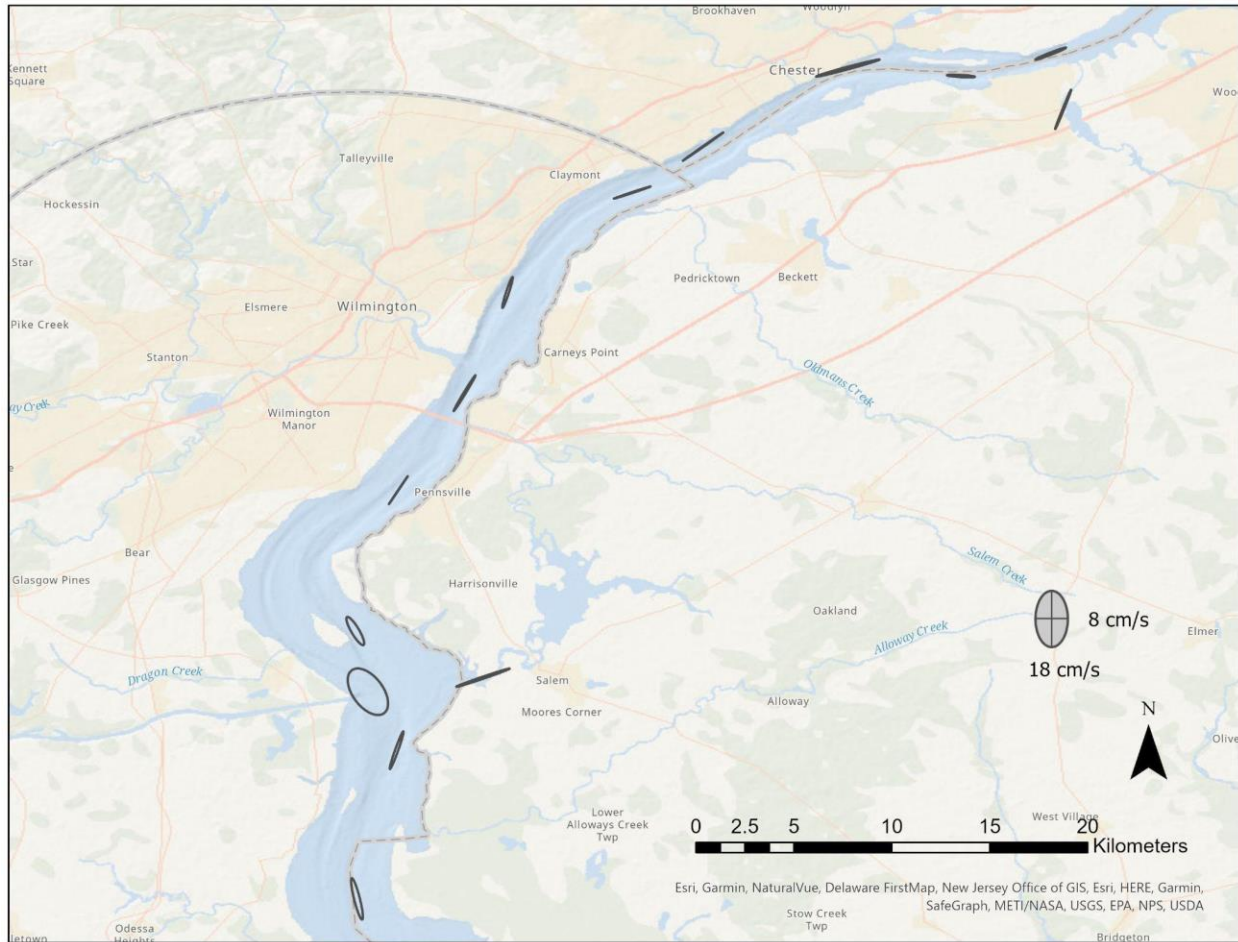


Figure 67. S2 tidal ellipses for prediction stations in the lower Delaware River, showing the topographic steering of the ellipses. Note that these are on a different scale than M2 in order to better visualize the ellipses. These data are at about 1/2 the scale of the M2 data.

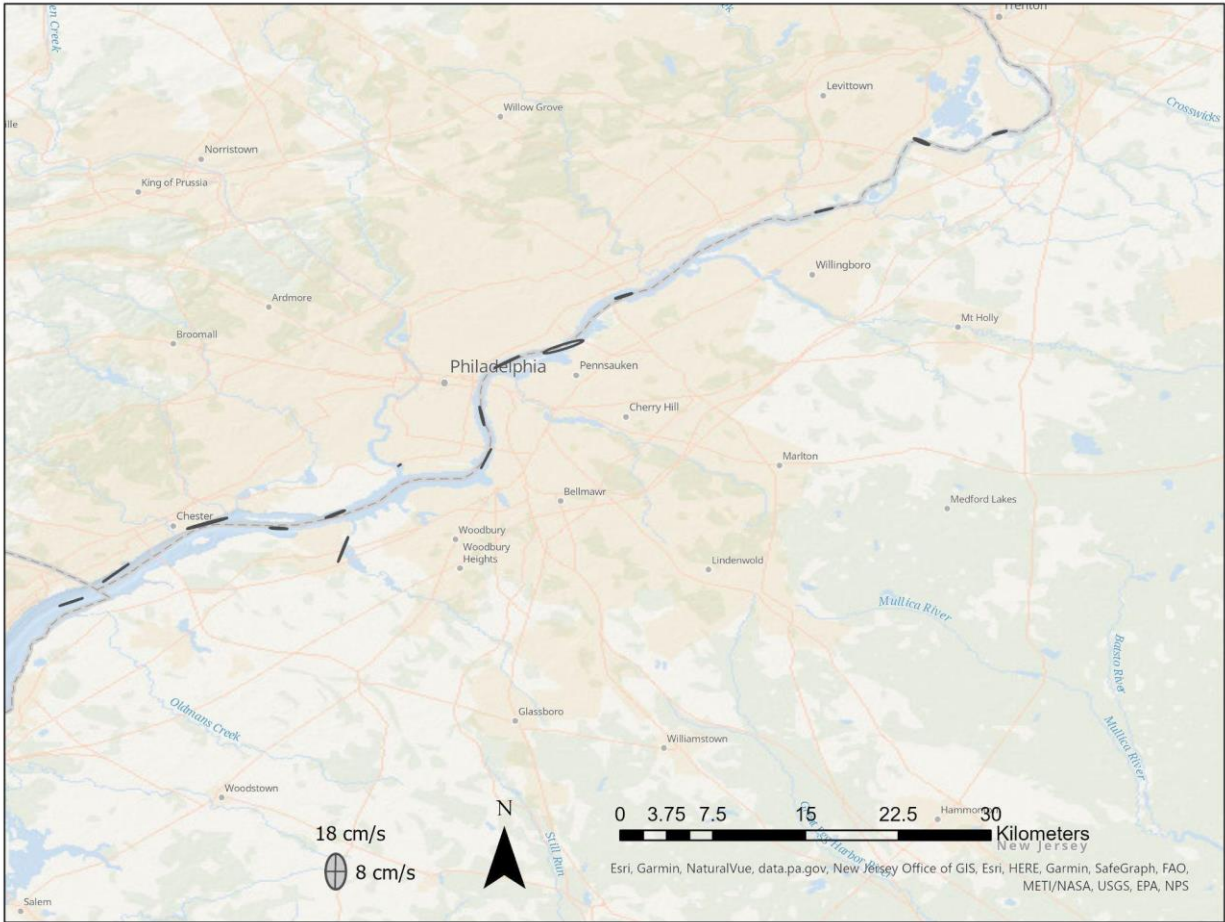


Figure 68. S2 tidal ellipses for prediction stations in the upper Delaware River, showing the topographic steering of the ellipses. Note that these are on a different scale than M2 in order to better visualize the ellipses. These data are at about 1/2 the scale of the M2 data.

6.2 Near-Surface Magnitude & Phases of the Tidal Current

Spatial representation of the magnitude and timing of mean ebb and flood currents show the progression of the tides within the estuary and the changes in amplitude due to bathymetry.

Figures 69-71 show the spatial distribution of the mean current magnitude and direction at each station during the maximum flood and ebb currents. In general, the current directions follow the channel orientation. Figures 72 and 73 show the corresponding GI timing of ebb and flood. These data are from the near-surface prediction bin.

Figures 25 (DEB2101), 30 (DEB2105), 32 (DEB2117), 45 (DEB2128), and 50 (DEB2132) from Section 5 above show the depth derived from the pressure sensor (magenta dots) relative to the tidal current velocity (green dots). The relationship between the timing of the high and low water relative to the max flood and ebb speeds indicates the character of the tidal wave being either progressive, standing, or a combination. At the mouth of the Bay (DEB2101, Figure 25) the max flood and ebb current speeds occur just prior to the high and low water with a very minor phase lag between the two indicating the tidal wave to be primarily progressive. Moving upriver, this phase lag increases, indicating a combination of progressive and standing tidal wave behavior. Near the tidal limit of the River, DEB2132 (Figure 50) shows the high and low water nearly corresponding to the slack currents indicating primarily standing wave behavior.

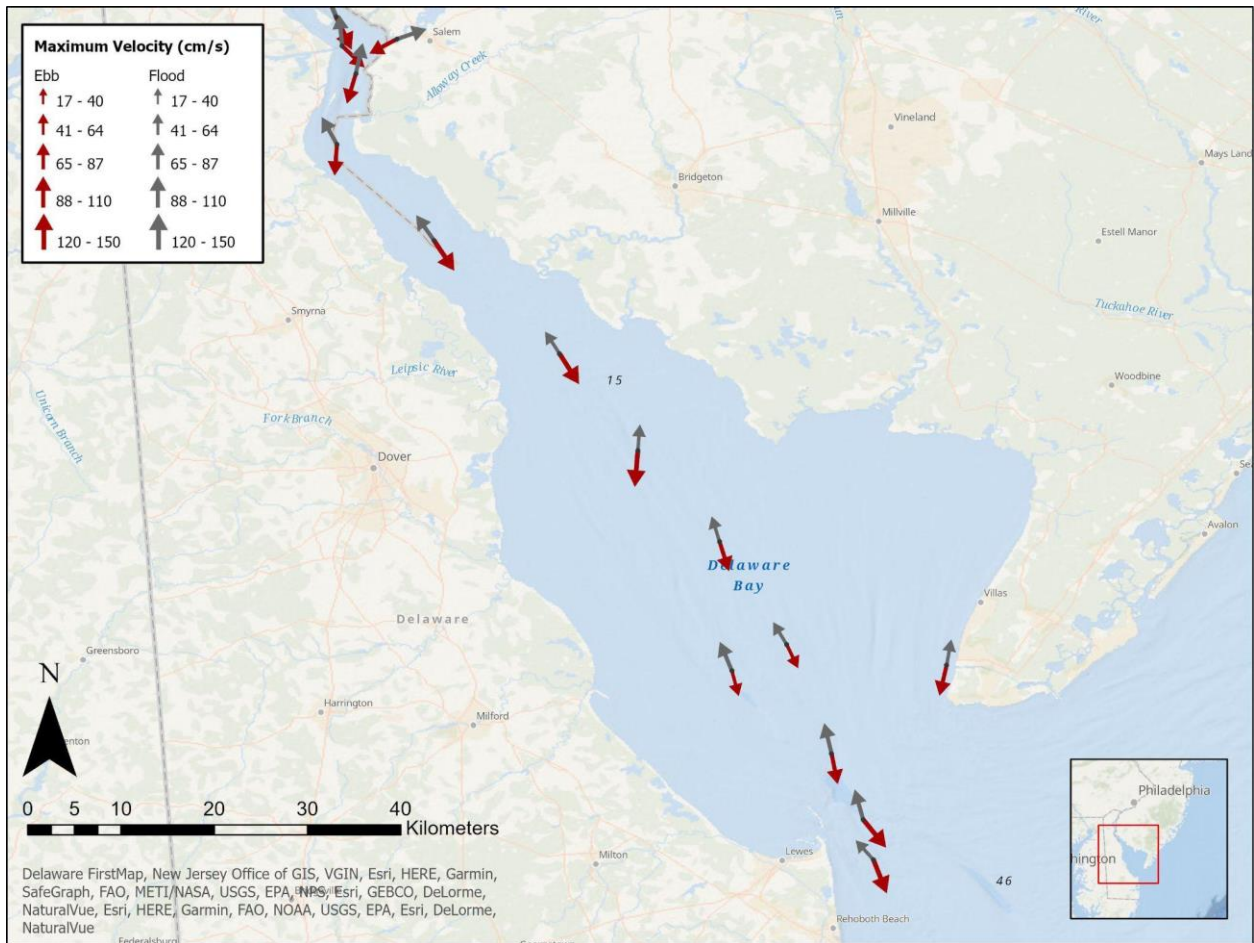


Figure 69. Mean values for the tidal currents during maximum flood and ebb for near-surface bins at all stations in the lower Delaware Bay.

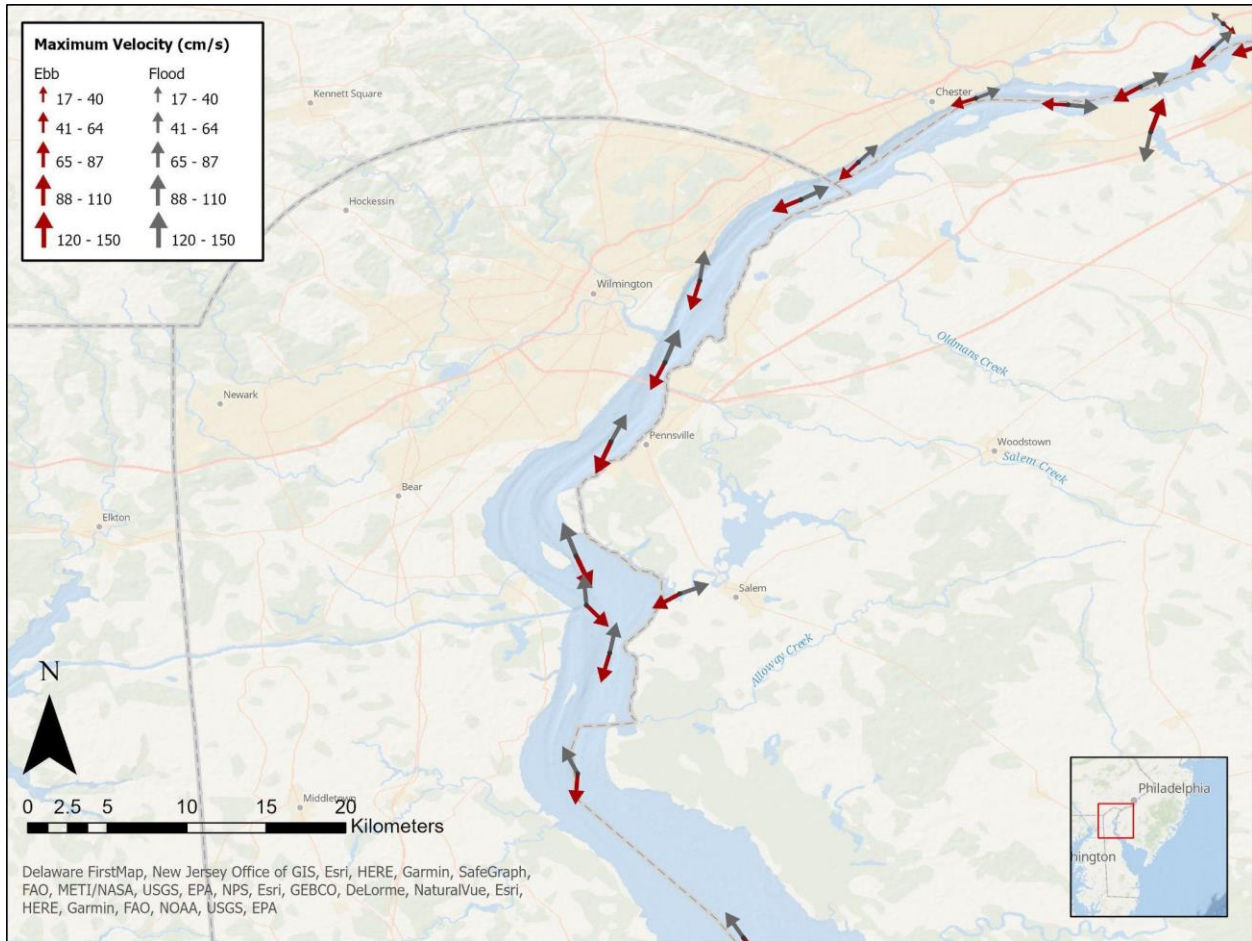


Figure 70. Mean values for the tidal currents during maximum flood and ebb for near-surface bins at all stations in the lower Delaware River.

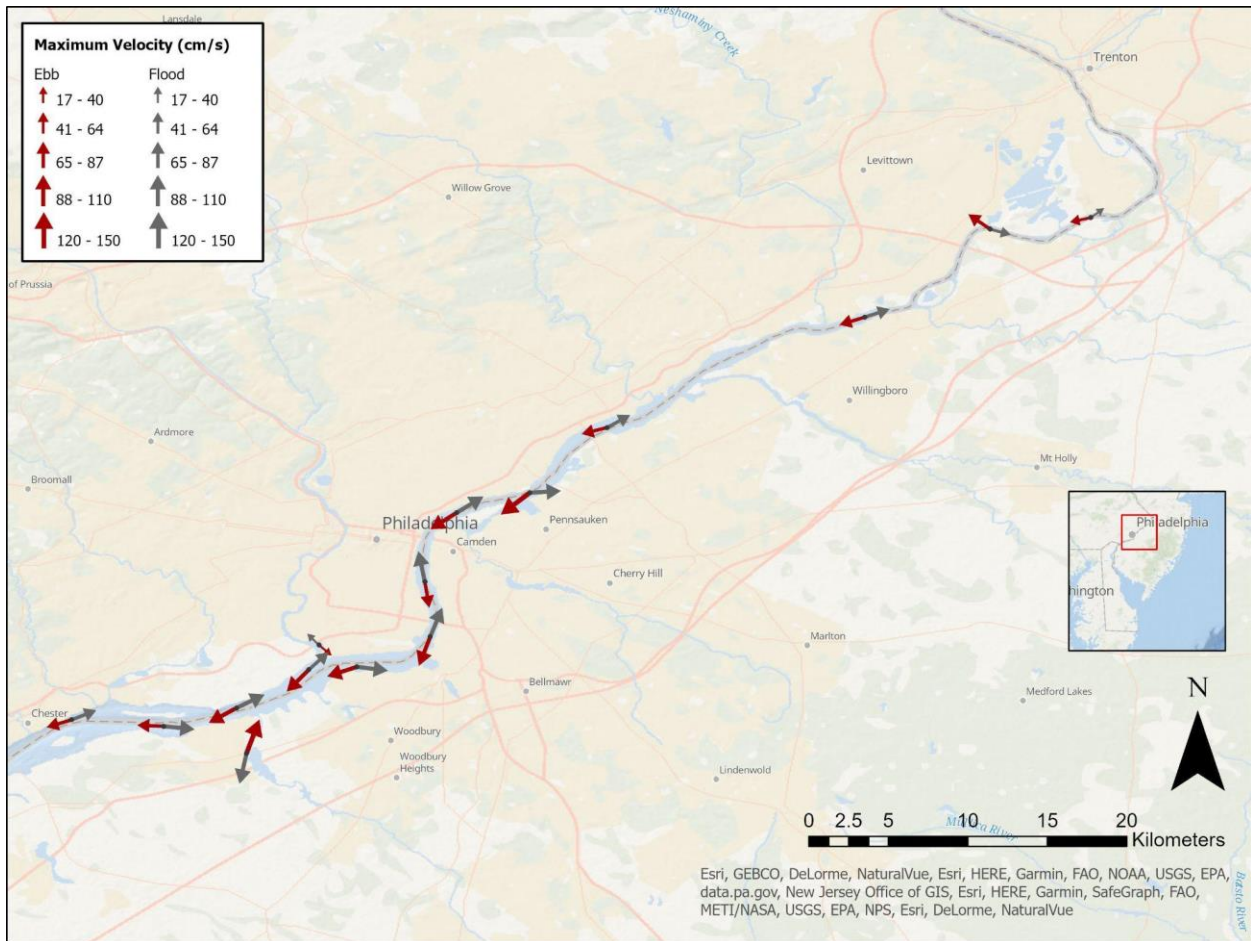


Figure 71. Mean values for the tidal currents during maximum flood and ebb for near-surface bins at all stations in the upper Delaware River.

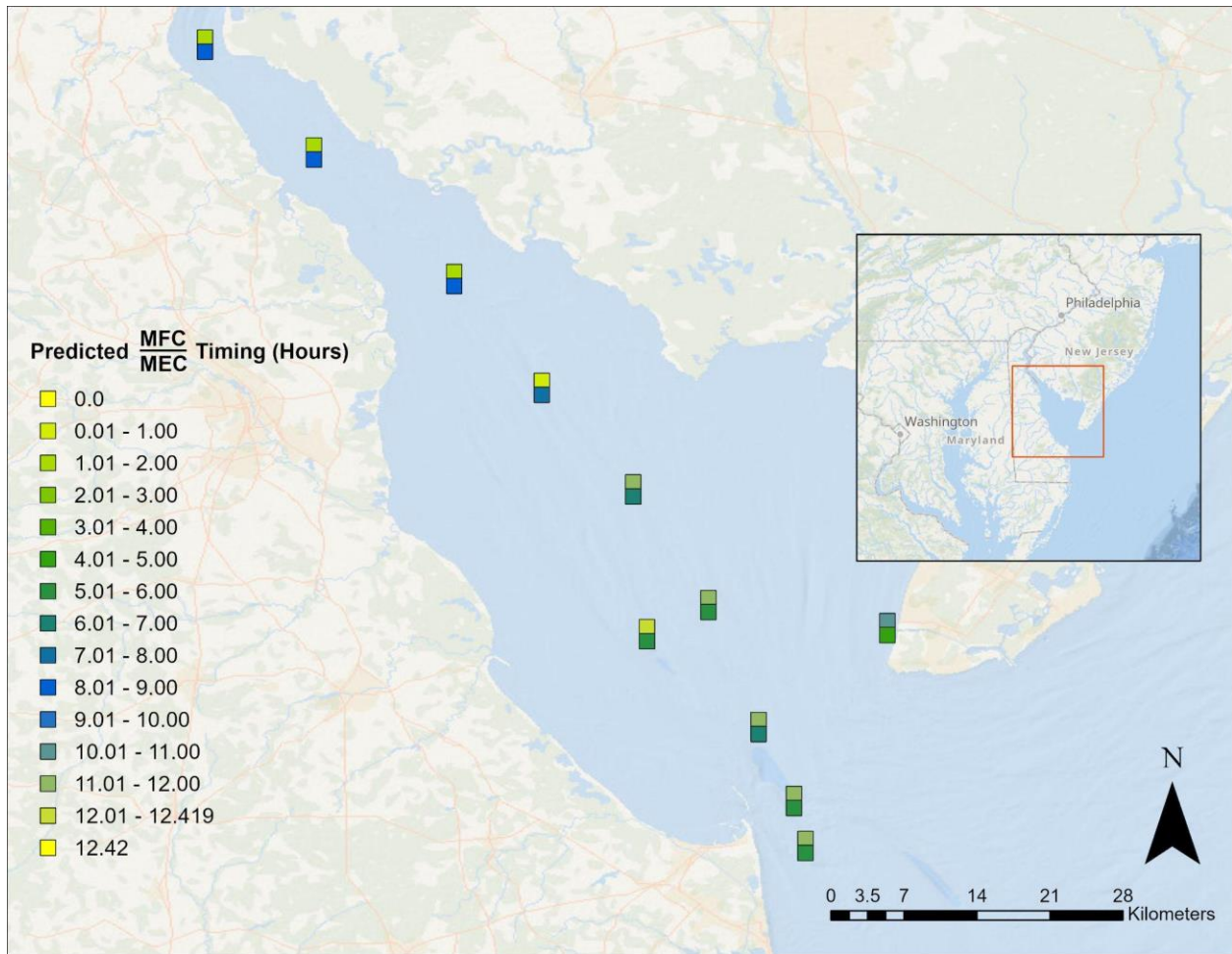


Figure 72. GI timing of maximum flood (top) and ebb (bottom) at stations in the lower Delaware Bay. Note that the colors represent hours from 0 to 12.42 with the end interval limits having the same colors to represent the cyclical tides.

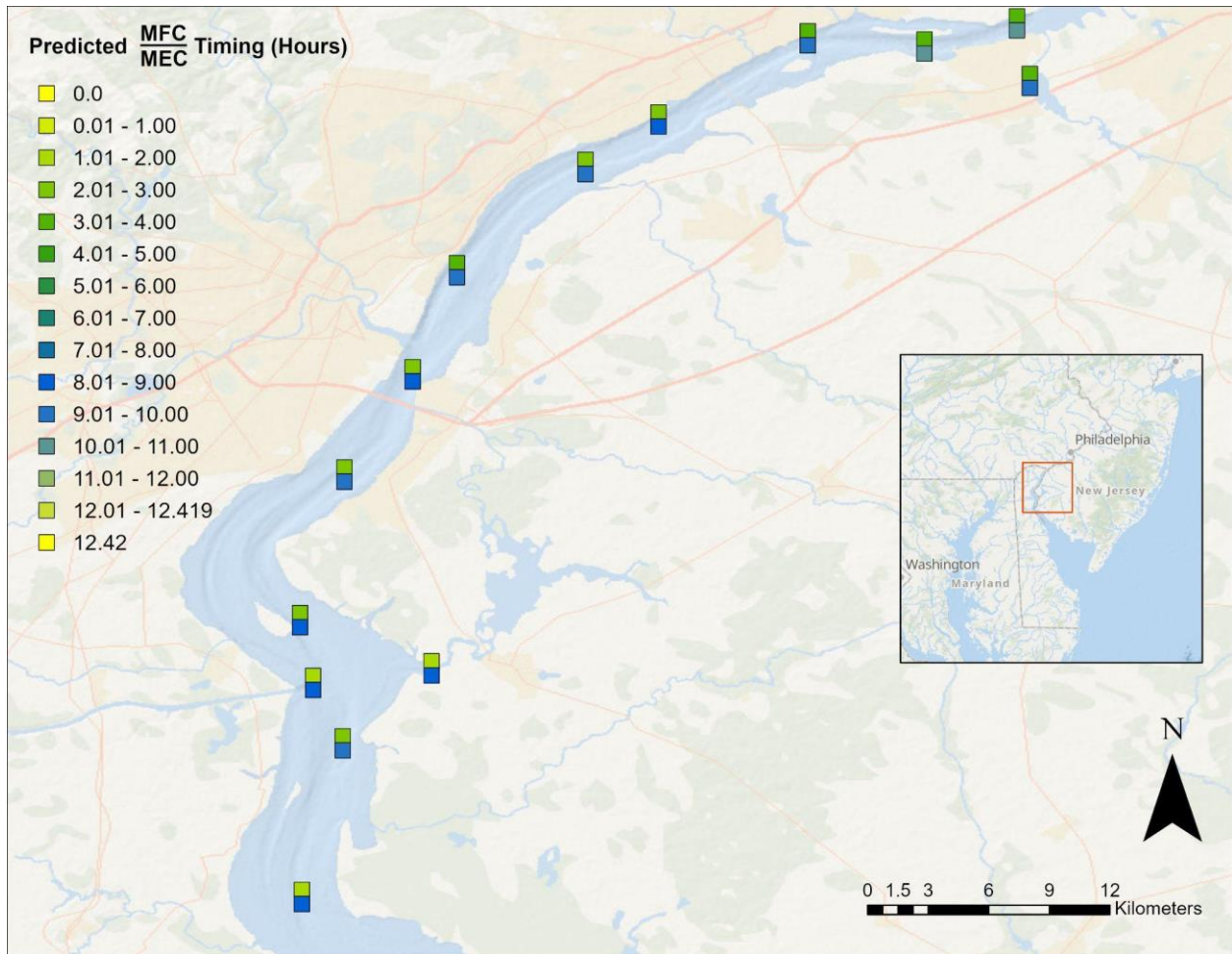


Figure 73. GI timing of maximum flood (top) and ebb (bottom) at stations in the lower Delaware River. Note that the colors represent hours from 0 to 12.42 with the end interval limits having the same colors to represent the cyclical tides.

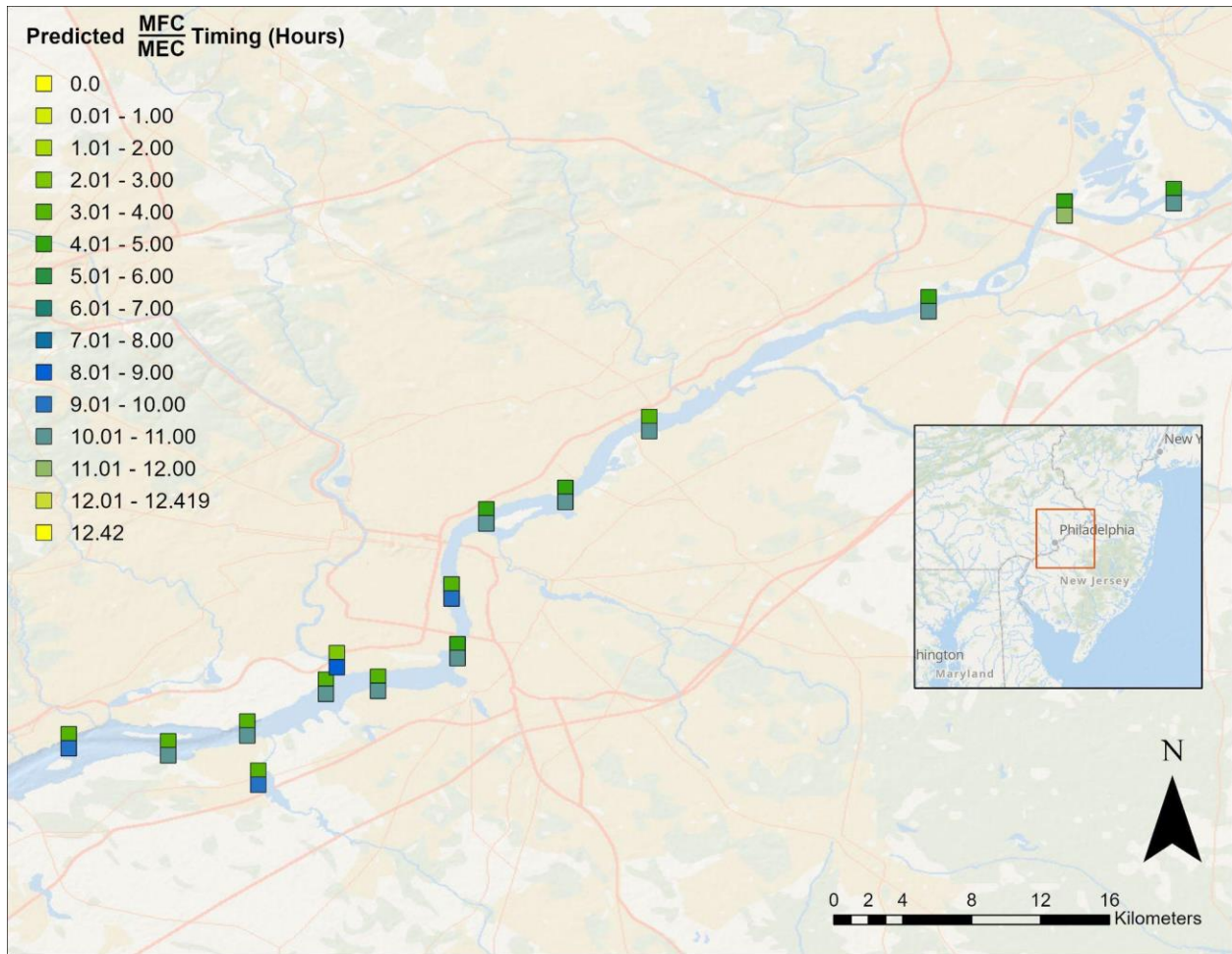


Figure 74. GI timing of maximum flood (top) and ebb (bottom) at stations in the upper Delaware River. Note that the colors represent hours from 0 to 12.42 with the end interval limits having the same colors to represent the cyclical tides.

6.3 Salinity

There is a strong spatial salinity gradient spanning the saline ocean seawater flowing through the mouth of the Bay up into the lower River where it meets relatively fresh water getting discharged down through the upper River (Figure 75). In an effort to help NOAA modelers better resolve this salinity gradient, 3 CTDs were deployed near the mouth of the Bay at DEB2101, DEB2105, and DEB2107 (Figure 3). In support of NOAA’s partners at USGS, 2 CTDs were deployed in the lower River (DEB2117 and DEB2119; Figure 3) in support of model development through the NGWOS program. All CTD data collected in both the 2019 reconnaissance as well as the 2021 survey was shared with NOAA and USGS modelers.

The vertical CTD cast at DEB2101 (Figure 76) shows stratification in the upper water column in July, creating relatively shallow (<2 m) thermoclines and pycnoclines, below which is relatively well mixed. The temperature decreases with depth by nearly 4°C (Figure 76) and warms through August, then begins to cool off in late August into September (Figure 77). The salinity increases with depth by 1.7 practical salinity units (PSU; Figure 76) and becomes fresher through August, then begins to become more saline in late August into September, following the temperature trend (Figure 77). The SEABY released early and drifted to shore, where the equipment was recovered. Therefore, a recovery CTD cast was not completed, and the time series

of the CTD data (Figure 77) was trimmed to only include the time period the SEABY was on station prior to premature surfacing.

The vertical CTD casts at DEB2105 (Figure 78) show strong stratification in the upper water column in September creating strong thermoclines and pycnoclines. However, the water column becomes well mixed by November when the recovery of equipment occurred (Figure 78). The water cooled and freshened causing an increase in density between the deployments in September and the recoveries in November, which can also be seen in both the vertical casts and the time series (Figures 78 and 79). The depth data show the semidiurnal tidal signal with a flooding event that occurs in late October (Figure 79).

The vertical CTD casts at DEB2117 and DEB2119 show the water column is well mixed in the River with little to no stratification in the density, especially in November (Figures 80 and 82). The water cooled and freshened, causing an increase in density between the deployments in July and the recoveries in November, which can also be seen in both the vertical casts and the time series (Figures 80-83). Changes in salinity in late August and early September may be attributed to Hurricane Ida (Figures 81 and 83). A minor flooding event in late October is evident in the depth and pressure time series data at DEB2117 and DEB2119 (Figures 81 and 83).

Comparing the stations at the mouth of the Bay to the ones upriver, the water is much more saline near the mouth due to the ocean influence and much fresher upriver due to river runoff. The temperature in November was colder farther upriver than the warmer water at the mouth possibly due to differences in depth and heat capacity. Stations near the mouth and upriver both show evidence of the flooding event in October in the depth data.

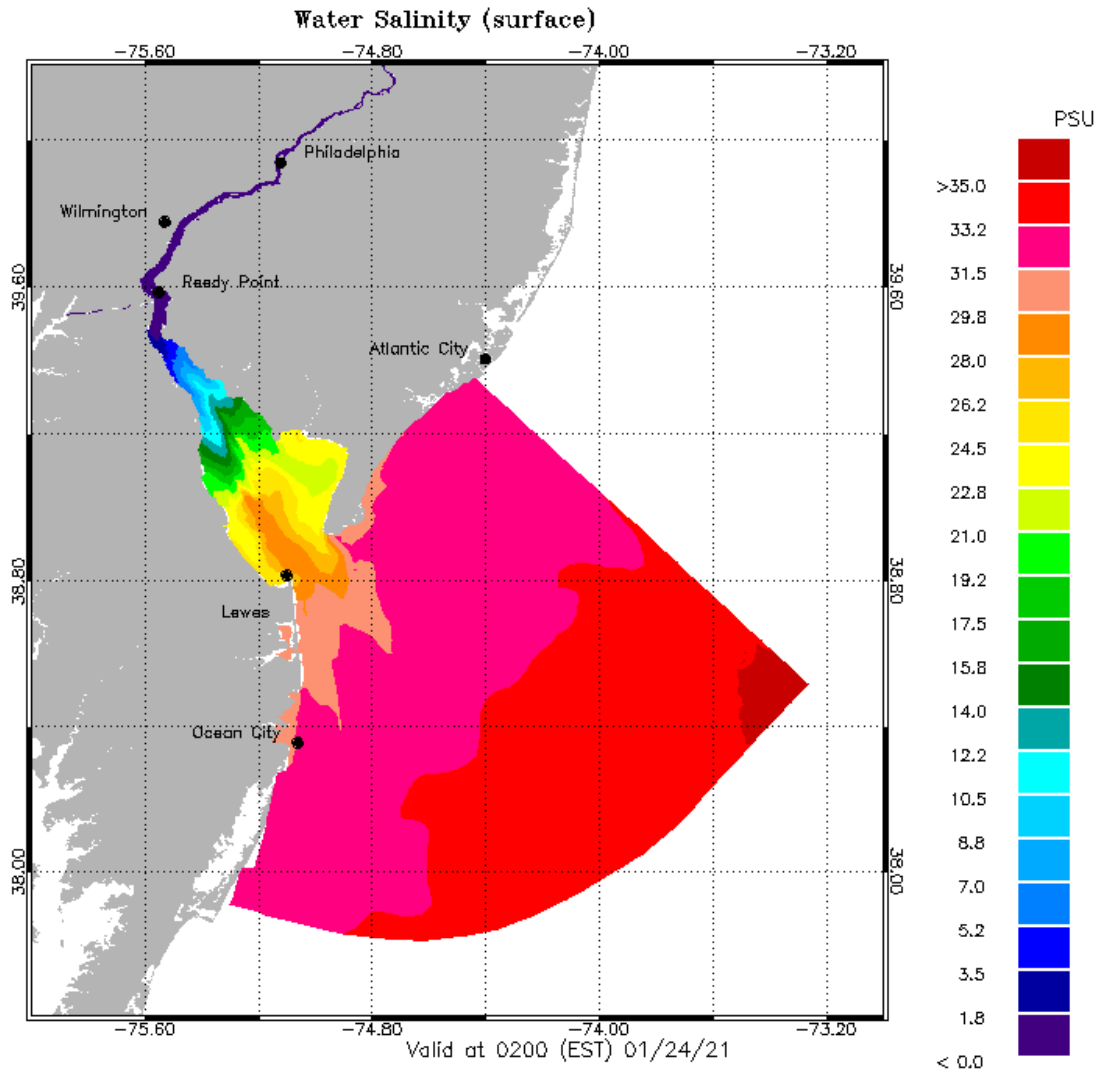


Figure 75. Delaware Bay Operation Forecast (DBOFS) nowcast surface salinity practical salinity units (PSU) output on January 24, 2021, showing the salinity gradient from the mouth of the Bay (>30 PSU) that decreases moving upriver (~0 PSU).

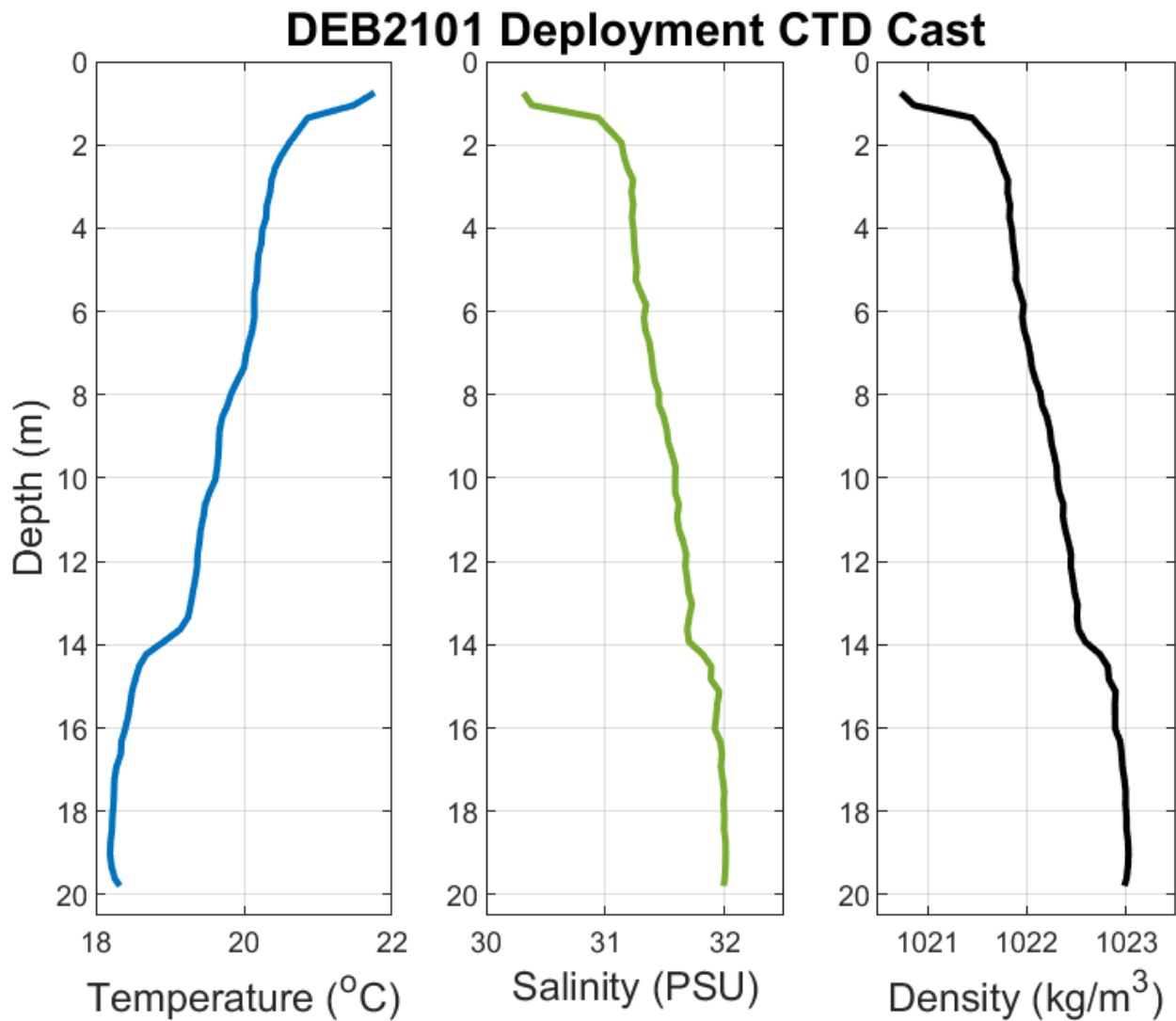


Figure 76. Raw conductivity, temperature, and depth (CTD) sensor (YSI Castaway) vertical downcast at DEB2101 upon deployment (on July 15, 2021) of the acoustic Doppler current profiler (ADCP) and CTD platform. The subsurface ellipsoid ADCP buoy (SEABY) released early and drifted to shore, so a recovery CTD cast was not completed.

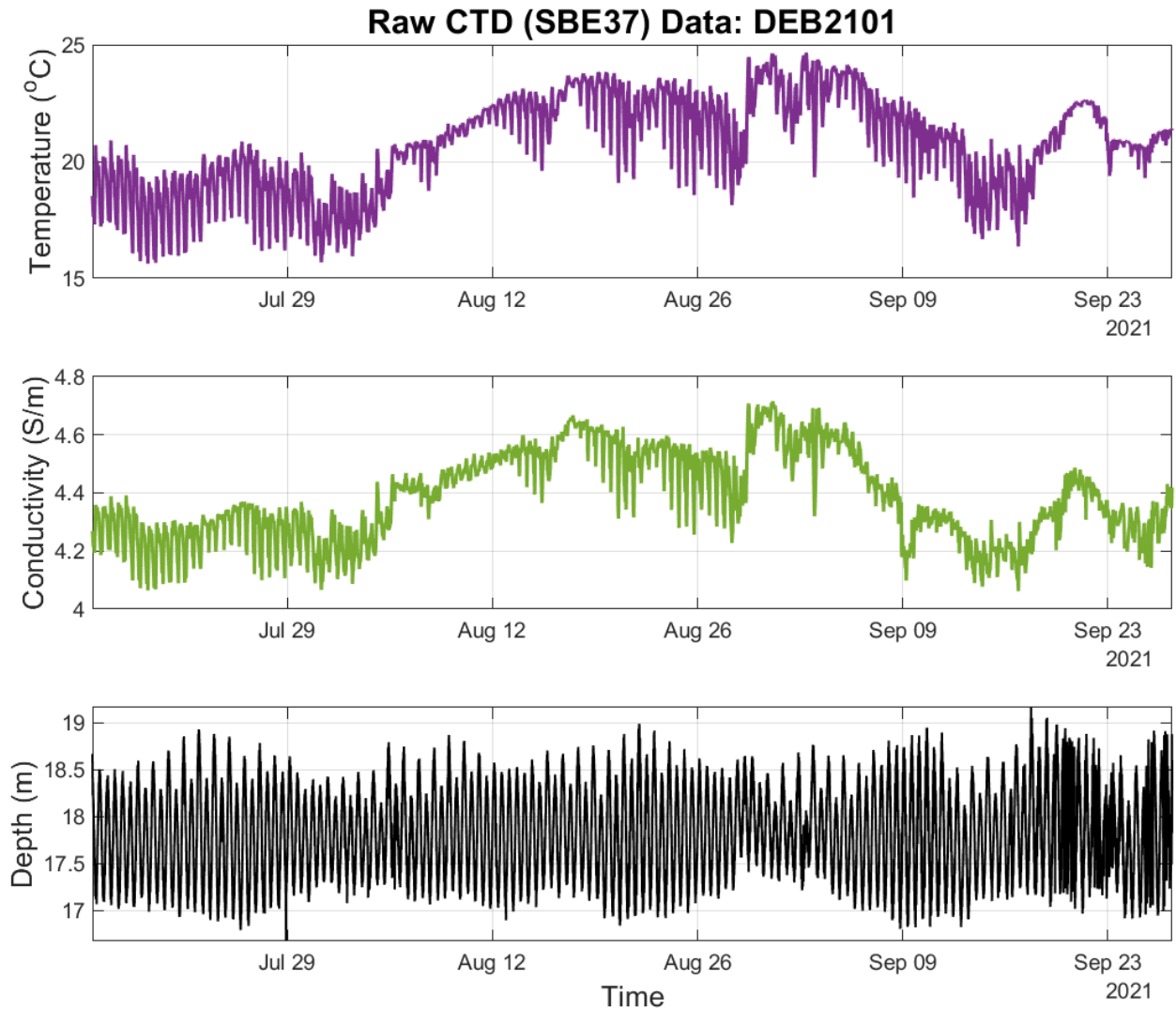


Figure 77. Raw water temperature (top), conductivity (middle), and depth (bottom) data collected with an SBE37 conductivity, temperature, and depth (CTD) sensor at DEB2101. The data was trimmed to exclude the time period at the end of the deployment when the subsurface ellipsoid ADCP buoy (SEABY) released early and drifted to shore.

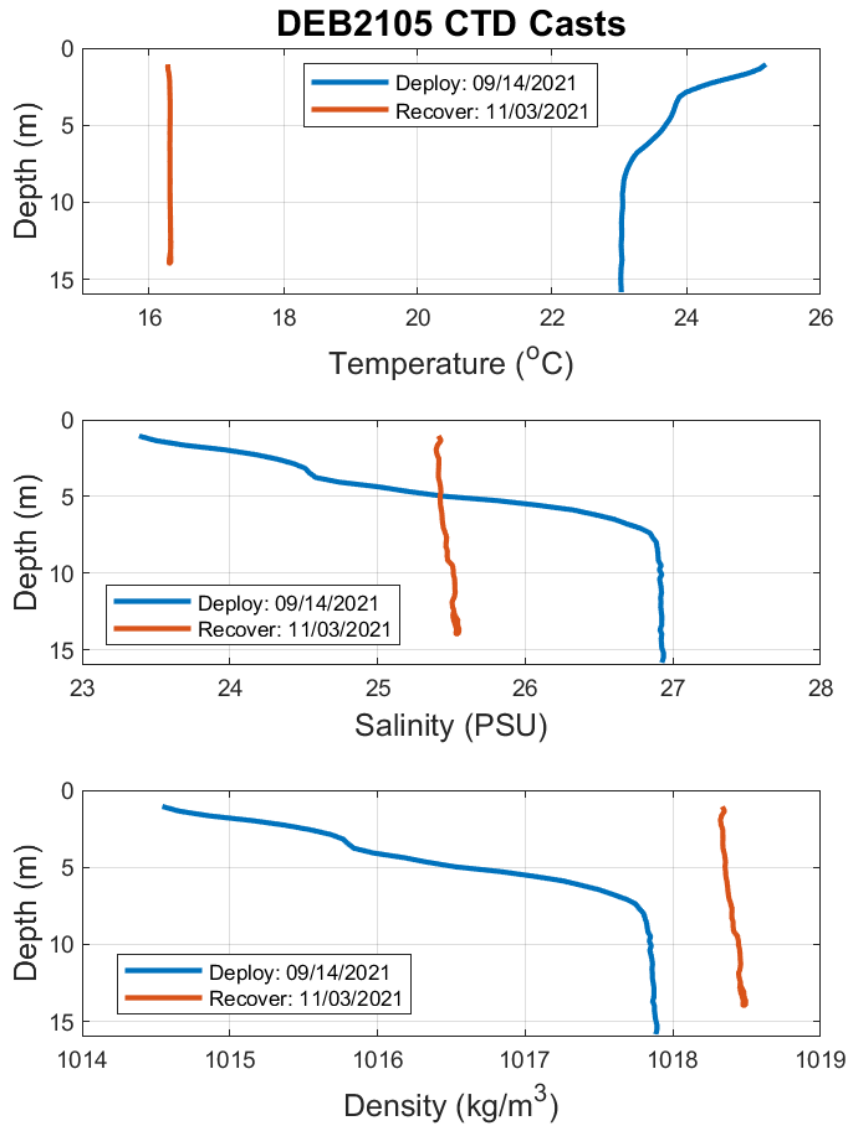


Figure 78. Raw conductivity, temperature, and depth (CTD) sensor (YSI Castaway) vertical downcast at DEB2105 upon deployment (on September 14, 2021) and recovery (on November 3, 2021) of the acoustic Doppler current profiler (ADCP) and CTD platform.

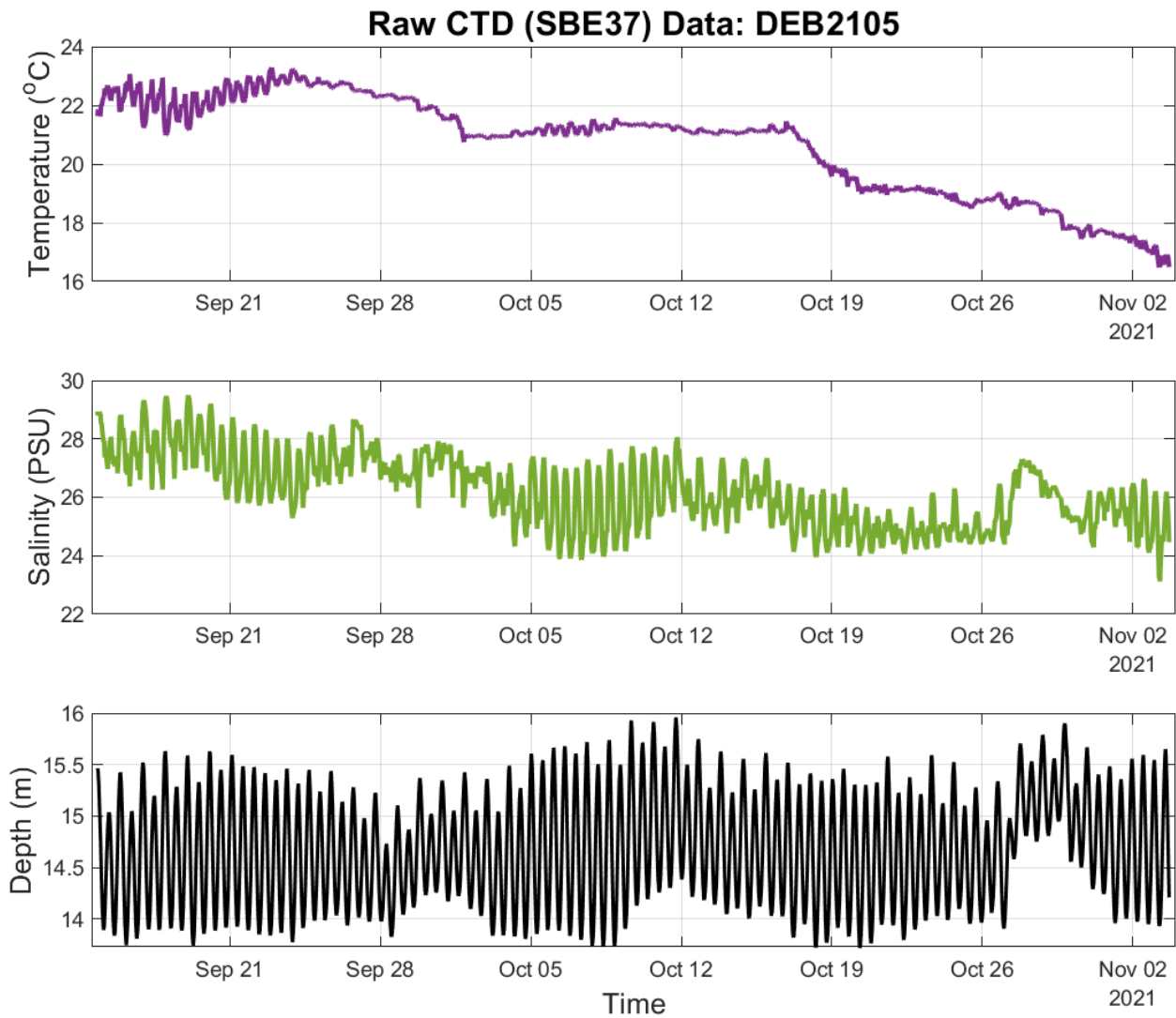


Figure 79. Raw water temperature (top), practical salinity (middle), and depth (bottom) data collected with an SBE37 conductivity, temperature, and depth (CTD) sensor at DEB2105.

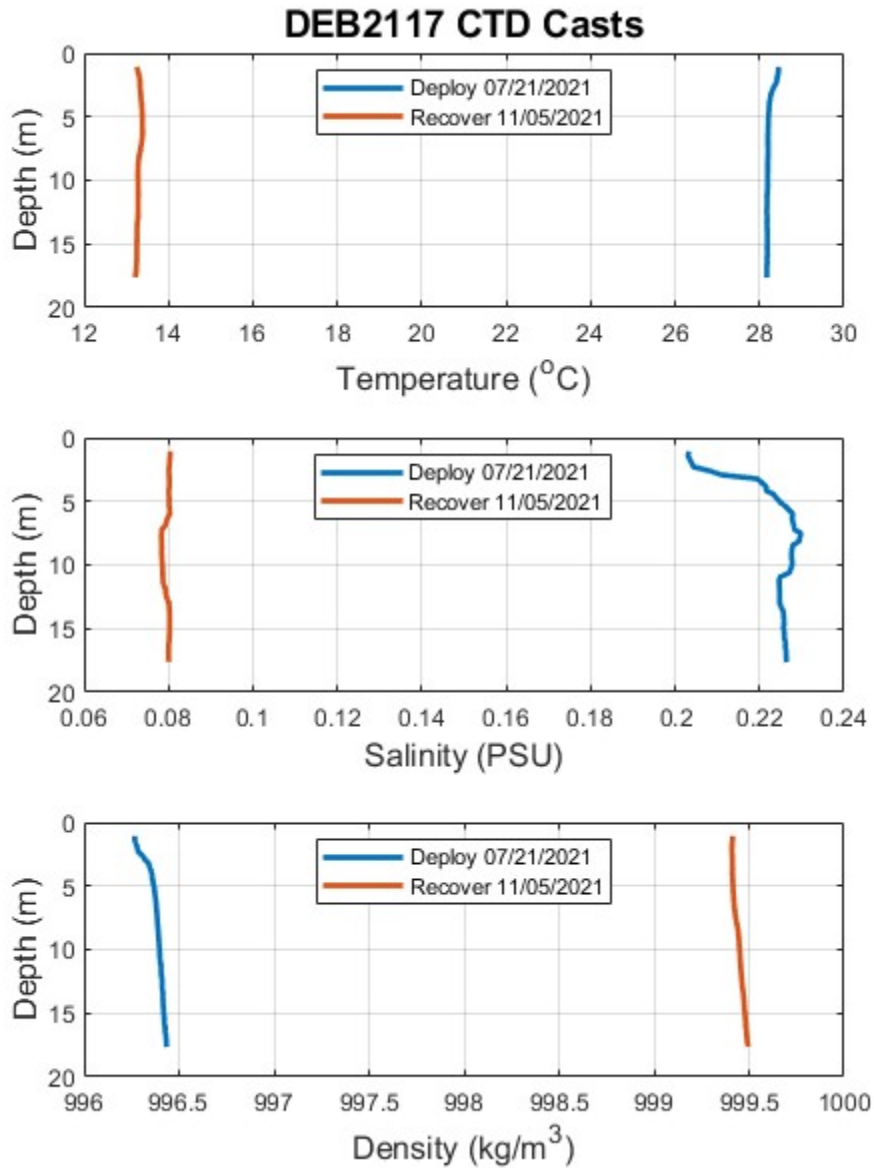


Figure 80. Raw conductivity, temperature, and depth (CTD) sensor (YSI Castaway) vertical downcast at DEB2117 upon deployment (on July 21, 2021) and recovery (on November 5, 2021) of the acoustic Doppler profiler (ADCP) and CTD platform.

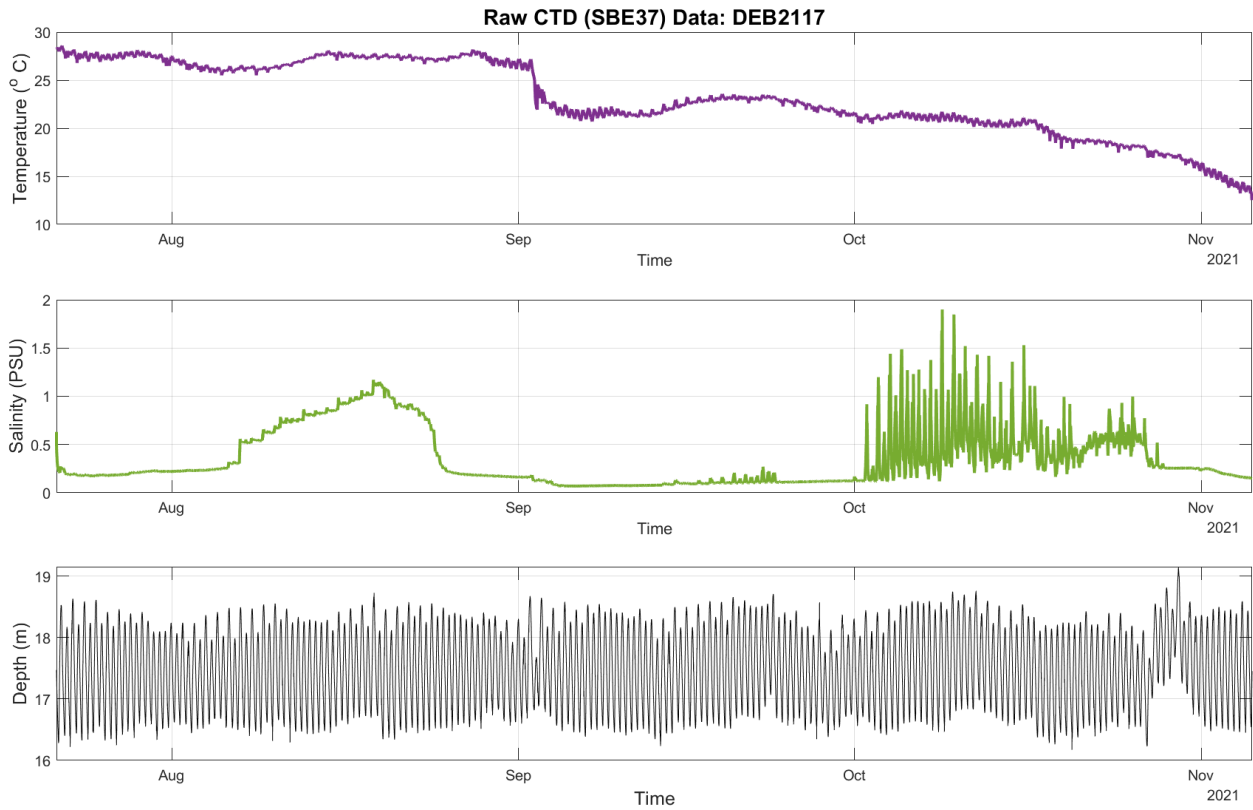


Figure 81. Raw conductivity, temperature, and depth (CTD) sensor (SBE37) time series of water temperature (top), salinity (middle), and depth (bottom) collected at DEB2117.

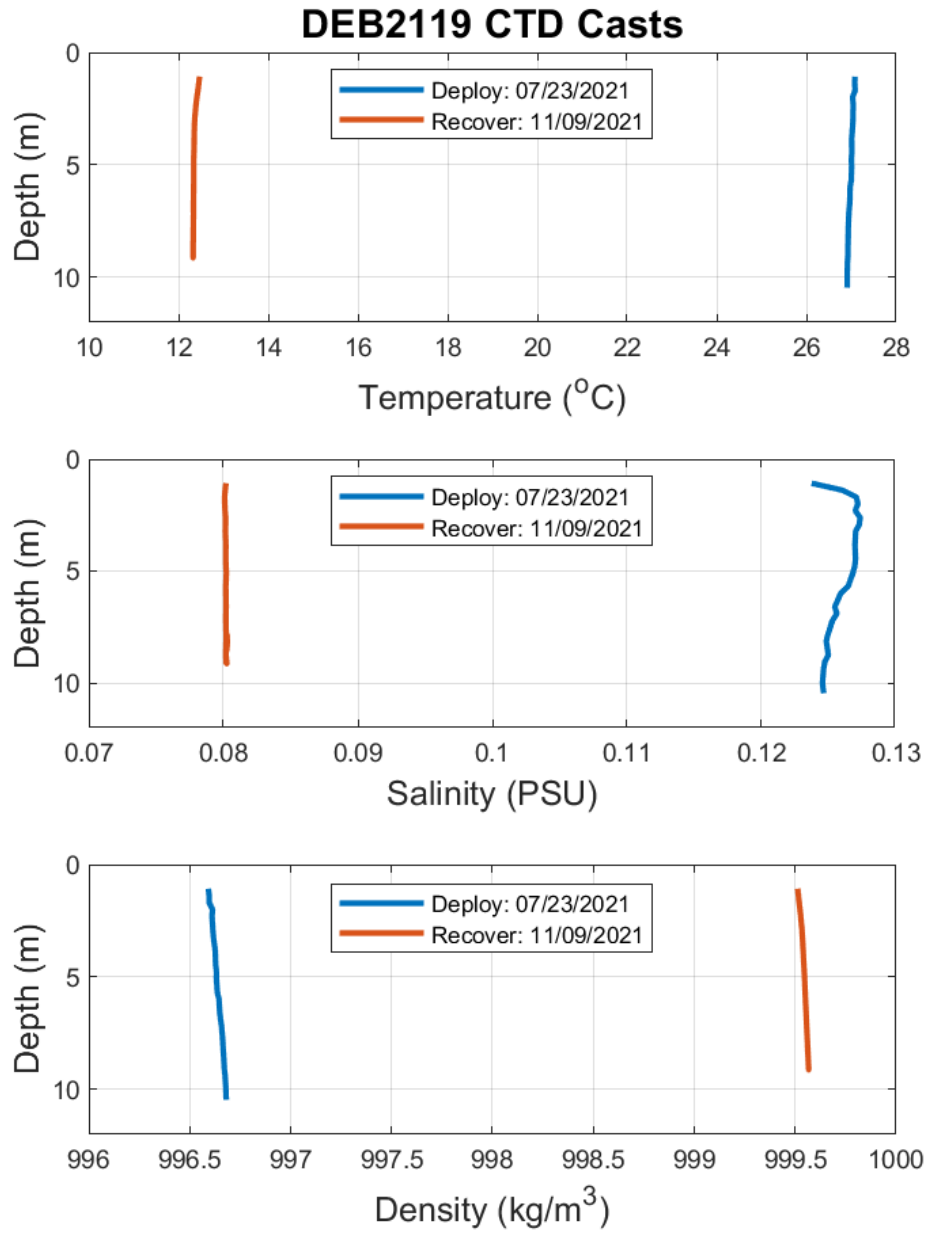


Figure 82. Raw conductivity, temperature, and depth (CTD) sensor (YSI Castaway) vertical downcast at DEB2119 upon deployment (on July 21, 2021) and recovery (on November 5, 2021) of the acoustic Doppler profiler (ADCP) and CTD platform.

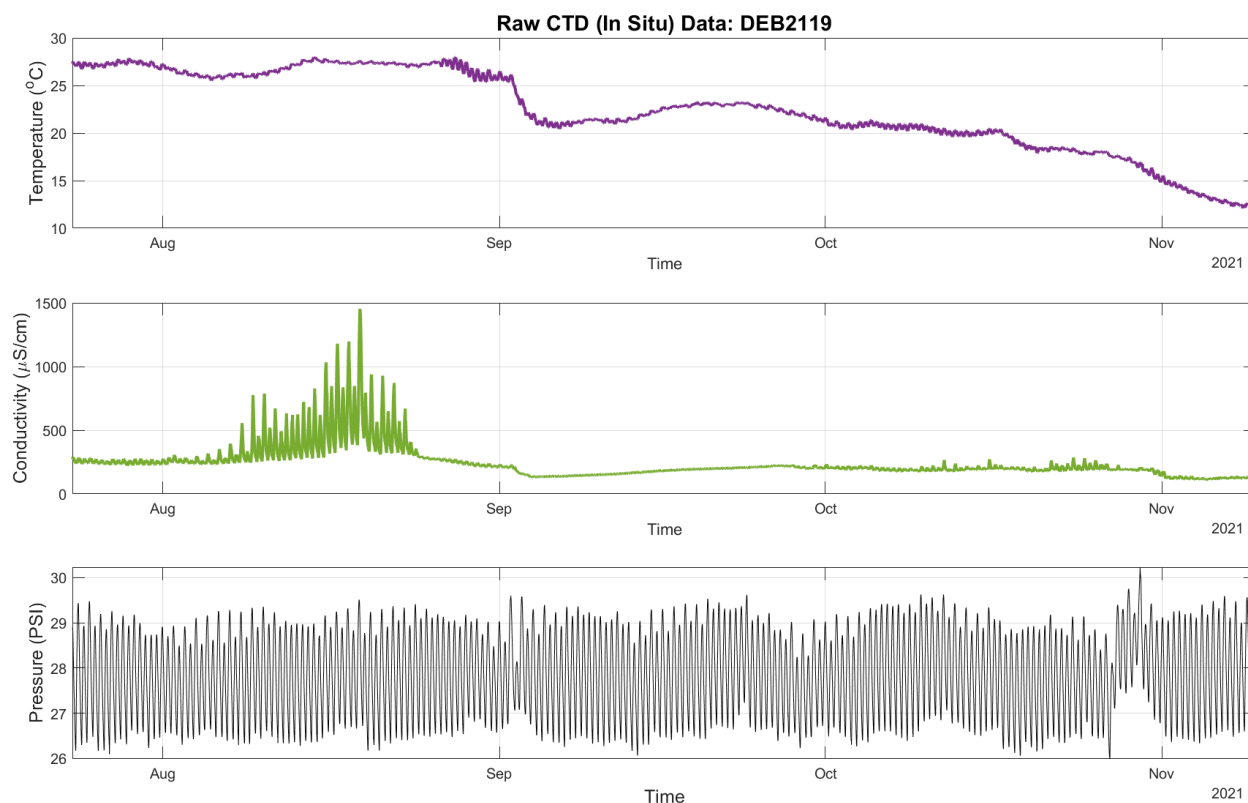


Figure 83. Raw conductivity, temperature, and depth (CTD) sensor (In Situ Aqua TROLL) time series of water temperature (top), conductivity (middle), and pressure (bottom) collected at DEB2119.

7.0 SUMMARY

CO-OPS occupied one station in 2019 and 35 stations in 2021 throughout the Delaware Bay and River. In addition to the current data obtained by the ADCPs, CTD profiles were collected at each station during deployment and recovery of the ADCP. CTDs were also deployed co-located with the ADCPs at 5 stations in support of modeling, and one external pressure sensor was deployed at one station to better understand a new mooring design.

This current survey resulted in a set of measured currents, water temperature, salinity, and pressure observations. The analysis showed that stations in the region are semidiurnal and primarily rectilinear. The tidal currents data were used to update NOAA tidal current predictions and inform future enhancements to a regional hydrodynamic model in Delaware Bay, which will support safe and efficient navigation by improving the accuracy of the model predictions and providing a higher density of observations to validate these predictions in the region.

All analyses and plots for the entire time series at all depths are available in detailed station reports (Tide.Predictions@noaa.gov). Updated tidal current predictions for each station are also available online via the CO-OPS Tides and Currents website (NOAA Current Predictions). Members of the public and research community who wish to further investigate the circulation of this region or obtain detailed information in support of safe navigation can request the full data set by contacting CO-OPS' Stakeholder Services Branch at Tide.Predictions@noaa.gov.

ACKNOWLEDGEMENTS

We would like to thank Eddie Roggenstein, who was the CO-OPS Field Lead throughout the project, as well as the Atlantic Operations Branch personnel who supported field operations. We would also like to thank all of the CO-OPS technicians, engineers, physical scientists, analysts,

and oceanographers who assisted in station planning, the preparation of equipment, field operations, and the processing and dissemination of the data. Special thanks to Hailey Foglio for manuscript editing and Virginia Dentler for final publishing.

REFERENCES CITED

- Bosley KT, McGrath CR, Dussault JP, Bushnell M, Evans MJ, French GW, Earwaker KL. 2005. Test, evaluation, and implementation of current measurement systems on aids-to-navigation. US Dept Commer NOAA NOS CO-OPS. Technical Report No. 043. 140 p. Accessible at: <https://repository.library.noaa.gov/view/noaa/14668>
- Charts and publications, 33 C.F.R. Sect. 164.33 (2022)
- [DBOFS] Delaware Bay Operational Forecast System. Silver Spring (MD): NOAA Tides & Currents. Accessible at: <https://tidesandcurrents.noaa.gov/ofs/dbofs/dbofs.html>
- Defant A. 1958. Ebb and flow: the tides of earth, air, and water. Ann Arbor (MI): University of Michigan Press. Ann Arbor Paperbacks Series. Vol. 506.
- Delaware River Main Channel Deepening. 2023. Philadelphia (PA): U.S. Army Corps of Engineers Philadelphia District & Marine Design Center; [accessed 19 July 2022]. <https://www.nap.usace.army.mil/Missions/Factsheets/Fact-Sheet-Article-View/Article/490804/delaware-river-main-channel-deepening/>
- Dissemination of data; further activities, 33 U.S.C. 883b (2021)
- Fanelli P, Paternostro C, Dusek G, Kammerer C, Park J, Carisio A. 2014. Potential Location Assessment of Coastal and Estuarine Surveys (PLACES). NOAA CO-OPS-NCOP.
- Fiorentino L, Heitsenrether R, Kirk K, Krug W, Breuer E, Hensley W. 2022. Recent development and field test of CO-OPS' real-time, shallow water CURrents BuoY (CURBY). Mar Technol Soc J. 56(6):58-69.
- [IHO] International Hydrographic Organization. 2008. IHO standards for hydrographic surveys. 5th ed. Special Publication No. 44. Monaco: International Hydrographic Bureau. 32 p. Accessible at: <https://repository.oceanbestpractices.org/handle/11329/388>
- [IOOS] Integrated Ocean Observing System. 2019. Manual for real-time quality control of in-situ current observations: a guide to quality control and quality assurance of acoustic doppler current profiler observations. Version 2.1. Silver Spring (MD): Quality Assurance/Quality Control of Real-Time Oceanographic Data (QARTOD). 50 p. Accessible at: <https://doi.org/10.25923/sqe9-e310>
- [IOOS] Integrated Ocean Observing System. 2020. Manual for real-time oceanographic data quality control flags. Version 1.2. Silver Spring (MD): Quality Assurance/Quality Control of Real-Time Oceanographic Data (QARTOD). 20 p. Accessible at: <https://repository.oceanbestpractices.org/handle/11329/1372>
- Klavans AS, Stone PJ, Stoney GA. 1986. Delaware River and Bay Circulation Survey: 1984-1985. NOS Oceanographic Circulation Survey Report No. 9. 92 p. Accessible at: <https://repository.library.noaa.gov/view/noaa/2584>

- Lanerolle LWJ, Patchen RC, Aikman F. 2011. The second-generation Chesapeake Bay Operational Forecast System (CBOFS2) model development and skill assessment. US Dept Commer NOAA NOS CS Technical Report No. 29. 87 p. Accessible at: <https://repository.library.noaa.gov/view/noaa/2589>
- [NOAA] National Oceanic and Atmospheric Administration. 2018. NOAA's contribution to the economy; powering America's economy and protecting Americans. 46 p. <https://repository.library.noaa.gov/view/noaa/20604>
- NOAA Current Predictions. Silver Spring (MD): NOAA Tides & Currents; Accessible at: <https://tidesandcurrents.noaa.gov/noaacurrents/Regions>
- Parker BB. 2007. Tidal analysis and prediction. US Dept Commer NOAA Special Report NOS CO-OPS 3. 384 p. Accessible at: <https://repository.oceanbestpractices.org/handle/11329/632>
- Haaf L, Morgan L, Kreeger D, editors. 2022. Technical Report for the Delaware Estuary and Basin (TREB). Wilmington (DE): Partnership for the Delaware Estuary. PDE Report No. 22-05. 445 pages.
- Paternostro CL, Pruessner A, Semkiw R. 2005. Designing a quality oceanographic data processing environment. Proceedings of OCEANS 2005 IEEE MTT-S; 2005 Sept 17-23; Washington, DC. Elkrigde (MD): IEEE Microwave Theory and Technology Society.
- Surveys and other activities, 33 U.S.C. 883a (2012)
- Swanson RL. 1974. Variability of tidal datums and accuracy in determining datums from short series of observations. US Dept Commer NOAA NOS Technical Report No. 64. 44 p. Accessible at: <https://repository.library.noaa.gov/view/noaa/2944>
- The Top 25 Container Port Rankings in North America. 2017. Medley (FL): Lilly & Associates International. <https://www.shiplilly.com/blog/top-25-container-port-rankings-north-america/>
- [USACE] U.S. Army Corps of Engineers. 2018. Waterborne tonnage for principal U.S. ports and all 50 states and U.S. territories; Waterborne tonnages for domestic, foreign, imports, exports and intra-state waterborne traffic. USACE. 23 p. Accessible at: <https://usace.contentdm.oclc.org/digital/collection/p16021coll2/id/1492>
- Valle-Levinson A, editor. 2010. Contemporary issues in estuarine physics. Cambridge: Cambridge University Press. <https://doi.org/10.1017/CBO9780511676567>
- Vessel traffic data. MarineCadastre.gov. Accessible at: <https://marinecadastre.gov/ais/>
- Zervas C. 1999. Tidal current analysis procedures and associated computer programs. US Dept Commer NOAA NOS CO-OPS Tech Memo No. 0021. 104 p. Accessible at: <https://repository.library.noaa.gov/view/noaa/50573>

APPENDIX A. STATION LISTING

Table A1. Station location and deployment information. Measurements in meters (m).

Station ID	Station Name	Latitude	Longitude	Depth (m)	Deployment Date	Recovery Date	Number of Days of Good Data	Predictions Generated
DEB2101	Delaware Bay Entrance	38.7813	-75.0430	18.8	7/15/2021	10/19/2021	87.3	Yes
DEB2102	Cape Henlopen, 2 mi NE of	38.8199	-75.0528	29.13	9/13/2021	11/14/2021	60.4	Yes
DEB2103	Cape Henlopen, 5 mi north of	38.8834	-75.0833	23.23	7/15/2021	9/11/2021	57.8	Yes
DEB2104	Cape May Canal, west end	38.9684	-74.9724	6.8	7/19/2021	9/14/2021	57.1	Yes
DEB2105	Brandywine Shoal Light, 0.5 nm west of	38.9882	-75.1265	14.57	9/14/2021	11/3/2021	50.0	Yes
DEB2106	Big Stone Beach Anchorage "G" buoy	38.9632	-75.1794	18.6	7/15/2021	9/11/2021	57.9	Yes
DEB2107	Brandywine Range at Miah Maull Range	39.0875	-75.1913	13.3	7/16/2021	9/11/2021	57.1	Yes
DEB2108	Cross Ledge Light	39.1747	-75.2700	14.02	7/16/2021	9/15/2021	60.8	Yes
DEB2109	Ben Davis Point, 3.2 nm southwest of	39.2682	-75.3454	15.13	9/15/2021	11/6/2021	52.0	Yes
DEB2110	Arnold Point, 1.8 nm WSW of	39.3768	-75.4662	12.4	7/17/2021	9/18/2021	57.6	Yes
DEB2111	Baker Range Channel	39.4694	-75.5600	12.4	9/17/2021	11/5/2021	16.1	Yes
DEB2112	Reedy Island Wreck	39.5375	-75.5418	16.2	9/17/2021	11/9/2021	53.0	Yes
DEB2113	Chesapeake and Delaware Canal Entrance	39.5644	-75.5549	11.5	7/17/2021	9/18/2021	30.7	Yes
DEB2114	Salem River Entrance, east of marker 11	39.5708	-75.5022	7.4	9/17/2021	11/4/2021	44.7	Yes
DEB2115	Pea Patch Island	39.5922	-75.5607	14.3	9/17/2021	11/4/2021	47.9	Yes
DEB2116	Kelly Point, 0.7nm N of	39.6568	-75.5410	15.8	7/23/2021	9/17/2021	56.1	Yes
DEB2117	Deepwater Point, 0.5 nm NW of	39.7013	-75.5106	17.39	7/21/2021	11/5/2021	106.9	Yes
DEB2118	Edgemoor	39.7475	-75.4909	15.06	9/21/2021	11/5/2021	43.7	Yes
DEB2119	Marcus Hook Bar (north)	39.7933	-75.4338	9.7	7/23/2021	11/9/2021	109.0	Yes

DEB2120	Marcus Hook	39.8144	-75.4013	10.5	9/21/2021	11/10/2021	10.7	No
DEB2121	Eddystone	39.8504	-75.3348	12.5	7/20/2021	9/9/2021	39.3	Yes
DEB2122	Crab Point, 0.5 mi East of	39.8468	-75.2830	17.4	9/21/2021	11/11/2021	50.9	Yes
DEB2123	Mantua Creek US 44 Bridge Paulsboro	39.8315	-75.2360	3.92	9/24/2021	11/18/2021	54.0	Yes
DEB2124	Mantua Creek Anchorage	39.8570	-75.2418	13.4	9/21/2021	11/11/2021	51.0	Yes
DEB2125	Schuylkill River Entrance	39.8794	-75.2007	11.3	9/19/2021	11/10/2021	0.0	No
DEB2126	Girard Point	39.8925	-75.1951	5.1	7/20/2021	9/9/2021	51.1	Yes
DEB2127	Eagle Point, 0.2 nm northwest of	39.8803	-75.1736	12.4	9/20/2021	11/11/2021	1.3	No
DEB2128	Gloucester Point	39.8973	-75.1322	15.9	7/20/2021	11/16/2021	119.1	Yes
DEB2129	Kaighn Point	39.9282	-75.1353	13.6	7/22/2021	9/20/2021	60.2	Yes
DEB2130	Fisher Point	39.9785	-75.0760	13.7	7/14/2021	9/10/2021	50.0	Yes
DEB2131	Frankford Range at Tacony Range	40.0153	-75.0323	12.3	9/20/2021	11/16/2021	57.0	Yes
DEB2132	Edgewater Range at Devlin Range	40.0776	-74.8866	12.5	9/22/2021	11/15/2021	54.0	Yes
DEB2133	Florence Bend	40.1273	-74.8158	13.58	9/22/2021	11/15/2021	53.9	Yes
DEB2134	Newbold Island north of, Main Channel	40.1337	-74.7589	12.1	7/14/2021	9/10/2021	42.2	Yes
db1935	Petty Island	39.9673	-75.1172	11.9	7/9/2019	10/17/2019	98.9	Yes
DEB2136	ATON Can Test at Schuylkill River Entrance	39.8787	-75.2008	13.1	9/9/2021	11/10/2021	8.3	No

APPENDIX B. STATION PLATFORM TYPES

Table B1. Platform and sensor information. Stations not used for predictions are italicized. ADCP = acoustic Doppler current profiler. MLLW = mean lower low water. Measurements in meters (m).

Station ID	Mount Class	ADCP Orientation	Mount Type	ADCP Make	ADCP Freq. (kHz)	ADCP Height Above Bottom (m)	Station Depth, MLLW (m)	Total Bins	Bin Size (m)
DEB2101	Bottom	Up	SEABY	TRDI WH	600	2.95	18.59	20	1
DEB2102	Bottom	Up	SEABY	TRDI WH	600	2.95	29.7	32	1
DEB2103	Bottom	Up	SEABY	TRDI WH	600	2.95	23.77	25	1
DEB2104	Bottom	Up	mTRBM	TRDI WH	1200	0.5	7.54	20	0.5
DEB2105	Bottom	Up	mTRBM	TRDI WH	1200	0.5	14.47	17	1
DEB2106	Bottom	Up	SEABY	TRDI WH	600	2.95	18.6	21	1
DEB2107	Bottom	Up	mTRBM	TRDI WH	1200	0.5	12.94	19	1
DEB2108	Bottom	Up	mTRBM	TRDI WH	1200	0.5	14.02	17	1
DEB2109	Bottom	Up	SEABY	TRDI WH	600	2.95	15.13	17	1
DEB2110	Bottom	Up	GP48	TRDI WH	600	0.66	13.47	17	1
DEB2111	Surface	Down	ATON	Nortek AqD	1000	10.3	12.4	18	1
DEB2112	Bottom	Up	mTRBM	TRDI WH	1200	0.5	15.35	17	1
DEB2113	Surface	Down	ATON	Nortek AqD	1000	9.3	11.5	22	0.5
DEB2114	Bottom	Up	Grate	Nortek AqD	2000	0.18	6.82	20	0.5
DEB2115	Bottom	Up	mTRBM	TRDI WH	1200	0.5	13.26	15	1
DEB2116	Surface	Down	ATON	Nortek AqD	1000	13.6	15.8	18	1
DEB2117	Bottom	Up	mTRBM	TRDI WH	600	0.5	16.93	21	1
DEB2118	Surface	Down	ATON	Nortek AqD	1000	13.06	15.06	18	1
DEB2119	Bottom	Up	mTRBM	Nortek AqD	1000	0.5	8.78	15	1
<i>DEB2120</i>	<i>Bottom</i>	<i>Up</i>	<i>mTRBM</i>	<i>TRDI WH</i>	<i>1200</i>	<i>0.5</i>	<i>9.36</i>	<i>24</i>	<i>0.5</i>
DEB2121	Bottom	Up	mTRBM	TRDI WH	1200	0.5	11.94	28	0.5
DEB2122	Bottom	Up	mTRBM	TRDI WH	600	0.5	17.2	20	1
DEB2123	Side	Side	Pipe Clamp	Nortek AqD 2D	600	2.02	3.86	27	1
DEB2124	Bottom	Up	mTRBM	TRDI WH	1200	0.5	12.4	17	1
<i>DEB2125</i>	<i>Bottom</i>	<i>Up</i>	<i>GP-35</i>	<i>Nortek AqD</i>	<i>1000</i>	<i>0.61</i>	<i>11.3</i>	<i>17</i>	<i>1</i>
DEB2126	Bottom	Up	Grate	Nortek AqD	2000	0.18	5.1	10	1
<i>DEB2127</i>	<i>Surface</i>	<i>Down</i>	<i>ATON</i>	<i>Nortek AqD</i>	<i>600</i>	<i>10.2</i>	<i>12.4</i>	<i>18</i>	<i>1</i>
DEB2128	Bottom	Up	mTRBM	TRDI WH	1200	0.5	15.52	16	1
DEB2129	Bottom	Up	GP35	TRDI WH	1200	0.47	13.4	16	1
DEB2130	Surface	Down	ATON	Nortek AqD	600	11.6	13.7	20	1
DEB2131	Surface	Down	ATON	Nortek AqD	1000	10.1	12.3	16	1
DEB2132	Bottom	Up	GP-48	TRDI WH	600	0.66	12.53	17	1
DEB2133	Surface	Down	ATON	Nortek AqD	1000	11.6	13.58	17	1
DEB2134	Surface	Down	ATON	Nortek AqD	1000	10	12.1	17	1
db1935	Surface	Down	CURBY	Nortek AqD	600	11.4	11.9	16	0.5
<i>DEB2136</i>	<i>Surface</i>	<i>Down</i>	<i>ATON</i>	<i>Nortek AqD</i>	<i>1000</i>	<i>10.12</i>	<i>13.1</i>	<i>17</i>	<i>1</i>

ACRONYMS

ADCP	acoustic Doppler current profiler
AIS	Automatic identification system
AqD	Nortek Aquadopp current meter
ATON	Aids to Navigation
C	Celsius
cm/s	Centimeters per second
CO-OPS	Center for Operational Oceanographic Products and Services
CTD	conductivity, temperature, and depth
CURBY	CUrrents Real-time BuoY
DBOFS	Delaware Bay Operational Forecast System
ENU	Earth-oriented (East-North-Up) coordinates.
ft	feet
GI	Greenwich Interval
GP35	General Purpose 35-inch bottom mount platform from Mooring Systems, Inc. This platform has been renamed as H-TRBM-35 by the manufacturer.
IHO	International Hydrographic Organization
kg	kilogram
kHz	kilohertz
km	kilometer
kn	knots
LSQHA	Least squares harmonic analysis
m	meter
MEC	maximum ebb current
MFC	maximum flood current
MHHW	mean higher high water
MLLW	mean lower low water
MSI	Mooring Systems, Inc.
mTRBM	miniature trawl-resistant bottom mount

NCOP	National Current Observation Program
NOAA	National Oceanic and Atmospheric Administration
NOS	National Ocean Service
QARTOD	Quality Assurance/Quality Control of Real-Time Oceanographic Data
R/V	Research Vessel
s	second
SEABY	Subsurface Ellipsoid ADCP BuoY
TCP	NOAA tidal current predictions
TRDI	Teledyne RD Instruments
WH	(TRDI) Workhorse ADCP
USACE	U. S. Army Corps of Engineers